

Vrije Universiteit Brussel



Faculteit Toegepaste Wetenschappen  
Werktuigkunde

# **Identification of the material properties of slender composite structures**

Promotor: Prof. Dr. Ir. Hugo Sol  
Academiejaar 2003 - 2004

Proefschrift ingediend tot het behalen van de academische graad van  
Burgerlijk Werktuigkundig-Elektrotechnisch Ingenieur

door  
Erik Eüler

## Abstract

This thesis investigates if **global effective orthotropic material properties** can be **determined by** measuring a certain amount of **natural frequencies of composite structures**. Natural frequencies contain mass and stiffness information and as such there is a possibility that this goal can be reached. The developed procedure belongs to the group of mixed numerical experimental methods. The procedure can be explained as follows.

First, experimental modal analysis (EMA) is used to extract the natural frequencies of the physical structure. This modal data is used as reference response data during the procedure.

Next, a mathematical model of the structure is created. In the physical model all mass and stiffness related properties are known except for the anisotropic material properties. All known properties are implemented as such into the mathematical model. One is interested in global properties of the structure (e.g. stiffness) and not in local properties (e.g. ply orientation, ply properties). Therefore, the real composite material is modelled as a global homogeneous orthotropic material in the mathematical model. This mathematical model is solved for modal data using finite element analysis.

Finally, two sets of non matching modal data are available. One set composed of experimentally obtained reference data. The other set contains calculated data from the mathematical model. The orthotropic material properties, also called parameters, are then modified in such a way that both sets of modal data match. If those two sets match, the virtual model has “in a global sense” the same mass and stiffness properties as the real model.

A program written in FEMtools is applied to five test cases. A first test case considers a beam made out of steel. The program correctly identifies the isotropic properties of steel, making use of analytical calculated natural frequencies. Afterwards, the program is used to identify the orthotropic material properties of four different composite beams. One closed box beam and three beams with open cross section. In each case, the program is able to identify certain orthotropic material properties. Which property can be identified, varies from case to case. It is also shown that the program can be used to detect a most optimal length to identify a certain preferred material property.

# **Table of Contents**

## **Introduction**

### **Chapter One: Literature review**

**page**

1.1 Mechanical behavior of composite materials	1
1.1.1 Linear elastic stress-strain characteristics of Fiber-reinforced material	
1.1.2 The plane-stress assumption	
1.1.3 Plane-stress stress-strain relations in a global coordinate system	
1.1.4 Classical Lamination Theory: The Kirchhoff Hypothesis	
1.1.5 Classical Lamination Theory: Laminate Stiffness Matrix	
1.1.6 Laminate Inplane Moduli	
1.2 Mechanical behavior of structural elements	16
1.2.1 Structural elements of homogeneous isotropic material	
1.2.2 Structural elements of composite material	
1.2.3 More advanced theories	

1.3 Production process: pultrusion	26
------------------------------------	----

### **Chapter Two: Experimental Modal Analysis (EMA)**

2.1 Introduction	27
2.2 Assumptions	28
2.3 Experimental setup	29

### **Chapter Three: The virtual model**

3.1 Mathematical model	33
3.1.1 Main assumptions in mathematical model	
3.1.2 Formulation of the equation of motion	
3.1.3 Solution methods	
3.2 The finite element solution	44
3.2.1 The finite element method as a generalization of the Rayleigh-Ritz method	
3.2.2 Derivation of element matrices	
3.2.3 Derivation of structural matrices	
3.2.4 Solving the equation of motion for modal data	
3.2.5 Sources of error	

<b><u>Chapter Four: Model Updating</u></b>	<b>page</b>
4.1 Principle of model updating	55
4.2 Mathematics of model updating	56
4.3 Successful model updating	59
4.4 Model updating using FEMtools	62

### **Chapter Five: Outline program**

5.1 Flowchart program	64
5.2 Input box “Define Geometry Beam”	65
5.3 Input box “Inputmenu Resonalyser”	70
5.4 Generate converged mesh	71
5.5 Check sensitivy Box	73
5.6 Input box “Tune InputBox”	74

### **Chapter Six: Application of the program**

6.1 Closed box profile made out of steel	76
6.2 Closed box profile	79
6.3 SymmetricU-profile	83
6.4 AsytermicU-profile	87
6.5 Complex-profile	92

### **Chapter Seven: Conclusions**

### **References**

### **Addendum**

## Introduction

Most engineers have considerable experience in the design of simple structural components using isotropic materials. However, today more and more composite materials are used for structural elements. Mainly because of their superior properties, such as high stiffness- and strength-to-weight ratios, excellent fatigue resistance and high resistance to environmental degradation. Secondly, production techniques are available to produce such components of constant quality in a cost efficient way.

In load carrying applications one is mainly interested in the stiffness properties of the structural component. Elastic and shear moduli supplemented with section properties render the stiffness properties of the component. Moduli of isotropic materials are well known and well documented. This is not the case for composite materials. The effective laminate properties depend on fiber material, matrix material, ply orientation, laminate thickness, stacking sequence, etc ... . Infinite combinations are possible, resulting in a huge amount of different moduli. It is clear that not all possible scenarios are studied in literature.

If all the details of the composite material are known, the engineer can calculate effective laminate properties and use them in theories like for example the first-order shear deformation theory for thin-walled laminated beams. If the ply lay-up results in coupling phenomena, the engineer has to use advanced software to simulate the behavior of the structure. All this requires substantial effort.

In some cases, not all the details of the composite material are known. For example, the exact fiber orientation at a certain area of the structure. Here, elastic properties can be determined by experiment. Drawback, these experiments are destructive in nature. Another possibility is to obtain stiffness properties of the whole structure by conducting an experiment. Drawback here, influence of boundary conditions. All this requires substantial effort.

Above reflections are discussed and explained in Chapter One: Literature review.

This thesis investigates if **global effective orthotropic material properties** for the composite material can be **determined by** measuring a certain amount of **natural frequencies of the structure**. Natural frequencies contain mass and stiffness information and as such there is a possibility that this goal can be reached. The developed procedure belongs to the group of mixed numerical experimental methods. The procedure can be explained as follows.

First, experimental modal analysis (EMA) is used to extract the natural frequencies of the physical structure. This modal data is used as reference response data during the procedure. Aspects concerning experimental modal analysis are discussed in Chapter Two: Experimental modal analysis.

Next, a mathematical model of the structure is created. In the physical model all mass and stiffness related properties are known except for the anisotropic material properties. All known properties are implemented as such into the mathematical model. One is interested in global properties of the structure (e.g. stiffness) and not in local properties (e.g. ply orientation, ply properties). Therefore, the real composite material is modelled as a global homogeneous orthotropic material in the mathematical model. This mathematical model is solved for modal data using finite element analysis. More information can be found in Chapter Three: The virtual model.

Finally, two sets of non matching modal data are available. One set composed of experimentally obtained reference data. The other set contains calculated data from the mathematical model. The orthotropic material properties, also called parameters, are then modified in such a way that both sets of modal data match. If those two sets match, the virtual model has “in a global sense” the same mass and stiffness properties as the real model. This principle is called model updating and is discussed in Chapter Four: Model updating.

If it is possible to identify orthotropic material properties by natural frequency measurement, then **the procedure** must be **automated**. User input is restricted to coordinate points to define the geometry, initial parameter values and reference responses. Information about program input is found in Chapter Five: Program Outline.

Chapter Six and Seven give an idea of how the program can be used in practise to estimate stiffness properties of structural elements.

The mixed numerical experimental approach offers a number of advantages:

- Natural frequencies of structures can be measured conveniently and accurately
- Vibration test are repeatable and non-destructive
- Tailor-made holding fixtures are not required as in conventional tests
- No specialized training required to use the application
- Minimum amount of calculation to obtain stiffness properties of the beam

## Chapter One: Literature review

### 1.1 Mechanical behavior of composite materials

#### **1.1.1 Linear elastic stress-strain characteristics of fiber-reinforced material**

The study of the mechanics of fiber-reinforced composites could begin at several points. Because the fiber plays a key role in the performance of the material, one logical starting point would be to study the interaction of the fiber with the matrix. One might address a host of problems: stresses in the fiber, stresses in the matrix around the fiber, adhesive stresses at the interface, breaking of the fiber, etc ... . This localized look at the interaction of the fibers and the matrix is called micromechanics. On the other end of the spectrum, interest centers on the behavior of structures made using fiber-reinforced material. Deflections, vibration frequencies and many other more global responses are of interest.

It is convenient to use an orthogonal coordinate system that has one axis aligned with the fiber direction. The system is identified as the 1-2-3 coordinate system or the principal material coordinate system. Figure 1.1 illustrates an isolated layer and the orientation of the principal material coordinate system. The 1 axis is aligned with the fiber direction, the 2 axis is in the plane of the layer and perpendicular to the fibers and the 3 axis is perpendicular to the plane of the layer. The 1 direction is the fiber direction, while the 2 and 3 directions are the matrix directions.

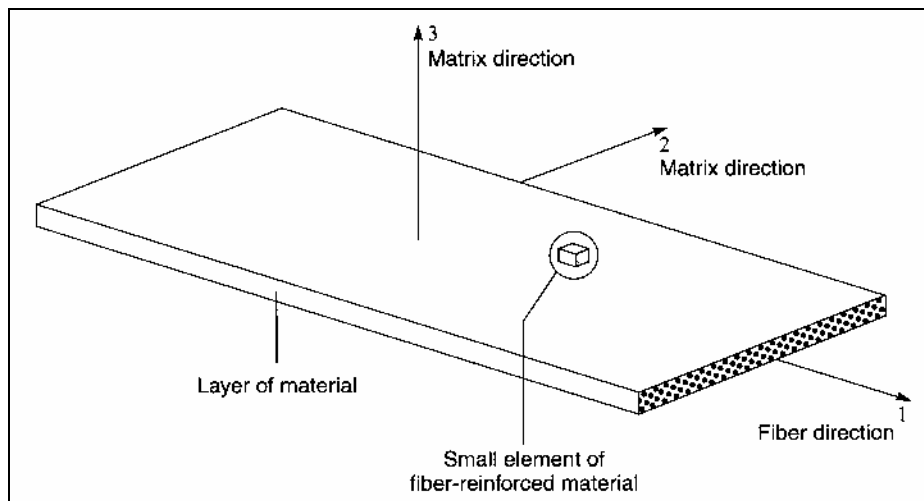


Figure 1.1 : Principal material coordinate system

The effect of the fiber reinforcement is smeared over the volume of the material and the fiber-matrix system is replaced by a single homogenous material. This single material has different properties in three mutually perpendicular directions and thus considered as orthotropic. As a result, a layer is said to be orthotropic.

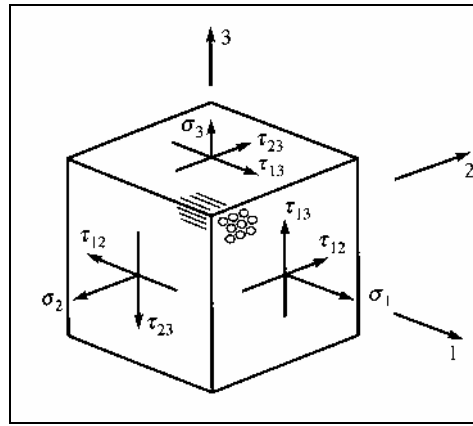


Figure 1.2 : Stresses acting on a small element of fiber-reinforced material

Figure 1.2 illustrates a small element of smeared fiber-reinforced material subject to stresses on its six bounding surfaces. This small volume of material has been considered removed from the plate in the previous figure. The normal stress acting on the element face with its outward normal in the 1 direction is denoted as  $\sigma_1$ . The shear stress acting in the 2 direction on that face is denoted as  $\tau_{12}$  and the shear stress acting in the 3 direction on that face is denoted as  $\tau_{13}$ . The normal and shear stresses acting on the other faces are similarly labeled. The extensional strain responses in the 1-2-3 coordinate system are denoted as  $\varepsilon_1$ ,  $\varepsilon_2$  and  $\varepsilon_3$  while the engineering shearing strain responses are denoted as  $\gamma_{12}$ ,  $\gamma_{23}$  and  $\gamma_{13}$ . With this notation  $\varepsilon_1$  is the stretching of the element in the 1 direction,  $\gamma_{12}$  is the change of right angle in the 1-2 plane, and so on.

The stress-strain relation for the small element of material can be constructed by considering the response of the element to each of the six stress components. As only linear elastic response is to be considered, superposition of the responses will be used to determine the response of the element to a complex or combined stress state. Only the relevant results are mentioned here, for details see reference (Ref.1). All the relationships between the stresses and strains take the collective form

$$\begin{Bmatrix} \varepsilon_1 \\ \varepsilon_2 \\ \varepsilon_3 \\ \gamma_{23} \\ \gamma_{13} \\ \gamma_{12} \end{Bmatrix} = \begin{bmatrix} \frac{1}{E_1} & -\nu_{21} & -\nu_{31} & 0 & 0 & 0 \\ -\nu_{12} & \frac{1}{E_2} & -\nu_{32} & 0 & 0 & 0 \\ -\nu_{13} & -\nu_{23} & \frac{1}{E_3} & 0 & 0 & 0 \\ 0 & 0 & 0 & \frac{1}{G_{23}} & 0 & 0 \\ 0 & 0 & 0 & 0 & \frac{1}{G_{13}} & 0 \\ 0 & 0 & 0 & 0 & 0 & \frac{1}{G_{12}} \end{bmatrix} \begin{Bmatrix} \sigma_1 \\ \sigma_2 \\ \sigma_3 \\ \tau_{23} \\ \tau_{13} \\ \tau_{12} \end{Bmatrix}$$

or

$$\begin{Bmatrix} \varepsilon_1 \\ \varepsilon_2 \\ \varepsilon_3 \\ \gamma_{23} \\ \gamma_{13} \\ \gamma_{12} \end{Bmatrix} = \begin{bmatrix} S_{11} & S_{12} & S_{13} & 0 & 0 & 0 \\ S_{21} & S_{22} & S_{23} & 0 & 0 & 0 \\ S_{31} & S_{32} & S_{33} & 0 & 0 & 0 \\ 0 & 0 & 0 & S_{44} & 0 & 0 \\ 0 & 0 & 0 & 0 & S_{55} & 0 \\ 0 & 0 & 0 & 0 & 0 & S_{66} \end{bmatrix} \begin{Bmatrix} \sigma_1 \\ \sigma_2 \\ \sigma_3 \\ \tau_{23} \\ \tau_{13} \\ \tau_{12} \end{Bmatrix}$$

where:

- $\{\varepsilon\}$  = strain vector
- $[S]$  = compliance matrix
- $\{\sigma\}$  = stress vector
- $E_i$  = Young's modulus in the  $i$  direction
- $\nu_{ij}$  = Poisson's ratio
- $G_{ij}$  = shear modulus in the  $ij$  plane

The inverse of the compliance matrix is called the stiffness matrix or elasticity matrix and is commonly denoted by  $[C]$ . With the inverse defined, the stress-strain relations become

$$\begin{Bmatrix} \sigma_1 \\ \sigma_2 \\ \sigma_3 \\ \tau_{23} \\ \tau_{13} \\ \tau_{12} \end{Bmatrix} = \begin{bmatrix} C_{11} & C_{12} & C_{13} & 0 & 0 & 0 \\ C_{21} & C_{22} & C_{23} & 0 & 0 & 0 \\ C_{31} & C_{32} & C_{33} & 0 & 0 & 0 \\ 0 & 0 & 0 & C_{44} & 0 & 0 \\ 0 & 0 & 0 & 0 & C_{55} & 0 \\ 0 & 0 & 0 & 0 & 0 & C_{66} \end{bmatrix} \begin{Bmatrix} \varepsilon_1 \\ \varepsilon_2 \\ \varepsilon_3 \\ \gamma_{23} \\ \gamma_{13} \\ \gamma_{12} \end{Bmatrix}$$

The compliance matrix involves 12 engineering properties. However, these properties are not all independent. There are actually only nine independent material properties. So-called reciprocity relationships can be established among the extensional moduli and the Poisson's ratios. As a result the compliance matrix is symmetric. To establish these relations, it is convenient to use the Maxwell-Betti Reciprocal Theorem. See reference (Ref. 1) for more details.

$$\text{Reciprocity relationships: } \frac{\nu_{12}}{E_1} = \frac{\nu_{21}}{E_2} ; \quad \frac{\nu_{13}}{E_1} = \frac{\nu_{31}}{E_3} ; \quad \frac{\nu_{23}}{E_2} = \frac{\nu_{32}}{E_3}$$

$$\begin{Bmatrix} \varepsilon_1 \\ \varepsilon_2 \\ \varepsilon_3 \\ \gamma_{23} \\ \gamma_{13} \\ \gamma_{12} \end{Bmatrix} = \begin{bmatrix} \frac{1}{E_1} & \frac{-\nu_{12}}{E_1} & \frac{-\nu_{13}}{E_1} & 0 & 0 & 0 \\ \frac{-\nu_{12}}{E_1} & \frac{1}{E_2} & \frac{-\nu_{23}}{E_2} & 0 & 0 & 0 \\ \frac{-\nu_{13}}{E_1} & \frac{-\nu_{23}}{E_2} & \frac{1}{E_3} & 0 & 0 & 0 \\ 0 & 0 & 0 & \frac{1}{G_{23}} & 0 & 0 \\ 0 & 0 & 0 & 0 & \frac{1}{G_{13}} & 0 \\ 0 & 0 & 0 & 0 & 0 & \frac{1}{G_{12}} \end{bmatrix} \begin{Bmatrix} \sigma_1 \\ \sigma_2 \\ \sigma_3 \\ \tau_{23} \\ \tau_{13} \\ \tau_{12} \end{Bmatrix}$$

or

$$\begin{Bmatrix} \varepsilon_1 \\ \varepsilon_2 \\ \varepsilon_3 \\ \gamma_{23} \\ \gamma_{13} \\ \gamma_{12} \end{Bmatrix} = \begin{bmatrix} S_{11} & S_{12} & S_{13} & 0 & 0 & 0 \\ S_{12} & S_{22} & S_{23} & 0 & 0 & 0 \\ S_{13} & S_{23} & S_{33} & 0 & 0 & 0 \\ 0 & 0 & 0 & S_{44} & 0 & 0 \\ 0 & 0 & 0 & 0 & S_{55} & 0 \\ 0 & 0 & 0 & 0 & 0 & S_{66} \end{bmatrix} \begin{Bmatrix} \sigma_1 \\ \sigma_2 \\ \sigma_3 \\ \tau_{23} \\ \tau_{13} \\ \tau_{12} \end{Bmatrix}$$

Because of the three reciprocity relations, only nine independent constants are needed to describe the linear elastic behavior of a fiber reinforced material.

### 1.1.2 The plane-stress assumption

The plane stress assumption is based on the manner in which fiber reinforced composite materials are used in many structures. Specifically, fiber reinforced materials are utilized in beams, plates and other structural shapes which have at least one characteristic geometric dimension an order of magnitude less than the other two dimensions. In these applications, three of the six components of stress are generally much smaller than the other three. In the context of fiber reinforced plates, the stress components  $\sigma_3$ ,  $\tau_{23}$  and  $\tau_{13}$  are set to zero with the assumption that the 1-2 plane of the coordinate system is in the plane of the plate.

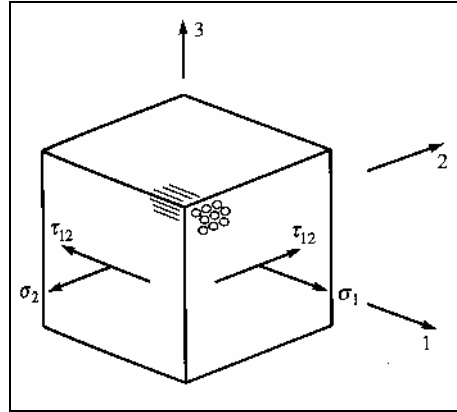


Figure 1.3 : Stresses acting on a small element of fiber-reinforced material in a state of plane stress

$$\begin{Bmatrix} \varepsilon_1 \\ \varepsilon_2 \\ \varepsilon_3 \\ \gamma_{23} \\ \gamma_{13} \\ \gamma_{12} \end{Bmatrix} = \begin{bmatrix} S_{11} & S_{12} & S_{13} & 0 & 0 & 0 \\ S_{12} & S_{22} & S_{23} & 0 & 0 & 0 \\ S_{13} & S_{23} & S_{33} & 0 & 0 & 0 \\ 0 & 0 & 0 & S_{44} & 0 & 0 \\ 0 & 0 & 0 & 0 & S_{55} & 0 \\ 0 & 0 & 0 & 0 & 0 & S_{66} \end{bmatrix} \begin{Bmatrix} \sigma_1 \\ \sigma_2 \\ 0 \\ 0 \\ 0 \\ \tau_{12} \end{Bmatrix}$$

From this relation it is obvious that

$$\gamma_{23} = 0 \quad \text{and} \quad \gamma_{13} = 0$$

so with the plane stress assumption there can be no shear strains whatsoever in the 2-3 and 1-3 planes. That is an important ramification of the assumption.

$$\begin{Bmatrix} \varepsilon_1 \\ \varepsilon_2 \\ \gamma_{12} \end{Bmatrix} = \begin{bmatrix} S_{11} & S_{12} & 0 \\ S_{12} & S_{22} & 0 \\ 0 & 0 & S_{66} \end{bmatrix} \begin{Bmatrix} \sigma_1 \\ \sigma_2 \\ \tau_{12} \end{Bmatrix}$$

The definitions of the compliances have not changed from the time they were first introduced, namely,

$$\begin{array}{ll} S_{11} = \frac{1}{E_1} & S_{12} = \frac{-\nu_{12}}{E_1} = \frac{-\nu_{21}}{E_2} \\ S_{22} = \frac{1}{E_2} & S_{66} = \frac{1}{G_{12}} \end{array}$$

The 3 x 3 matrix of compliances is called the reduced compliance matrix. This relationship can be inverted. This result in

$$\begin{Bmatrix} \sigma_1 \\ \sigma_2 \\ \tau_{12} \end{Bmatrix} = \begin{bmatrix} Q_{11} & Q_{12} & 0 \\ Q_{12} & Q_{22} & 0 \\ 0 & 0 & Q_{66} \end{bmatrix} \begin{Bmatrix} \varepsilon_1 \\ \varepsilon_2 \\ \gamma_{12} \end{Bmatrix}$$

$$\begin{array}{ll} Q_{11} = \frac{E_1}{1 - \nu_{12}\nu_{21}} & Q_{12} = \frac{\nu_{12}E_2}{1 - \nu_{12}\nu_{21}} = \frac{\nu_{21}E_1}{1 - \nu_{12}\nu_{21}} \\ Q_{22} = \frac{E_2}{1 - \nu_{12}\nu_{21}} & Q_{66} = G_{12} \end{array}$$

The  $[Q]$  3 x 3 matrix is called the reduced stiffness matrix.

The plane stress assumption reduces the number of independent constants from nine to four namely  $E_1$ ,  $E_2$ ,  $\nu_{12}$  and  $G_{12}$ . The elastic properties of a layer can be determined by mechanical testing or by micromechanical models.

### 1.1.3 Plane-stress stress-strain relations in a global coordinate system

To this point we have studied the response of fiber-reinforced materials in the principal material coordinate system. In the context of composite structures, interesting properties like the total deformation, stiffness, etc. are calculated with respect to a global or structural coordinate system. Therefore it is necessary to transform the stress-strain relations from the 1-2-3 coordinate system into the global x-y-z coordinate system.

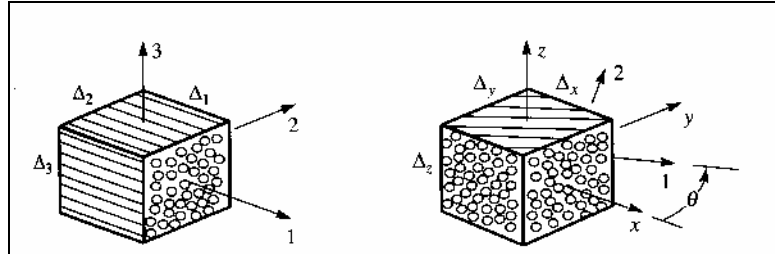


Figure 1.4 (a): element in 1-2-3 system

Figure 1.4 (b): element in x-y-z system

Figure 1.4 (a) illustrates an element in the principal material system. Next to it a similar element but one that is isolated in an x-y-z global coordinate system. The fibers are oriented at an angle  $\theta$  with respect to the positive x axis of the global system. The fibers are parallel to the x-y plane and the 3 and z axes coincide.

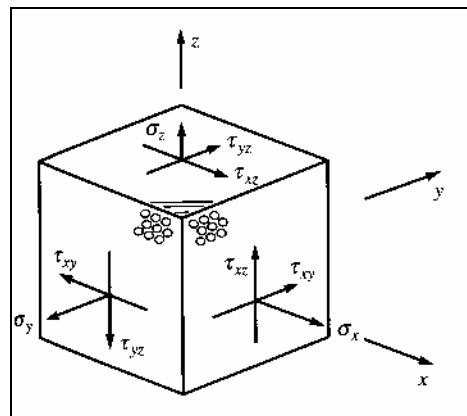


Figure 1.5 : Stress components in x-y-z coordinate system

Figure 1.5 should be interpreted quite literally; “What is the relation between the stresses and deformations for a small volume of material whose fibers are oriented at some angle relative to the boundaries of the element rather than parallel to them?”. Loads will not be always applied parallel to the fibers. Intuition indicates that unusual deformations are likely to occur. The skewed orientation of the fibers must certainly cause unusual distortions of the originally cubic volume element.

Transforming the stress-strain relations from the 1-2-3 coordinate system into the global x-y-z coordinate system is done using the standard transformation relations for stresses and strains. This transformation can be done for a general state of stress. However, in this paper only the plane-stress situation is considered and only the final result is stated. More information can be found in (Ref. 1).

$$\begin{Bmatrix} \varepsilon_x \\ \varepsilon_y \\ \gamma_{xy} \end{Bmatrix} = \begin{bmatrix} \bar{S}_{11} & \bar{S}_{12} & \bar{S}_{16} \\ \bar{S}_{12} & \bar{S}_{22} & \bar{S}_{26} \\ \bar{S}_{16} & \bar{S}_{26} & \bar{S}_{66} \end{bmatrix} \begin{Bmatrix} \sigma_x \\ \sigma_y \\ \tau_{xy} \end{Bmatrix}$$

The  $\bar{S}_{ij}$  are called the transformed reduced compliances. These are defined by

$$\begin{Bmatrix} \bar{S}_{11} \\ \bar{S}_{22} \\ \bar{S}_{12} \\ \bar{S}_{66} \\ \bar{S}_{16} \\ \bar{S}_{26} \end{Bmatrix} = \begin{bmatrix} c^4 & s^4 & 2c^2s^2 & c^2s^2 \\ s^4 & c^4 & 2c^2s^2 & c^2s^2 \\ c^2s^2 & c^2s^2 & c^4 + s^4 & -c^2s^2 \\ 4c^2s^2 & 4c^2s^2 & -8c^2s^2 & (c^2 - s^2)^2 \\ 2c^3s & -2cs^3 & 2(cs^3 - c^3s) & cs^3 - c^3s \\ 2cs^3 & -2c^3s & 2(c^3s - cs^3) & c^3s - cs^3 \end{bmatrix} \begin{Bmatrix} S_{11} \\ S_{22} \\ S_{12} \\ S_{66} \end{Bmatrix}$$

where  $c$  and  $s$  respectively stands for  $\cos\theta$  and  $\sin\theta$ . This equation relate the strains of an element of fiber-reinforced material as measured in the  $x$ - $y$ - $z$  global coordinate system to the applied stresses measured in that coordinate system. Consider that a normal stress  $\sigma_x$  will cause a shearing deformation  $\gamma_{xy}$  through the  $\bar{S}_{16}$  term, and similarly a normal stress  $\sigma_y$  will cause a shearing deformation through the  $\bar{S}_{26}$  term. Equally important, because of the existence of these same  $\bar{S}_{16}$  and  $\bar{S}_{26}$  terms at other locations in the compliance matrix, a shear stress  $\tau_{xy}$  will cause strains  $\varepsilon_x$  and  $\varepsilon_y$ . Such responses are totally different from those in metals. This coupling found in fiber-reinforced composites is termed shear-extension coupling.

The same techniques can be used to deduce the transformed reduced stiffnesses  $\bar{Q}_{ij}$ . These are defined by

$$\begin{Bmatrix} \sigma_x \\ \sigma_y \\ \tau_{xy} \end{Bmatrix} = \begin{bmatrix} \bar{Q}_{11} & \bar{Q}_{12} & \bar{Q}_{16} \\ \bar{Q}_{12} & \bar{Q}_{22} & \bar{Q}_{26} \\ \bar{Q}_{16} & \bar{Q}_{26} & \bar{Q}_{66} \end{bmatrix} \begin{Bmatrix} \varepsilon_x \\ \varepsilon_y \\ \gamma_{xy} \end{Bmatrix}$$

$$\begin{Bmatrix} \bar{Q}_{11} \\ \bar{Q}_{22} \\ \bar{Q}_{12} \\ \bar{Q}_{66} \\ \bar{Q}_{16} \\ \bar{Q}_{26} \end{Bmatrix} = \begin{bmatrix} c^4 & s^4 & 2c^2s^2 & 4c^2s^2 \\ s^4 & c^4 & 2c^2s^2 & 4c^2s^2 \\ c^2s^2 & c^2s^2 & c^4 + s^4 & -4c^2s^2 \\ c^2s^2 & c^2s^2 & -2c^2s^2 & (c^2 - s^2)^2 \\ c^3s & -cs^3 & cs^3 - c^3s & 2(cs^3 - c^3s) \\ cs^3 & -c^3s & c^3s - cs^3 & 2(c^3s - cs^3) \end{bmatrix} \begin{Bmatrix} Q_{11} \\ Q_{22} \\ Q_{12} \\ Q_{66} \end{Bmatrix}$$

where  $c$  and  $s$  respectively stands for  $\cos\theta$  and  $\sin\theta$ . Like the transformed compliances, the transformed stiffnesses relate the strains as defined in the  $x$ - $y$ - $z$  global coordinate system to the stresses defined in that system, and the existence of the  $\bar{Q}_{16}$  and  $\bar{Q}_{26}$  terms, like the existence of the  $\bar{S}_{16}$  and  $\bar{S}_{26}$  terms, represent shear-extension coupling effects.

### 1.1.4 Classical Lamination Theory: The Kirchhoff Hypothesis

In a typical structural application of a composite, multiple layers of unidirectional composites are stacked together at various angles to form a laminate. Some layers may use graphite fibers for reinforcement, while others may use glass fibers. Some laminates may consist of three or four layers, and some of several hundred layers. Figure 1.6 illustrates a global coordinate system and a general laminate consisting of  $N$  layers. The laminate thickness is denoted by  $H$  and the thickness of an individual layer by  $h$ . It is important that a geometric midplane can be defined. Herein the positive  $z$  axis will be downward and the laminate extends in the  $z$  direction from  $-H/2$  to  $+H/2$ .

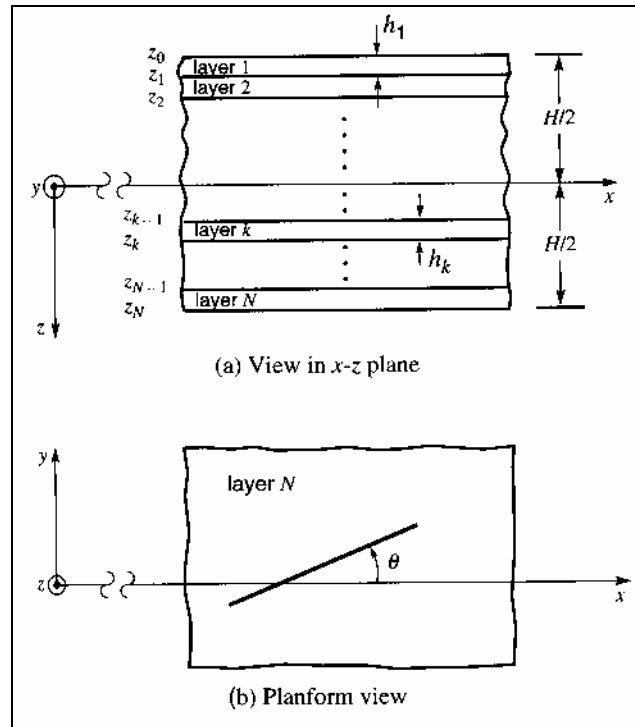


Figure 1.6 : Laminates nomenclature

It is assumed that all layers are perfectly bonded together. The Kirchhoff hypothesis focuses on the deformation of lines which before deformation are straight and normal to the laminate's geometric midsurface. It assumes that despite the deformations caused by the applied loads, such an initial line remains straight and normal to the deformed geometric midplane and does not change length. Generally there will be a through-thickness strain  $\varepsilon_z$  but the Kirchhoff hypothesis is inconsistent with this fact. Fortunately, the assumption that the normal remains fixed in length does not enter directly into the use of the hypothesis.

A corollary of the Kirchhoff hypothesis is that the in-plane displacements vary linearly through the entire thickness of the laminate, while the normal deflection is uniform through the thickness. The superscript  $o$  will be reserved to denote the kinematics of points on the geometric midsurface or reference surface.

$$\begin{aligned}
 u(x, y, z) &= u^o(x, y) - z \frac{\partial w^o(x, y)}{\partial x} \\
 v(x, y, z) &= v^o(x, y) - z \frac{\partial w^o(x, y)}{\partial y} \\
 w(x, y, z) &= w^o(x, y)
 \end{aligned}$$

With the assumptions regarding the displacement field established by way of the Kirchhoff hypothesis, the next step is to investigate the strains that result from the displacements. This can be done by using the strain-displacement relations from the theory of elasticity.

$$\begin{aligned}\varepsilon_x(x, y, z) &= \varepsilon_x^o(x, y) + z\kappa_x^o(x, y) \\ \varepsilon_y(x, y, z) &= \varepsilon_y^o(x, y) + z\kappa_y^o(x, y) \\ \gamma_{xy}(x, y, z) &= \gamma_{xy}^o(x, y) + z\kappa_{xy}^o(x, y)\end{aligned}$$

with

$$\begin{aligned}\varepsilon_x^o(x, y) &= \frac{\partial u^o(x, y)}{\partial x} \quad \text{and} \quad \kappa_x^o(x, y) = -\frac{\partial^2 w^o(x, y)}{\partial x^2} \\ \varepsilon_y^o(x, y) &= \frac{\partial v^o(x, y)}{\partial y} \quad \text{and} \quad \kappa_y^o(x, y) = -\frac{\partial^2 w^o(x, y)}{\partial y^2} \\ \gamma_{xy}^o(x, y) &= \frac{\partial v^o(x, y)}{\partial x} + \frac{\partial u^o(x, y)}{\partial y} \quad \text{and} \quad \kappa_{xy}^o(x, y) = -2\frac{\partial^2 w^o(x, y)}{\partial x \partial y}\end{aligned}$$

The equations show that if the reference surface strains and curvatures are known at every point within a laminate, then the strains at every point within the three-dimensional volume are known. This is an important advantage. Rather than treating a laminate as a three-dimensional domain, the analysis of laminates degenerates to studying what is happening to the reference surface, a two-dimensional domain.

Another important assumption of classical lamination theory is that each point within the volume of a laminate is in a state of plane stress. The stress-strain relation for layer  $k$  of a laminate become

$$\begin{Bmatrix} \sigma_x \\ \sigma_y \\ \tau_{xy} \end{Bmatrix}_k = \begin{bmatrix} \bar{Q}_{11} & \bar{Q}_{12} & \bar{Q}_{16} \\ \bar{Q}_{12} & \bar{Q}_{22} & \bar{Q}_{26} \\ \bar{Q}_{16} & \bar{Q}_{26} & \bar{Q}_{66} \end{bmatrix}_k \begin{Bmatrix} \varepsilon_x^o + z_k \kappa_x^o \\ \varepsilon_y^o + z_k \kappa_y^o \\ \gamma_{xy}^o + z_k \kappa_{xy}^o \end{Bmatrix}$$

The stresses are function of  $z$  not only because the strains vary linearly with  $z$  but also because the reduced stiffnesses vary with  $z$ . The reduced stiffnesses vary in piecewise constant fashion, having one set of values through the thickness of one layer, another set of values through another layer, and so forth. The net result is that, in general, the variation of the stresses through the thickness of the laminate is discontinuous.

### 1.1.5 Classical Lamination Theory: Laminate Stiffness Matrix

It is usually more convenient to work with the resultant forces and moments, expressed per unit width, than it is to deal with stress components in each individual layer. The stress resultants are defined as

$$\begin{array}{ll}
 N_x \equiv \int_{-\frac{H}{2}}^{\frac{H}{2}} \sigma_x dz & M_x \equiv \int_{-\frac{H}{2}}^{\frac{H}{2}} \sigma_x z dz \\
 N_y \equiv \int_{-\frac{H}{2}}^{\frac{H}{2}} \sigma_y dz & M_y \equiv \int_{-\frac{H}{2}}^{\frac{H}{2}} \sigma_y z dz \\
 N_{xy} \equiv \int_{-\frac{H}{2}}^{\frac{H}{2}} \tau_{xy} dz & M_{xy} \equiv \int_{-\frac{H}{2}}^{\frac{H}{2}} \tau_{xy} z dz
 \end{array}$$

$N_x, N_y$  the normal force resultants

$N_{xy}$  the shear force resultants

$M_x, M_y$  the bending moment resultants

$M_{xy}$  the twisting moment resultant

Next the stress-strain relations are substituted in the above definitions of the stress resultants. As such, one obtains the relationship between the resultants and the reference surface response.

$$\begin{Bmatrix} N_x \\ N_y \\ N_{xy} \\ M_x \\ M_y \\ M_{xy} \end{Bmatrix} = \begin{bmatrix} A_{11} & A_{12} & A_{16} & B_{11} & B_{12} & B_{16} \\ A_{12} & A_{22} & A_{26} & B_{12} & B_{22} & B_{26} \\ A_{16} & A_{26} & A_{66} & B_{16} & B_{26} & B_{66} \\ B_{11} & B_{12} & B_{16} & D_{11} & D_{12} & D_{16} \\ B_{12} & B_{22} & B_{26} & D_{12} & D_{22} & D_{26} \\ B_{16} & B_{26} & B_{66} & D_{16} & D_{26} & D_{66} \end{bmatrix} \begin{Bmatrix} \epsilon_x^o \\ \epsilon_y^o \\ \gamma_{xy}^o \\ \kappa_x^o \\ \kappa_y^o \\ \kappa_{xy}^o \end{Bmatrix}$$

$$A_{ij} = \sum_{k=1}^N \bar{Q}_{ij_k} (z_k - z_{k-1})$$

$$B_{ij} = \frac{1}{2} \sum_{k=1}^N \bar{Q}_{ij_k} (z_k^2 - z_{k-1}^2)$$

$$D_{ij} = \frac{1}{3} \sum_{k=1}^N \bar{Q}_{ij_k} (z_k^3 - z_{k-1}^3)$$

The six-by-six matrix consisting of the components  $A_{ij}$ ,  $B_{ij}$  and  $D_{ij}$  is called the laminate stiffness matrix. For obvious reasons it is also known as the  $ABD$  matrix. This form is a direct result of the Kirchhoff hypothesis, the plane-stress assumption and the definition of the stress resultants. The above matrix equation exhibits a variety of different kinds of coupling. All of the  $B$ 's represent bending-stretching coupling in general. All quantities with subscripts 16 and 26 involve normal-shear coupling. This degree of coupling depends strongly on stacking arrangement of the laminate.

### ***Symmetric Laminates***

A laminate is symmetric if for every layer to one side of the laminate reference surface with a specific thickness, specific material properties and specific fiber orientation, there is another layer the identical distance on the opposite side of the reference surface with the identical thickness, material properties and fiber orientation. For a symmetric laminate all the components of the  $B$  matrix are identically zero. Consequently, the full six-by-six set of equations decouples into two three-by-three sets of equations, namely

$$\begin{Bmatrix} N_x \\ N_y \\ N_{xy} \end{Bmatrix} = \begin{bmatrix} A_{11} & A_{12} & A_{16} \\ A_{12} & A_{22} & A_{26} \\ A_{16} & A_{26} & A_{66} \end{bmatrix} \begin{Bmatrix} \varepsilon_x^o \\ \varepsilon_y^o \\ \gamma_{xy}^o \end{Bmatrix}$$

and

$$\begin{Bmatrix} M_x \\ M_y \\ M_{xy} \end{Bmatrix} = \begin{bmatrix} D_{11} & D_{12} & D_{16} \\ D_{12} & D_{22} & D_{26} \\ D_{16} & D_{26} & D_{66} \end{bmatrix} \begin{Bmatrix} \kappa_x^o \\ \kappa_y^o \\ \kappa_{xy}^o \end{Bmatrix}$$

### ***Balanced Laminates***

A laminate is balanced if for every layer with a specified thickness, specific material properties and specific fiber orientation, there is another layer with the identical thickness, material properties but opposite fiber orientation somewhere in the laminate. The layer with opposite fiber orientation can be anywhere within the thickness. The  $ABD$  matrix of a balanced but otherwise general laminate is not that much simpler than the  $ABD$  matrix of a general laminate. The full six-by-six equation applies but with the  $A_{16}$  and  $A_{26}$  components set to zero.

### ***Cross-Ply Laminates***

A laminate is a cross-ply laminate if every layer has its fibers oriented at either  $0^\circ$  or  $90^\circ$ . The six equations decouple to a set of four equations and a set of two equations, namely

$$\begin{Bmatrix} N_x \\ N_y \\ M_x \\ M_y \end{Bmatrix} = \begin{bmatrix} A_{11} & A_{12} & B_{11} & B_{12} \\ A_{12} & A_{22} & B_{12} & B_{22} \\ B_{11} & B_{12} & D_{11} & D_{12} \\ B_{12} & B_{22} & D_{12} & D_{22} \end{bmatrix} \begin{Bmatrix} \varepsilon_x^o \\ \varepsilon_y^o \\ \kappa_x^o \\ \kappa_y^o \end{Bmatrix} ; \quad \begin{Bmatrix} N_{xy} \\ M_{xy} \end{Bmatrix} = \begin{bmatrix} A_{66} & B_{66} \\ B_{66} & D_{66} \end{bmatrix} \begin{Bmatrix} \gamma_{xy}^o \\ \kappa_{xy}^o \end{Bmatrix}$$

### ***Symmetric Balanced Laminates***

A laminate is symmetric balanced if it meets both the criterion for being symmetric and the criterion for being balanced. If this is the case, then the equation takes the decoupled form

$$\begin{Bmatrix} N_x \\ N_y \end{Bmatrix} = \begin{bmatrix} A_{11} & A_{12} \\ A_{12} & A_{22} \end{bmatrix} \begin{Bmatrix} \varepsilon_x^o \\ \varepsilon_y^o \end{Bmatrix}$$

$$N_{xy} = A_{66}\gamma_{xy}^o$$

$$\begin{Bmatrix} M_x \\ M_y \\ M_{xy} \end{Bmatrix} = \begin{bmatrix} D_{11} & D_{12} & D_{16} \\ D_{12} & D_{22} & D_{26} \\ D_{16} & D_{26} & D_{66} \end{bmatrix} \begin{Bmatrix} \kappa_x^o \\ \kappa_y^o \\ \kappa_{xy}^o \end{Bmatrix}$$

### ***Symmetric Cross-Ply Laminates***

A laminate is a symmetric cross-ply laminate if it meets the criterion for being symmetric and the criterion for being cross-ply. This results in the simplest form of the  $ABD$  matrix. The six equations decouple significantly. Specifically,

$$\begin{Bmatrix} N_x \\ N_y \end{Bmatrix} = \begin{bmatrix} A_{11} & A_{12} \\ A_{12} & A_{22} \end{bmatrix} \begin{Bmatrix} \varepsilon_x^o \\ \varepsilon_y^o \end{Bmatrix}$$

$$N_{xy} = A_{66}\gamma_{xy}^o$$

$$\begin{Bmatrix} M_x \\ M_y \end{Bmatrix} = \begin{bmatrix} D_{11} & D_{12} \\ D_{12} & D_{22} \end{bmatrix} \begin{Bmatrix} \kappa_x^o \\ \kappa_y^o \end{Bmatrix}$$

$$M_{xy} = D_{66}\kappa_{xy}^o$$

## 1.1.6 Laminate Inplane Moduli

The effective engineering properties of a laminate consist of the effective extensional modulus in the x direction, the effective extensional modulus in the y direction, the effective Poisson's ratio's and the effective shear modulus in the x-y plane. These particular effective properties can be defined for general laminates but they make the most sense when considering the inplane loading of symmetric balanced laminates. To introduce effective engineering properties, define the average laminate stress in the x direction, the average laminate stress in the y direction and the average laminate shear stress to be, respectively

$$\bar{\sigma}_x \equiv \frac{1}{H} \int_{-\frac{H}{2}}^{\frac{H}{2}} \sigma_x dz \quad \bar{\sigma}_y \equiv \frac{1}{H} \int_{-\frac{H}{2}}^{\frac{H}{2}} \sigma_y dz \quad \bar{\tau}_{xy} \equiv \frac{1}{H} \int_{-\frac{H}{2}}^{\frac{H}{2}} \tau_{xy} dz$$

In the definition of the average stresses, the integrals are actually the definitions of the normal and shear force resultants, consequently

$$\bar{\sigma}_x = \frac{1}{H} N_x \quad \bar{\sigma}_y = \frac{1}{H} N_y \quad \bar{\tau}_{xy} = \frac{1}{H} N_{xy}$$

or

$$N_x = H\bar{\sigma}_x \quad N_y = H\bar{\sigma}_y \quad N_{xy} = H\bar{\tau}_{xy}$$

The stiffness matrices for symmetric balanced laminates are:

$$\begin{Bmatrix} N_x \\ N_y \end{Bmatrix} = \begin{bmatrix} A_{11} & A_{12} \\ A_{12} & A_{22} \end{bmatrix} \begin{Bmatrix} \varepsilon_x^o \\ \varepsilon_y^o \end{Bmatrix}$$

$$N_{xy} = A_{66} \gamma_{xy}^o$$

If there are no bending loads, all the curvatures are zero, and the strains are constant through the thickness; that is  $\varepsilon_x = \varepsilon_x^o$ ,  $\varepsilon_y = \varepsilon_y^o$ ,  $\gamma_{xy} = \gamma_{xy}^o$ . Inverting the stress resultant midplane strain relations yields:

$$\begin{Bmatrix} \varepsilon_x \\ \varepsilon_y \\ \gamma_{xy} \end{Bmatrix} = \begin{bmatrix} a_{11} & a_{12} & 0 \\ a_{12} & a_{22} & 0 \\ 0 & 0 & a_{33} \end{bmatrix} \begin{Bmatrix} N_x \\ N_y \\ N_{xy} \end{Bmatrix}$$

Substituting the definitions for the average laminate stresses in the above equation:

$$\begin{Bmatrix} \varepsilon_x \\ \varepsilon_y \\ \gamma_{xy} \end{Bmatrix} = \begin{bmatrix} a_{11}H & a_{12}H & 0 \\ a_{12}H & a_{22}H & 0 \\ 0 & 0 & a_{33}H \end{bmatrix} \begin{Bmatrix} \bar{\sigma}_x \\ \bar{\sigma}_y \\ \bar{\tau}_{xy} \end{Bmatrix}$$

from which the laminate elastic constants are seen to be:

$$\begin{aligned} \bar{E}_x &= \frac{1}{a_{11}H} & \bar{G}_{xy} &= \frac{1}{a_{66}H} \\ \bar{E}_y &= \frac{1}{a_{22}H} & \bar{\nu}_{xy} &= -\frac{a_{12}}{a_{11}} \end{aligned}$$

Noting that the  $[A]$  matrix consists of  $[Q]$  matrices from each layer in the laminate, it is obvious that the laminate elastic properties are functions of the angular orientation of the plies. This is illustrated in figure 1.8 for a typical high-modulus graphite-epoxy system. The layer properties are indicated in figure 1.7.

$$\begin{aligned} E_1 &= 170 \text{ GPa } (25.0 \times 10^6 \text{ psi}) \\ E_2 &= 12 \text{ GPa } (1.7 \times 10^6 \text{ psi}) \\ G_{12} &= 4.5 \text{ GPa } (0.65 \times 10^6 \text{ psi}) \\ \nu_{12} &= 0.30 \\ \rho &= 0.056 \\ \alpha_1 &= -0.54 \times 10^{-6}/\text{K} \\ \alpha_2 &= 35.1 \times 10^{-6}/\text{K} \\ \sigma_{L1}^{\text{tu}} &= 758 \text{ MPa } (110.0 \text{ ksi}) \\ \sigma_{L1}^{\text{tu}} &= 28 \text{ MPa } (4.0 \text{ ksi}) \\ \sigma_{L1}^{\text{u}} &= 62 \text{ MPa } (9.0 \text{ ksi}) \\ \sigma_{L1}^{\text{tu}} &= 758 \text{ MPa } (110.0 \text{ ksi}) \\ \sigma_{L1}^{\text{tu}} &= 138 \text{ MPa } (20.0 \text{ ksi}) \\ V_f &= 0.6 \end{aligned}$$

Note: Ply thickness, 0.13 mm (0.0052 in.)

Figure 1.7 : Layer properties

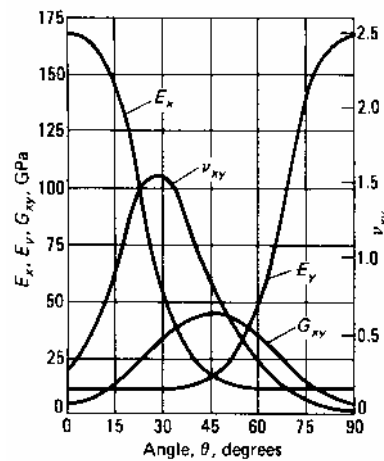


Figure 1.8 : Effective elastic properties for high-modulus graphite-epoxy system  $[\pm \theta]_s$

An interesting effect is seen in the variation of Poisson's ratio. The peak value in this example is greater than 1.5. In an orthotropic material, the isotropic restrictions do not hold and a Poisson's ratio greater than one is valid and realistic.

## **1.2 Mechanical behavior of structural elements**

The structural elements of interest are members with an I-, T- or box section. The elements are straight and long, with a small wall thickness compared with the overall cross-sectional dimension of the element. These components are often the primary load-carrying members in many constructions. Therefore, the knowledge of their stiffness properties is crucial. Stiffness properties depend on the material system and the geometry of the cross-section. In first instance, structural elements made of homogeneous isotropic material are discussed. This knowledge can be used in the design of fiber-reinforced plastic (FRP) structural members and is discussed next. Finally, an overview is given of more advanced theories to calculate the stiffness properties of FRP structures.

### **1.2.1 Structural elements of homogeneous isotropic material**

The discussion of the behavior of a structural member under any load, starts with the definition of the shear center. The shear center  $Q$  of any section is that point in the plane of the section through which a transverse load, applied at that section, must act if bending deflection only is to be produced, with no twist of the section. For any section having two or more axes of symmetry (rectangle, I-beam, etc) and for any section having a point of symmetry (equilateral triangle, Z-bar, etc),  $Q$  is at the centroid. For any section having only one axis of symmetry,  $Q$  is on that axis but in general not at the centroid. For such sections and for unsymmetrical sections in general, consult reference (Ref. 2).

In describing the mechanical behavior of structural elements, it is necessary to introduce some coordinate systems. Often reference is made to a global orthogonal rectangular coordinate system  $xyz$ . The origin of this system is placed in the centroid  $G$  of the section at hand. The  $x$ -axis is directed along the span direction of the beam; the  $y$ - and  $z$ -axis are the principal central axes of the section. Sometimes an additional coordinate system  $xns$  is introduced. The  $x$ -axis is still in the span direction of the beam. The  $s$ -axis is directed along the midline of the thickness of the section. The  $n$ -axis is perpendicular to the  $x$ - and  $s$ -axis.

#### ***Bending behavior***

The theory of bending is built on the next assumption (Euler-Bernoulli):

Plane cross sections of the beam perpendicular to its neutral line remain plane and perpendicular to the neutral line after deformation. Successive cross sections will only turn around their neutral line.

This will result in a linear longitudinal strain distribution through the height of the member. As an example consider figure 1.9. The structure is loaded by a transverse load  $V_y$  through the shear center  $Q$ . Therefore the structure will only bend around  $Gz$ . The figure also shows the longitudinal strain distribution  $\varepsilon_x$  through the height of the beam. The strain  $\varepsilon_x$  is almost uniform through the thickness of the flanges and is uniform through the thickness in the web.

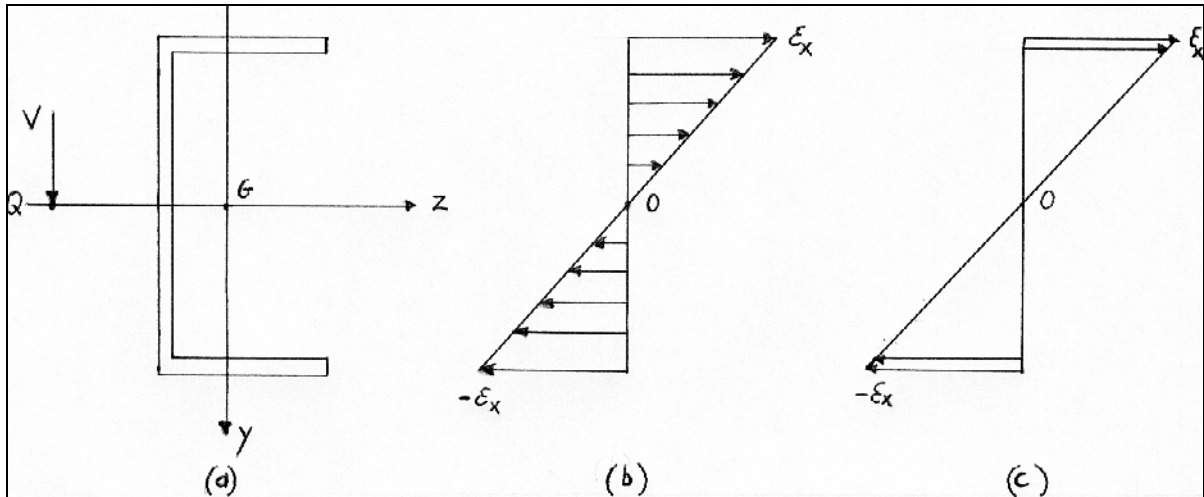


Figure 1.9 : (a) display cross-section; (b) longitudinal strain in web;  
(c) longitudinal strain in flanges

For an isotropic material, the linear strain distribution will cause a linear stress distribution through the height of the beam, namely  $\sigma_x = \frac{M_z y}{I_z}$ . The bending stiffness is defined as  $E I_z$ , with E the modulus of elasticity and  $I_z$  the moment of inertia of the section with respect to the z-axis.

The transverse force  $V_y$  will, in addition to normal stresses  $\sigma_x$ , also induce shear stresses. Consider the figure 1.10.

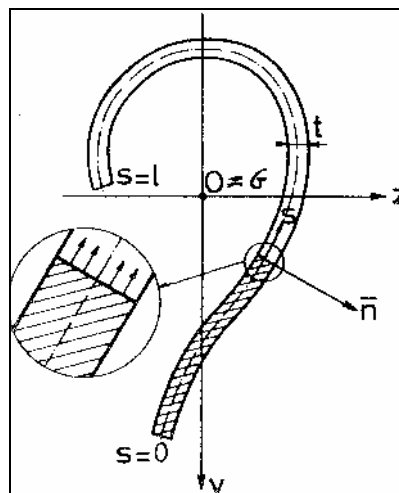


Figure 1.10 : Coordinate systems used in describing shear stress

The surface of the beam is stress free. Therefore it is assumed that  $\sigma_{xn}$  is zero. In addition, it is assumed that  $\sigma_{xs}$  is only function of the coordinate s or:  $\sigma_{xs}$  is constant through the wall thickness. By writing the equilibrium conditions of an isolated part of the beam, one obtains a formula for the shear stresses, namely  $\sigma_{xs} = \frac{V_y S_z(s)}{I_z t(s)}$ . With  $S_z(s)$  the static moment of the area from the spot of the stress  $\sigma_{xs}$  to the top with respect to z-axis.

The next figure shows the distribution of the shear stress due to a transverse force  $V_y$  through the shear center  $Q$ .

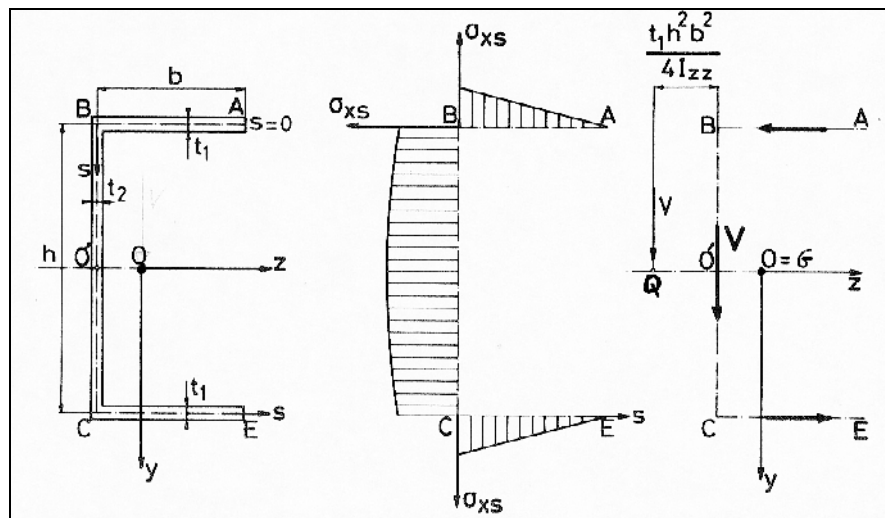


Figure 1.11 : Shear stress due to transverse force  $V_y$

Since the shear stress  $\sigma_{xs}$  and the resulting shear strain  $\epsilon_{xs}$  is never constant, a plane section can never remain plain after deformation. This is illustrated in figure 1.12.

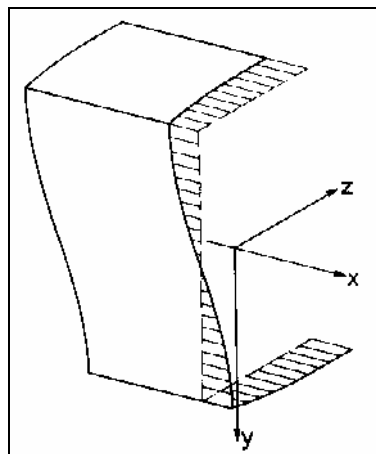


Figure 1.12 : Deformation due to transverse force  $V_y$

This is in contradiction with the Euler-Bernoulli hypothesis. In practice the problem is solved by retaining the assumption that a plane section originally normal to the neutral axis remains plane, but this section does not remain normal to the neutral axis. Usually the shear deflection is negligible in comparison with the deflection caused by bending.

### Torsional behavior

The torsional behavior of thin walled structural members is classically divided in two separate chapters: open thin walled sections and thin walled hollow or closed sections. This is because their behavior is quite different under torsion.

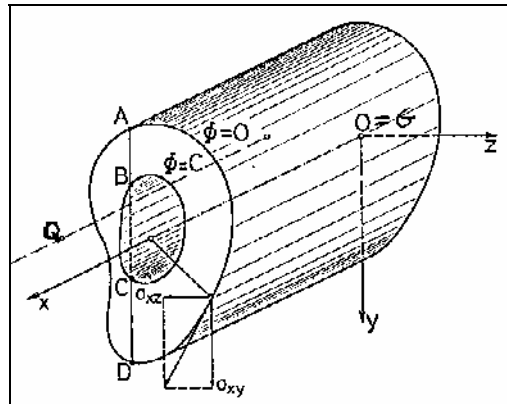


Figure 1.13 : Torsion of an arbitrary cylinder

The essential assumption in the theory of torsion concerning the deformation pattern is:

A plane cross section turns around an axis through the shear center  $Q$ , parallel to the longitudinal  $x$  axis, over an angle  $\alpha = \alpha' x$ . The torsional stiffness is defined as

$GJ = \frac{M_x}{\alpha'}$ , with  $G$  the shear modulus,  $J$  the torsional stiffness factor,  $M_x$  the torque and  $\alpha'$  a constant.

For noncircular bars, the cross sections do not remain plane but warp. All cross sections warp in the same manner.

This assumption together with equilibrium aspects, leads to a partial differential equation for the stress function  $\Phi(y, z)$ :

$$\frac{\partial^2 \Phi(y, z)}{\partial z^2} + \frac{\partial^2 \Phi(y, z)}{\partial y^2} = -2G\alpha'$$

$$\sigma_{xy} = \frac{\partial \Phi(y, z)}{\partial z} \quad ; \quad \sigma_{xz} = \frac{\partial \Phi(y, z)}{\partial y}$$

If for a given cross section a function  $\Phi(y, z)$  can be found which satisfies the differential equation and which also satisfies the boundary condition  $\Phi(y, z) = \text{constant}$  along the periphery, then the stresses derived from that function  $\Phi(y, z)$  are the true solution to the torsion problem. Prandtl (1903) observed that the differential equation for the stress function  $\Phi(y, z)$  is the same as the differential equation for the shape of a stretched membrane, originally flat, which is then blown up by air pressure from the bottom. This remark gives an extremely simple and clear manner of visualizing the shape of the function  $\Phi(y, z)$  and the stress distribution.

Consider open thin walled sections. I Shapes, T shapes , slit tubes and in general sections that can be built up of rectangles, all belong to this category. Figure 1.14 shows the stress function  $\Phi(n, s)$  for an open thin walled section loaded in torsion.

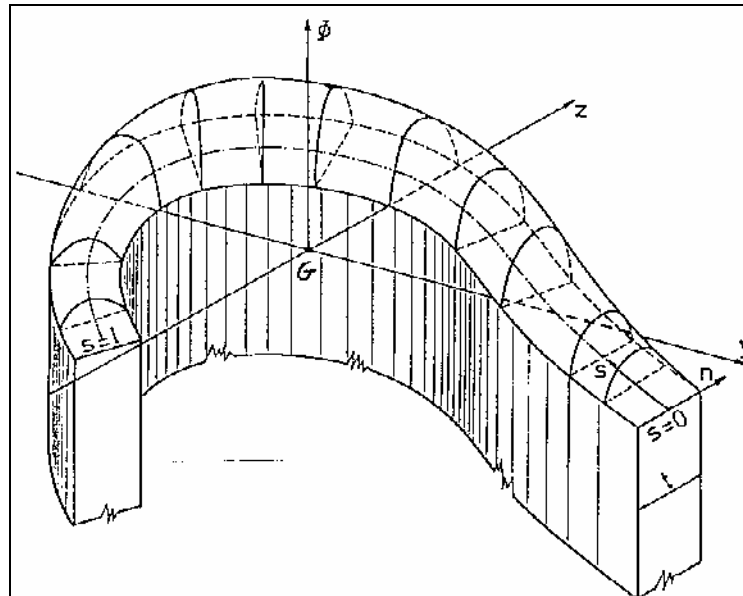


Figure 1.14 : Stress function  $\Phi(n, s)$  for an open thin walled section

The membrane has zero slope in the direction of the s-axis and the slope along the n-axis goes from negative over zero (at the top) to positive. The stresses become:

$$\sigma_{sn} = \frac{\partial \Phi(n, s)}{\partial s} = 0 \quad \sigma_{xs} = -\frac{\partial \Phi(n, s)}{\partial n} = 2G\alpha' n$$

The shear stress  $\sigma_{xs}$  is linear distributed through the wall thickness and the torsional stiffness factor is equal to  $J = \frac{1}{3} \int_0^l t^3 ds$ . Those important quantities are indicated for an I-profile in the figure below.

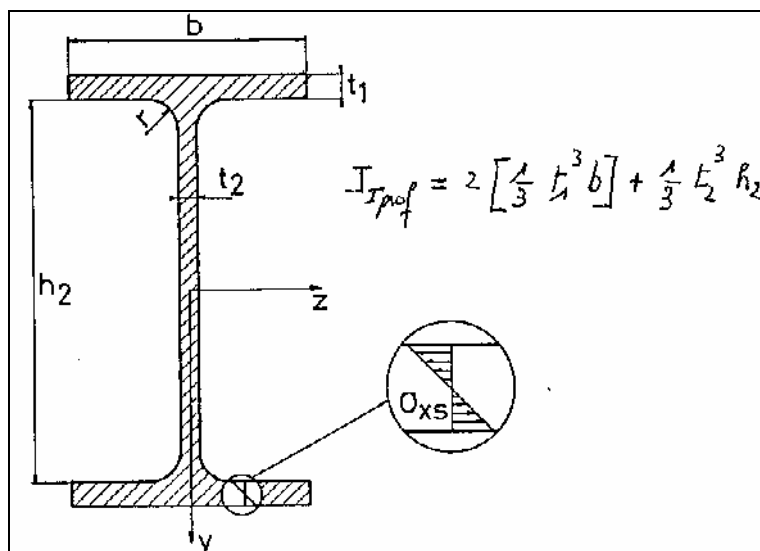


Figure 1.15 : Shear stress and torsional constant J for an I-profile

Consider thin walled closed sections. Thin walled closed tubes, circular, elliptic or square and even entire airplane wings or fuselages, all belong to this category. Figure 1.16 shows the stress function  $\Phi(n, s)$  for an thin walled closed section loaded in torsion.

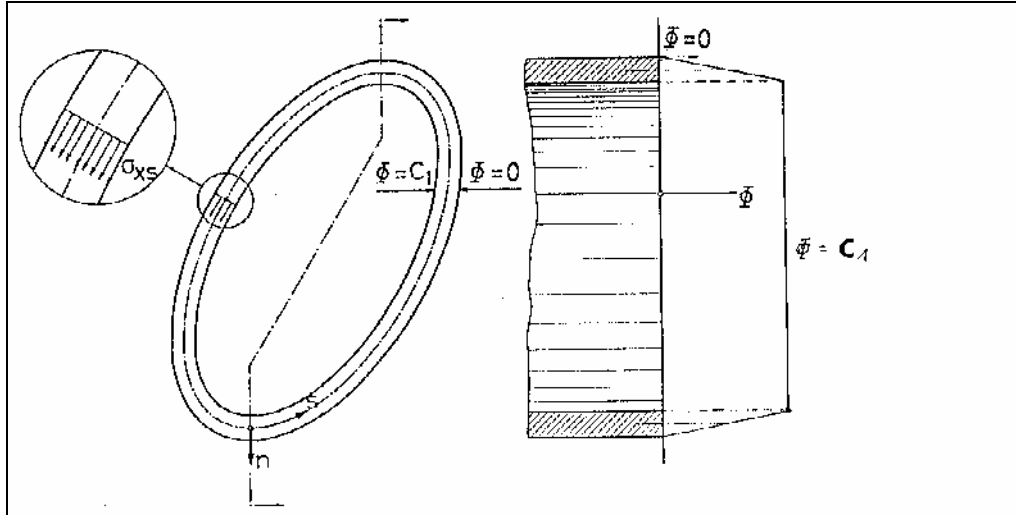


Figure 1.16 : Stress function  $\Phi(n, s)$  for a closed thin walled section

The membrane has zero slope in the direction of the s-axis and the slope along the n-axis is more or less constant. The stresses become:

$$\sigma_{sn} = \frac{\partial \Phi(n, s)}{\partial s} = 0 \quad \sigma_{xs} = -\frac{\partial \Phi(n, s)}{\partial n} = \frac{M_x}{2At}$$

The shear stress  $\sigma_{xs}$  is constant through the wall thickness and for sections with a constant wall thickness  $t$  the shear stress is the same all around. In the above formula  $A$  is the area of the entire area enclosed by the section and not the cross-sectional area of the material. The torsional

stiffness factor is equal to  $J = \frac{4(A)^2}{\oint \frac{ds}{t}}$ . Those important quantities are indicated for a circular

section in the figure below.

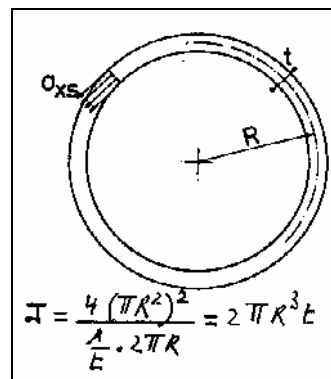


Figure 1.17 : Shear stress and torsional constant J for a circular section

It was pointed out that when noncircular bars are twisted, the sections do not remain plane but warp. The formulas presented so far, are based on the assumption that this warping is not prevented. If one or both ends of a bar are so fixed that warping is prevented, the stresses and the angle of twist produced by the given torque are affected. In compact sections the effect is slight, but in the case of open thin walled sections the effect may be considerable.

To visualize the additional support created by warping restraint, consider an I-beam with one end fixed. By applying a torque load, the built-in flanges of the I-beam act as cantilever beams. The shear forces developed in the flanges as a result of the bending of these cantilevers will assist the torsional shear stresses in carrying the applied torque and greatly increase the stiffness of the bar. Hence, the formulas for the torsional stiffness previously presented are modified by a warping stiffness factor (Ref. 2).

### *Principle of superposition*

With certain exceptions, the effect (stress, strain, or deflection) produced on an elastic system by any final state of loading is the same whether the forces that constitute that loading are applied simultaneously or in any given sequence and is the result of the effects that the several forces would produce if each acted singly.

The principle of superposition is used in the general case of a beam of any section loaded by a transverse load  $V$  in any plane. The solution comprises the following steps:

- (1) The load  $V$  is resolved into an equal and parallel force  $V'$  passing through the flexural center  $Q$  of the section, and a twisting couple  $T$  equal to the moment of  $V$  about  $Q$ .
- (2)  $V'$  is resolved at  $Q$  into rectangular components  $V'_y$  and  $V'_z$ , each parallel to a principal central axis of the section.
- (3) The flexural stresses and deflections due to  $V'_y$  and  $V'_z$  are calculated independently and superimposed to find the effect of  $V'$ .
- (4) The stresses due to  $T$  are computed independently and superimposed on the stresses due to  $V'$ , giving the stresses due to the actual loading.

If there are several loads, the effect of each is calculated separately and these effects added. For a distributed load the same procedure is followed as for a concentrated load.

## 1.2.2 Structural elements of composite material

Most engineers have considerable training and experience in the design of structural components using isotropic materials. Laminate inplane moduli  $\bar{E}_x$ ,  $\bar{E}_y$ ,  $\bar{G}_{xy}$  and  $\bar{\nu}_{xy}$  can be used to take advantage of this knowledge for the design of composite structures. However, these moduli are independent of the stacking sequence of the layers through the thickness of the laminate. Consequently, the inplane moduli are only valid when the strain distribution is more or less uniform through the thickness of the laminate. This is further explained in the next example.

Consider two composite beams with different stacking sequence under a tip force. Assume that the deflection at the end of both beams is the same. Consequently, both beams have the same linear strain distribution. Because beam (a) has axial plies at top and bottom, it will require more force to obtain this strain distribution in comparison with beam (b). Hence, the flexural stiffness of both beams is not the same.

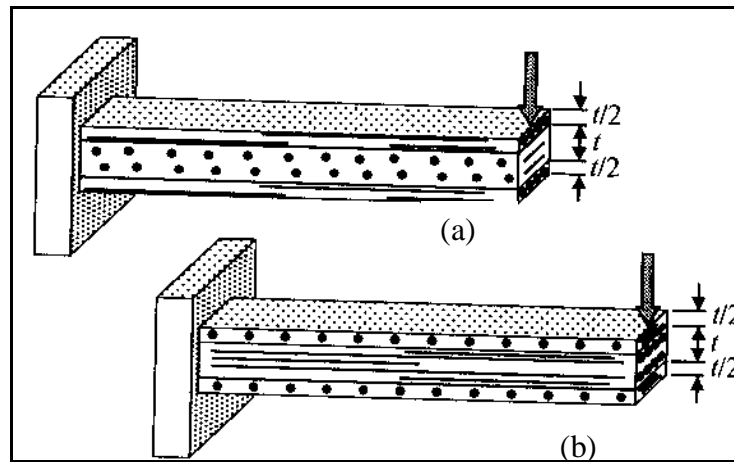


Figure 1.18 : Composite beams consisting of  
 (a) axial plies at top and bottom, middle plies transverse  
 (b) transverse plies at top and bottom, middle plies axial.

It is therefore not correct to use the laminate inplane modulus  $\bar{E}_x$  in the above situation. With this modulus both beams have the same bending stiffness, namely  $\bar{E}_x I_y$ .

In cases where the strain distribution is uniform through the thickness of the laminate, the formulas previously derived for structural elements made out of isotropic material are applicable to composite structures by using the inplane moduli instead of the isotropic properties. All load cases discussed, causes a more or less uniform strain distribution through the thickness of the thin walled structure. Torsion of a beam with an open section is an exception. Here the strain distribution is linear through the thickness and careful use of  $\bar{G}_{xy}$  is mandatory. As an example, consider a composite beam with a box section subject to a tip load P.

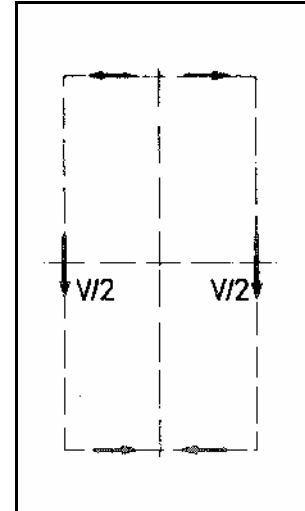
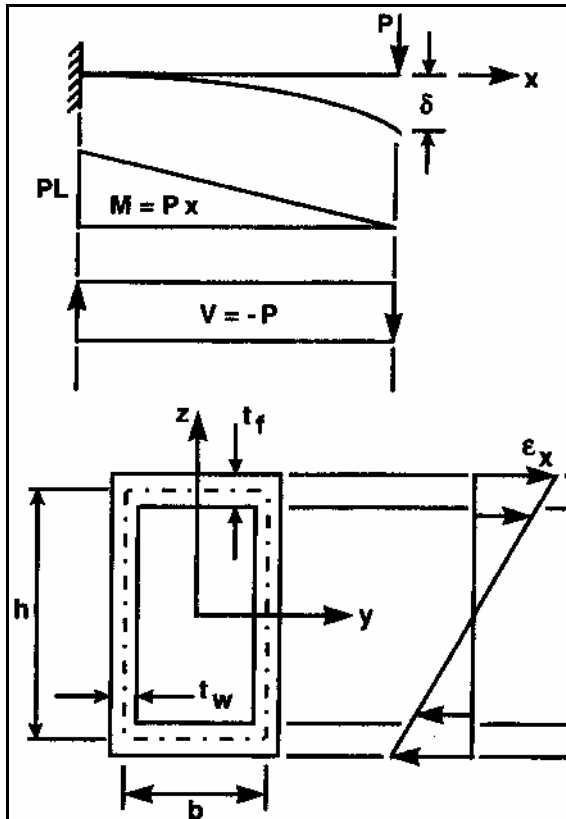


Figure 1.19 : Design of a doubly symmetric box section    Figure 1.20 : Shear flow distribution

For a double symmetric section loaded through the centroid, the strain distribution is as shown in figure 1.19 . The strain  $\epsilon_x$  is almost uniform through the thickness of the flanges and is uniform through the thickness in the web. Therefore, the laminate inplane modulus  $\bar{E}_x$  can be used to calculate the bending stiffness  $\bar{E}_x I_y$  . The transverse load  $V$  will cause inplane shear deformation. One can use the inplane shear modulus  $\bar{G}_{xy}$  in calculating the shear stiffness  $GA$ . It is assumed that the flanges do not contribute to the shear stiffness. Therefore,  $A$  can be taken as the area of the webs. If the box section is loaded in torsion, a corresponding shear flow will result. Also in this case, it is valid to use the inplane shear modulus  $\bar{G}_{xy}$  to calculate the torsion stiffness  $GJ$ , with  $J$  the torsional stiffness factor of the section.

### 1.2.3 More advanced theories

Three different methodologies have been used in the literature for the evaluation of the stiffness coefficients of composite beam elements.

First, Bert (Ref. 3) proposed beam stiffnesses for rectangular laminated beams based on an integration through the thickness of the piecewise-constant lamina longitudinal and shear moduli.

Second, stiffness coefficients for laminated beams were proposed by Vinson and Sierakowski (Ref. 4) by extending classical laminated plate theory to a simple theory for beams. They derived beam stiffness coefficients from the corresponding laminate stiffness coefficients by neglecting lateral strains and curvatures.

Third, effective moduli of laminated beams were proposed by Whitney et al. (Ref. 5) and Tsai (Ref. 6) from the reciprocals of the corresponding laminate compliances. Barbero et al. (Ref. 7) adopted this approach in order to develop a first-order shear deformation theory for thin-walled laminated beams. They modeled a thin-walled beam as an assembly of laminated panels with stiffnesses characterized by effective beam moduli.

### 1.3 Production process: pultrusion

Pultrusion is a continuous manufacturing process used to manufacture constant cross-section shapes of any length. Pultrusion is a low-cost process because it achieves direct conversion of continuous fibers and resin into a finished part. The fibers are continuously impregnated and pulled through a heated die, where they are shaped and cured.

Figure 1.21 shows the simplest pultrusion line. Here, roving and mat are dispensed from the creel and mat racks and guided through preforming guides. The preforming guides position the reinforcements in the appropriate locations in the cross section of the product, as specified by the design. The reinforcements enter dry into the injection chamber where they are wetted by resin supplied under pressure. Frequently, the injection chamber is an integral part of the die. The cross section of the die gives the final shape to the product. As the wet reinforcement travels through the die, the curing takes place aided by the heat supplied by the in-line heaters. As it cures, the composite shrinks and separates from the walls of the die, leaving the die as a finished product.

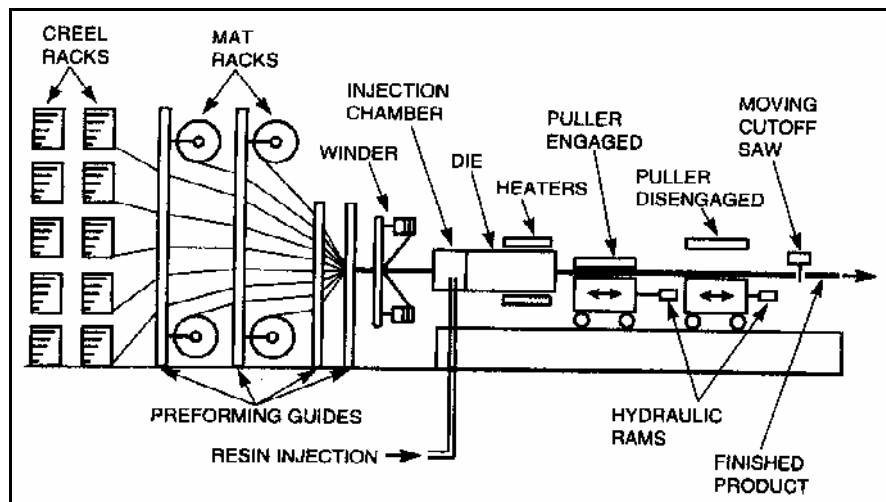


Figure 1.21 : Pultrusion line

The cured part is then pulled by reciprocating pullers, synchronized to provide a constant speed. The product is therefore continuously produced in virtually infinite length. A moving cutoff saw clamps itself to the moving product whenever a preset length of product is available, thus cutting the part without stopping the process.

Operational costs of pultrusion are low. The major cost of the process is in equipment, the chrome plated dies and the design and tune-up of the guiding system. For these reasons, pultrusion is ideally suited for high volume applications. Any type of fibers can be used, but glass dominates the market because of cost. Special formulations of various resins have been developed for pultrusion, but polyesters and vinyl esters dominate the market because of cost. The main fiber form used is roving and continuous strand mat (CSM), the latter used to provide transverse strength and to facilitate production.

Pultrusion has some constraints regarding fiber orientation and content. A minimum of roving or longitudinal fibers must be used to be able to pull the product. Fiber volume fraction can seldom exceed 45%, with 30% being a more typical value.

## **Chapter Two: Experimental Modal Analysis (EMA)**

### **2.1 Introduction**

This chapter focuses on experimental modal analysis (EMA), which is the determination of natural frequencies, mode shapes and damping ratios from experimental vibration measurements. The subject of modal testing is very broad and strongly depends on the following areas:

- The theoretical basis of vibration
- Accurate measurement of vibration
- Realistic and detailed data analysis

No attempt is made to give a comprehensive description of the subject. The interested reader is referred to the extensive literature on the subject (Ref. 8).

In the context of this work, the desired output from the modal test are the natural frequencies and corresponding mode shapes of the composite beams. This modal data will be used as the reference response data during model updating.

The fundamental idea behind modal testing is that of resonance. If a structure is excited at resonance, its response exhibits two distinct phenomena. As the driving frequency approaches the natural frequency of the structure, the magnitude at resonance rapidly approaches a sharp maximum value. The second phenomena of resonance is that the phase of the response shifts by  $180^\circ$  as the frequency sweeps through resonance. Next figure shows a typical frequency response function for a single degree of freedom system.

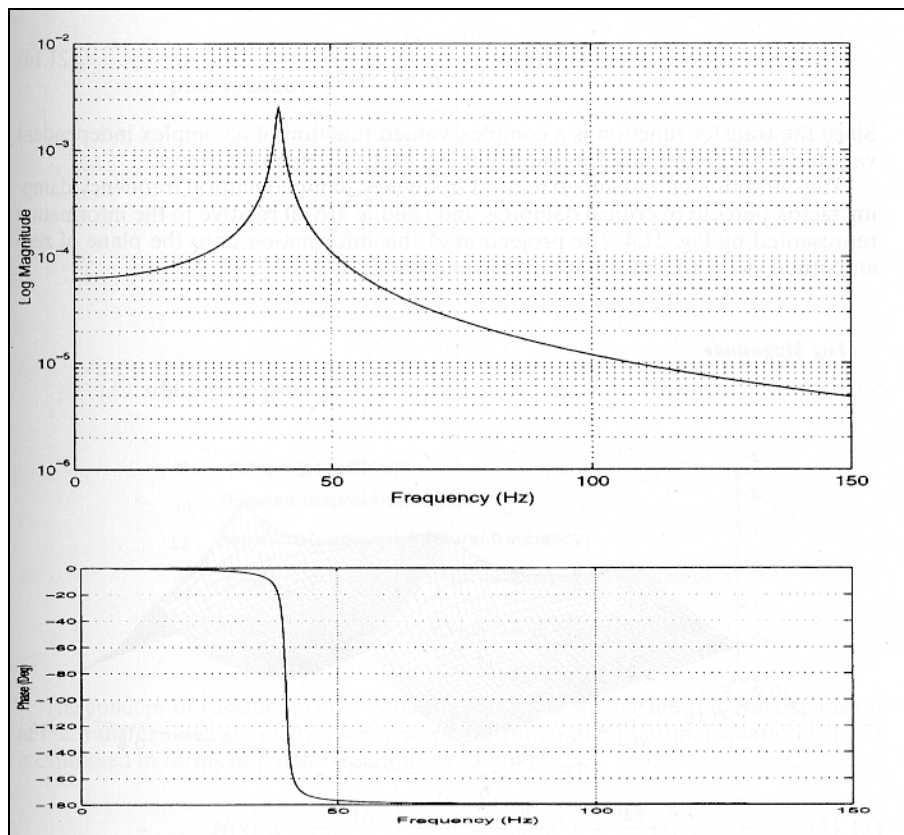


**Figure 2.1 :** Single degree of freedom frequency response function (log magnitude / phase format).

In fact, it is sufficient to measure one “good” frequency response function to obtain the natural frequencies of the structure. However, if one is interested in the corresponding mode shapes it is necessary to measure multiple frequency response functions.

## **2.2 Assumptions**

There are four basic assumptions that are made in order to perform an experimental modal analysis:

1. ***The structure is assumed to be linear***, the response of the structure to any combination of forces, simultaneously applied, is the sum of the individual responses to each of the forces acting alone. When a structure is linear, its behavior can be characterized by a controlled excitation experiment in which the forces applied to the structure have a form that is convenient for measurement and parameter estimation rather than being similar to the forces that are actually applied to the structure in its normal environment. For a wide variety of structures this is a good assumption.
2. ***The structure is time invariant***, the parameters that are to be determined are constants. In general, a system which is not time invariant has components whose mass, stiffness or damping depend on factors that are not measured or are not included in the model.
3. ***The structure obeys Maxwell’s reciprocity***, a force applied at degree-of-freedom  $p$  causes a response at degree-of-freedom  $q$  that is the same as the response at degree-of-freedom  $p$  caused by the same force applied at degree-of-freedom  $q$ . With respect to frequency response function measurements, the frequency response function between points  $p$  and  $q$  determined by exciting at  $p$  and measuring the response at  $q$  is the same frequency response function found by exciting at  $q$  and measuring the response at  $p$ .
4. ***The structure is observable***, the input-output measurements that are made contain enough information to generate an adequate behavioral model of the structure. Structures and machines which have degrees-of-freedom of motion that are not measured, are not completely observable.

## 2.3 Experimental setup

Obtaining multiple frequency response functions of the test structure at hand, generally requires several hardware components. The basic hardware consists of three major items:

An excitation mechanism

A transduction system (to measure the various parameters of interest)

An analyzer, to extract the desired information

The next figure shows a typical layout for the measurement system, detailing some of the standard items which are usually found.

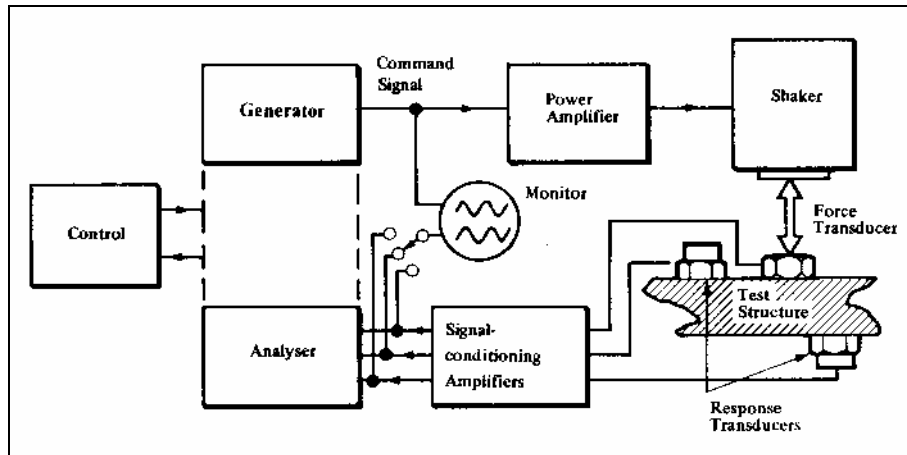


Figure 2.2 : General layout of mobility measurement system

The structure at hand is freely suspended in space. This is achieved by supporting the structure on very soft springs, such as might be provided by light elastic bands. In this configuration the suspension system has no significant influence on the natural frequencies. One added precaution which can be taken to ensure minimum interference by the suspension on the lowest bending mode is to attach the suspension as close as possible to nodal points of the mode in question.

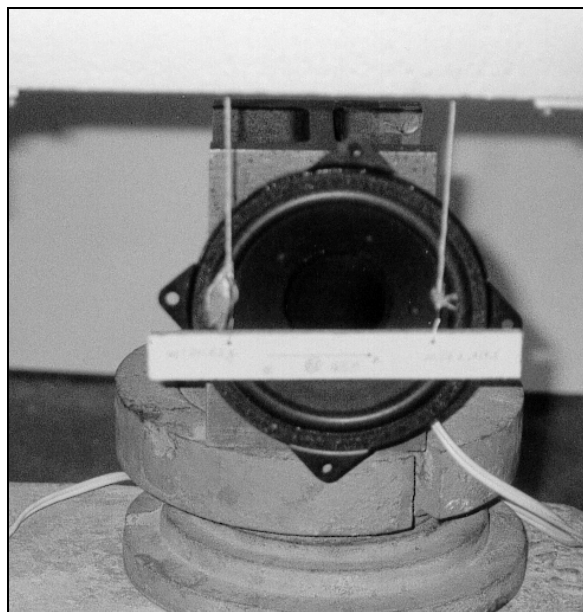


Figure 2.3 : Suspension system; Acoustical excitation

Next consider the excitation system. The physical device may take several forms, depending on the desired input and the physical properties of the test structure. The preferred device for the composite beams is the electromagnetic exciter also called shaker. A shaker can provide inputs large enough to result in easily measured responses. The shaker is attached to the structure through a stinger. A stinger consists of a short thin rod running from the driving point of the shaker to a force transducer mounted directly on the structure. The stinger serves to isolate the shaker from the structure, minimizes mass loading and causes the force to be transmitted axially along the stinger, controlling the direction of the applied force more precisely. Acoustical excitation is used for small test structures. Irrespective of the excitation method used, the structure must be excited in the frequency range of interest. This can be done with a swept sinusoidal, random or other appropriate signal.

To construct frequency response functions one has to measure both input force and resulting response. The input force is measured with a force transducer. The response in different points is measured using a laser vibrometer. More information about this device can be found on [www.polytec.com](http://www.polytec.com). Finally, the measurements are analyzed and frequency response functions are obtained.

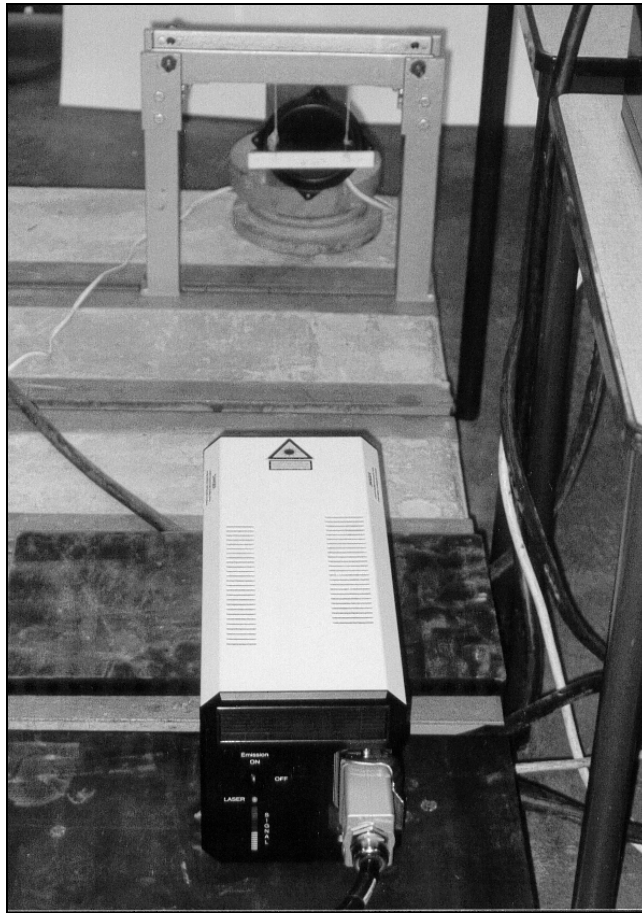


Figure 2.4 : Laser vibrometer in action

Remain to extract the modal data from the measured frequency response functions. There are several ways in which this can be accomplished (Ref. 8). In this thesis the “peak-picking” method is used to obtain the modal data. The method is applied as follows:

- (1) individual resonance peaks are detected on the frequency response function plot and the frequency of maximum response taken as the damped natural frequency  $\omega_d$  of that mode.
- (2) The damping ratio associated with each peak is assumed to be the modal damping ratio  $\xi_i$ . The modal damping ratio  $\xi_i$  is related to the frequencies corresponding to the

two points on the magnitude plot, where  $|H(\omega_a)| = |H(\omega_b)| = \frac{|H(\omega_d)|}{\sqrt{2}}$

By  $\omega_b - \omega_a = 2\xi\omega_d$ , so that  $\xi = \frac{\omega_b - \omega_a}{2\omega_d}$ .

The “peak-picking” method is illustrated in figure 2.5 .

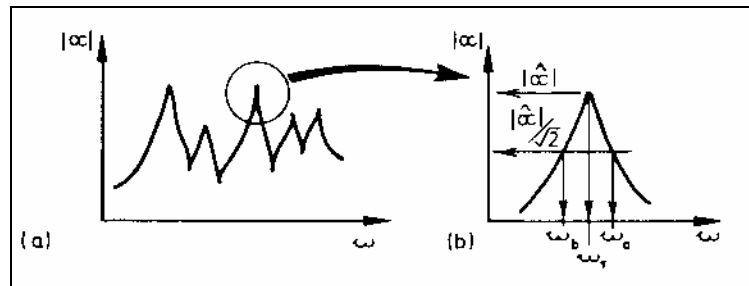


Figure 2.5 : (a) Overall FRF; (b) Resonance Detail

Experimental measurements of the FRF show that the modal damping ratio's  $\xi_i$  have a value around 2.6%. For the small damping case  $\xi < 1/\sqrt{2}$ , next equality holds  $\omega_d = \omega\sqrt{1 - 2\xi^2}$ . The error made by working with the undamped natural frequency  $\omega$  is minimal for small values of modal damping.

Finally, mode shapes can be visualized in the post processing module of the software. Mode shapes are saved as avi-files.

## Chapter Three: The virtual model

The finite element method is used to solve physical problems in engineering analysis. The figure below summarizes the process of finite element analysis. The physical problem typically involves a structural component subjected to certain loads. The idealization of the physical problem to a mathematical problem requires certain assumptions that together lead to differential equations governing the mathematical model. The finite element analysis solves this mathematical model. Since the finite element solution technique is a numerical procedure, it is necessary to assess the solution accuracy. If the accuracy criteria are not met, the numerical solution has to be repeated with refined solution parameters until a sufficient accuracy is reached.

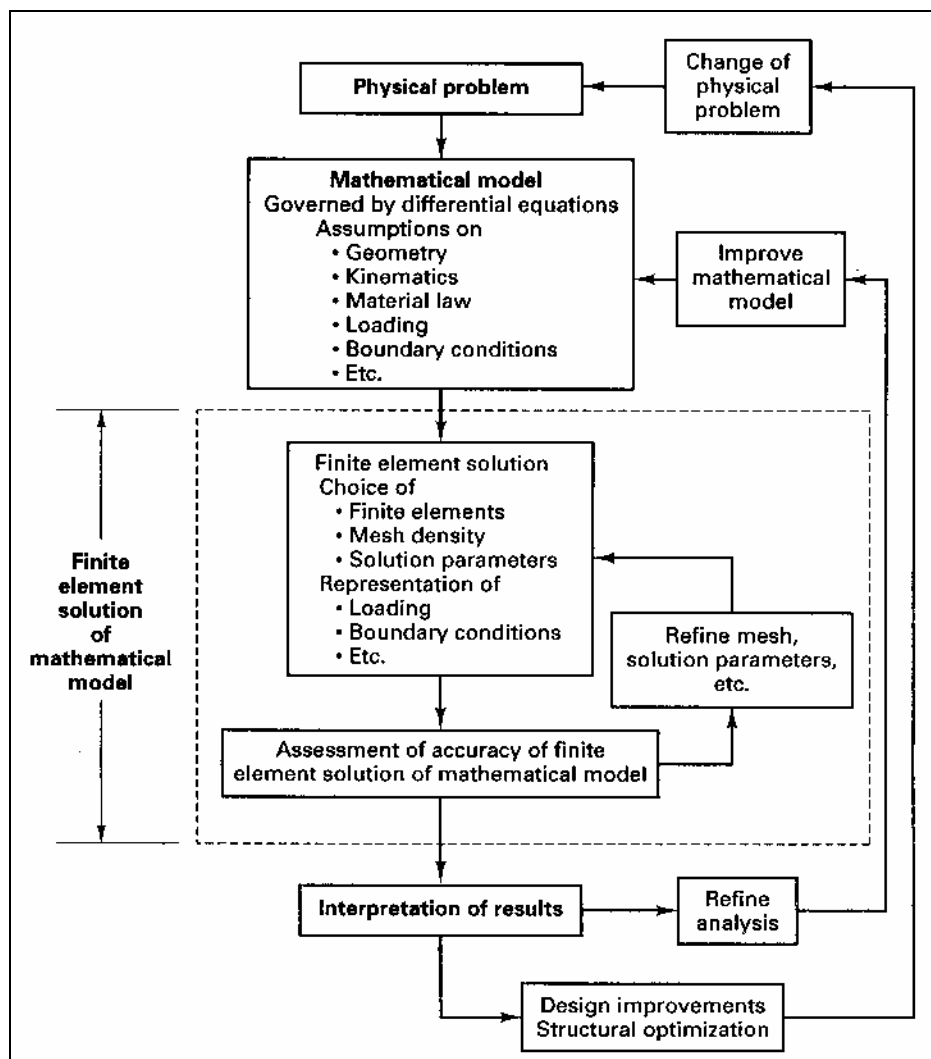


Figure 3.1 : The process of finite element analysis

## **3.1 Mathematical model**

The finite element solution will solve the selected mathematical model and all assumptions in this model will be reflected in the predicted response. One can not expect any more information in the prediction of physical phenomena than the information contained in the mathematical model. Hence the choice of an appropriate mathematical model is crucial.

In the context of material identification using modal data, the mathematical model has to reflect the properties of the composite beams in sufficient detail. The properties of interest are all mass and stiffness related. Consider the main assumptions in the mathematical model.

### **3.1.1 Main assumptions in mathematical model**

#### *Assumptions on geometry*

The structures considered all have a relatively small wall thickness in comparison with their other dimensions. Therefore, a plate or shell theory is used to model the behavior of the member. The mathematical model do not take into account geometrical details of the physical beams such as corner rounds and small holes through the thickness. The small holes are made to suspend the structure during experimental modal analysis. The thicknesses of the walls are sufficiently constant to justify constant thickness shell elements.

#### *Assumptions on kinematics*

To start the discussion, the author refers to Chapter One section: Mechanical behavior of structural elements. In this section it is illustrated that only the inplane strain components are different from zero. This is the case irrespective of the loadcase. Moreover, the inplane strain components are uniform or linear distributed through the thickness of the plate. This deformation pattern can be described by thin shell small-deflection theory. Membrane and bending effects are included and the Kirchhoff hypothesis is the main kinematic assumption. Information about the Kirchhoff hypothesis can be found in Chapter One section Classical Lamination Theory: The Kirchhoff Hypothesis.

In the small-deflection theory of thin plates the transverse deflections  $w^o$  are uncoupled from the in-plane deflections  $u^o$  and  $v^o$ . Consequently, the stiffness matrices for the in-plane and transverse deflections are also uncoupled, and they can be calculated independently. Hence, in the sequel membrane and bending effects are treated separately.

The use of thin plate theory does not exclude shear deformation of the structural element. The shear deformation of the structural element is due to inplane shear strains. Consequently, it is not necessary to include shear strains transverse to the plane as in thick plate theory.

### Assumptions on material law

The real composite material is modeled as a global homogeneous orthotropic material in the mathematical model. Material irregularities and nonuniformities are ignored in the mathematical model. An orthotropic material has two lines of symmetry. One line of symmetry is aligned with the span direction of the structural element. The other line of symmetry is perpendicular to the previous one and lies in the plane of the plate.

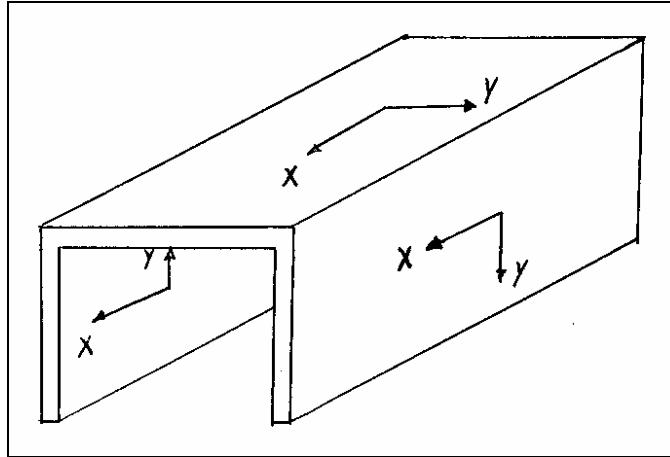


Figure 3.2 : Orthotropic lines of symmetry

In this coordinate system the transformed reduced stiffness matrix has the form;

$$\begin{Bmatrix} \sigma_x \\ \sigma_y \\ \tau_{xy} \end{Bmatrix} = \begin{bmatrix} \bar{Q}_{11} & \bar{Q}_{12} & 0 \\ \bar{Q}_{12} & \bar{Q}_{22} & 0 \\ 0 & 0 & \bar{Q}_{66} \end{bmatrix} \begin{Bmatrix} \varepsilon_x \\ \varepsilon_y \\ \gamma_{xy} \end{Bmatrix}$$

with

$$\begin{array}{ll} \bar{Q}_{11} = \frac{E_x}{1 - \nu_{xy}\nu_{yx}} & \bar{Q}_{12} = \frac{\nu_{xy}E_y}{1 - \nu_{xy}\nu_{yx}} = \frac{\nu_{yx}E_x}{1 - \nu_{xy}\nu_{yx}} \\ \bar{Q}_{22} = \frac{E_y}{1 - \nu_{xy}\nu_{yx}} & \bar{Q}_{66} = G_{xy} \end{array}$$

The  $ABD$  matrix is a result of the Kirchhoff hypothesis, the plane-stress assumption and the definition of the stress resultants. This matrix is shown for a laminate with one orthotropic layer and thickness  $H$ .

$$\begin{Bmatrix} N_x \\ N_y \\ N_{xy} \\ M_x \\ M_y \\ M_{xy} \end{Bmatrix} = \begin{bmatrix} \bar{Q}_{11}H & \bar{Q}_{12}H & 0 & 0 & 0 & 0 \\ \bar{Q}_{12}H & \bar{Q}_{22}H & 0 & 0 & 0 & 0 \\ 0 & 0 & \bar{Q}_{66}H & 0 & 0 & 0 \\ 0 & 0 & 0 & \frac{1}{12}\bar{Q}_{11}H^3 & \frac{1}{12}\bar{Q}_{12}H^3 & 0 \\ 0 & 0 & 0 & \frac{1}{12}\bar{Q}_{12}H^3 & \frac{1}{12}\bar{Q}_{22}H^3 & 0 \\ 0 & 0 & 0 & 0 & 0 & \frac{1}{12}\bar{Q}_{66}H^3 \end{bmatrix} \begin{Bmatrix} \varepsilon_x^o \\ \varepsilon_y^o \\ \gamma_{xy}^o \\ \kappa_x^o \\ \kappa_y^o \\ \kappa_{xy}^o \end{Bmatrix}$$

Composites have ten to hundred times the damping of metals, but the damping is still relatively low. Experimental measurements corroborate this statement. As discussed in Chapter Two: Experimental modal analysis, the measured modal damping ratio's  $\xi_i$  have a value around 2.6%. The damping in the system is mainly due to material damping, which is inherent in the material. As the largest damping ratio encountered in the present study is only 0.026 or 2.6%, the damped natural frequencies should be less than the undamped ones by at most 0.034%. Therefore, damping properties of the composite material is not included in the mathematical model.

### *Assumptions on loading and boundary conditions*

Natural frequencies and mode shapes depend only on mass and stiffness distribution in the structure. No loading is required to calculate this modal data. Boundary conditions have great impact on natural frequencies and mode shapes. Boundary conditions influence the stiffness of the structure. Boundary conditions are always difficult to model. However, as explained in Chapter Two, the physical structure is freely suspended in space. Consequently, free boundary conditions are defined in the mathematical model.

### 3.1.2 Formulation of the equation of motion

The principle of virtual work for bodies in motion is used to derive the governing differential equations. The principle is also known as Hamilton's principle. It can be applied to both discrete, multi-degree of freedom systems and continuous systems. The advantage of this formulation is that it uses scalar energy quantities. An additional advantage of the energy method is that it contains information concerning the boundary conditions.

Hamilton's principle has the form:

$$\int_{t1}^{t2} (\delta(T - U) + \delta W_{nc}) dt = 0$$

where  $T$  is the kinetic energy,  $U$  the strain energy and  $\delta W_{nc}$  the virtual work done by non-conservative forces. Non-conservative forces are energy dissipating forces or forces imparting energy to the system.

Remain to derive the expressions for  $T$ ,  $U$  and  $\delta W_{nc}$  of an orthotropic plate. Here the assumptions on geometry, kinematics, etc enter the picture. Membrane and plate bending effects can be treated separately because small deflections are assumed. In the sequel, all displacement components are time dependent. In considering the spatial variation of these quantities explicit mention of time dependence is omitted.

#### *membrane element energy functions*

Membrane theory only considers inplane strain components  $\varepsilon_x$ ,  $\varepsilon_y$  and  $\tau_{xy}$ . These strain components are uniform distributed through the thickness  $H$  of the plate. The loads considered are applied in directions parallel to the midplane of the plate and are uniformly distributed through the thickness. Figure 3.3 shows a membrane element.

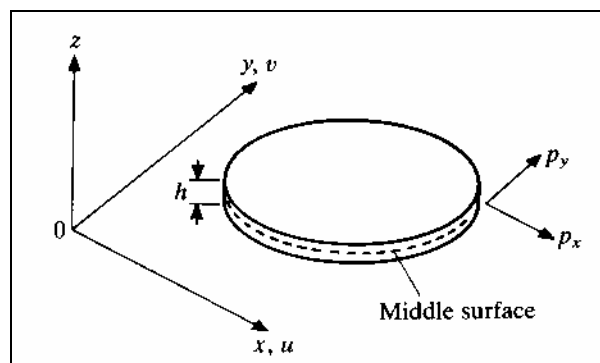


Figure 3.3 : Membrane element lying in xy-plane.

The strain energy stored in the element is given by

$$U = \frac{1}{2} \int_v (\sigma_x \varepsilon_x + \sigma_y \varepsilon_y + \tau_{xy} \gamma_{xy}) dV$$

which can be expressed in the following matrix form

$$U = \frac{1}{2} \int_v \left\{ \begin{matrix} \sigma_x & \sigma_y & \tau_{xy} \end{matrix} \right\} \left\{ \begin{matrix} \varepsilon_x \\ \varepsilon_y \\ \gamma_{xy} \end{matrix} \right\} dV$$

The constitutive equation for an orthotropic material is, as derived previously,

$$\left\{ \begin{matrix} \sigma_x \\ \sigma_y \\ \tau_{xy} \end{matrix} \right\} = \begin{bmatrix} \bar{Q}_{11} & \bar{Q}_{12} & 0 \\ \bar{Q}_{12} & \bar{Q}_{22} & 0 \\ 0 & 0 & \bar{Q}_{66} \end{bmatrix} \left\{ \begin{matrix} \varepsilon_x \\ \varepsilon_y \\ \gamma_{xy} \end{matrix} \right\}$$

and therefore,

$$U = \frac{1}{2} \int_v \left\{ \begin{matrix} \varepsilon_x & \varepsilon_y & \gamma_{xy} \end{matrix} \right\} \begin{bmatrix} \bar{Q}_{11} & \bar{Q}_{12} & 0 \\ \bar{Q}_{12} & \bar{Q}_{22} & 0 \\ 0 & 0 & \bar{Q}_{66} \end{bmatrix} \left\{ \begin{matrix} \varepsilon_x \\ \varepsilon_y \\ \gamma_{xy} \end{matrix} \right\} dV$$

In a membrane element the strains are uniform through the thickness of the plate and independent of  $z$ .

$$\left\{ \begin{matrix} \varepsilon_x \\ \varepsilon_y \\ \gamma_{xy} \end{matrix} \right\} = \begin{bmatrix} \partial u^o / \partial x \\ \partial v^o / \partial y \\ \partial u^o / \partial y + \partial v^o / \partial x \end{bmatrix}$$

Substituting the strain displacement equation in the expression of the strain energy and integrating with respect to  $z$  gives

$$U = \frac{1}{2} \int_A H \begin{bmatrix} \frac{\partial u^o}{\partial x} & \frac{\partial v^o}{\partial y} & \frac{\partial u^o}{\partial y} + \frac{\partial v^o}{\partial x} \end{bmatrix} \begin{bmatrix} \bar{Q}_{11} & \bar{Q}_{12} & 0 \\ \bar{Q}_{12} & \bar{Q}_{22} & 0 \\ 0 & 0 & \bar{Q}_{66} \end{bmatrix} \begin{bmatrix} \partial u^o / \partial x \\ \partial v^o / \partial y \\ \partial u^o / \partial y + \partial v^o / \partial x \end{bmatrix} dA$$

where  $A$  is the area of the middle surface.

The kinetic energy of the membrane element is given by

$$T = \frac{1}{2} \int_A \rho H (\dot{u}_o^2 + \dot{v}_o^2) dA$$

where  $\rho$  is the mass per unit volume of the material and the superposed dot indicates time derivative.

If  $p_x$ ,  $p_y$  are the components of the applied boundary forces per unit arc length of the boundary, then the virtual work is

$$\delta W_{nc} = \int_S (p_x \delta u^o + p_y \delta v^o) ds$$

where  $S$  denotes the boundary of the element.

### *thin plate bending element energy functions*

Thin plate bending theory only considers inplane strain components  $\varepsilon_x$ ,  $\varepsilon_y$  and  $\tau_{xy}$ . These strain components are linear distributed through the thickness  $H$  of the plate. The loads considered are applied normal to the middle surface. Figure 3.4 shows a thin plate element.

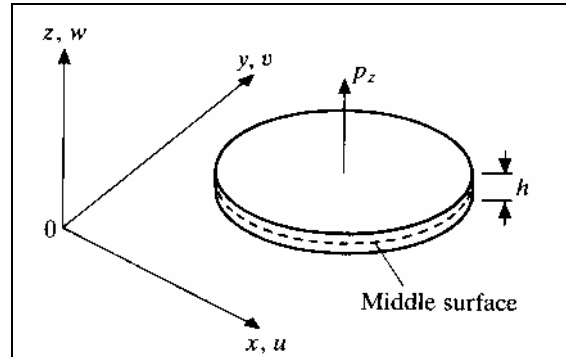


Figure 3.4 : Plate bending element

The strain energy for an orthotropic element, as previously derived:

$$U = \frac{1}{2} \int_V \left\{ \begin{matrix} \varepsilon_x & \varepsilon_y & \gamma_{xy} \end{matrix} \right\} \begin{bmatrix} \bar{Q}_{11} & \bar{Q}_{12} & 0 \\ \bar{Q}_{12} & \bar{Q}_{22} & 0 \\ 0 & 0 & \bar{Q}_{66} \end{bmatrix} \left\{ \begin{matrix} \varepsilon_x \\ \varepsilon_y \\ \gamma_{xy} \end{matrix} \right\} dV$$

In a plate bending element the strains are linear distributed through the thickness of the plate. This can be written as:

$$\begin{Bmatrix} \varepsilon_x \\ \varepsilon_y \\ \gamma_{xy} \end{Bmatrix} = -z \begin{bmatrix} \partial^2 w^o / \partial x^2 \\ \partial^2 w^o / \partial y^2 \\ 2\partial^2 w^o / \partial x \partial y \end{bmatrix}$$

Substituting the strain displacement equation in the expression of the strain energy and integrating with respect to  $z$  gives

$$U = \frac{1}{2} \int_A \frac{H^3}{12} \begin{bmatrix} \frac{\partial^2 w^o}{\partial x^2} & \frac{\partial^2 w^o}{\partial y^2} & 2\frac{\partial^2 w^o}{\partial x \partial y} \end{bmatrix} \begin{bmatrix} \bar{Q}_{11} & \bar{Q}_{12} & 0 \\ \bar{Q}_{12} & \bar{Q}_{22} & 0 \\ 0 & 0 & \bar{Q}_{66} \end{bmatrix} \begin{bmatrix} \partial^2 w^o / \partial x^2 \\ \partial^2 w^o / \partial y^2 \\ 2\partial^2 w^o / \partial x \partial y \end{bmatrix} dA$$

where  $A$  is the area of the middle surface.

The kinetic energy of the plate bending element is given by

$$T = \frac{1}{2} \int_A \rho H \dot{w}^o{}^2 dA$$

where  $\rho$  is the mass per unit volume of the material and the superposed dot indicates time derivative.

The virtual work of the transverse loading  $p_z$  becomes

$$\delta W_{nc} = \int_A p_z \delta w^o dA$$

where  $A$  denotes the area of the middle surface.

The derived energy functions are substituted into the statement of Hamilton. By doing so, one obtains the governing differential equations and the Neumann boundary conditions. The full derivation can be found in a book written by Reddy (Ref. 9). Here, the results are stated.

$$\bar{Q}_{11} H \frac{\partial^2 u^o}{\partial x^2} + \bar{Q}_{66} H \frac{\partial^2 u^o}{\partial y^2} + \{\bar{Q}_{12} H + \bar{Q}_{66} H\} \frac{\partial^2 v^o}{\partial x \partial y} = \rho H \frac{\partial^2 u^o}{\partial t^2}$$

$$\{\bar{Q}_{12} H + \bar{Q}_{66} H\} \frac{\partial^2 u^o}{\partial x \partial y} + \bar{Q}_{66} H \frac{\partial^2 v^o}{\partial x^2} + \bar{Q}_{22} H \frac{\partial^2 v^o}{\partial y^2} = \rho H \frac{\partial^2 v^o}{\partial t^2}$$

$$\frac{1}{12} \bar{Q}_{11} H^3 \frac{\partial^4 w^o}{\partial x^4} + 2 \left\{ \frac{1}{12} \bar{Q}_{12} H^3 + \frac{1}{6} \bar{Q}_{66} H^3 \right\} \frac{\partial^4 w^o}{\partial x^2 \partial y^2} + \frac{1}{12} \bar{Q}_{22} H^3 \frac{\partial^4 w^o}{\partial y^4} = p_z + \rho H \frac{\partial^2 w^o}{\partial t^2}$$

The differential equations contain second-order spatial derivatives of  $u^o(x, y, t)$  and  $v^o(x, y, t)$  and fourth-order spatial derivatives of  $w^o(x, y, t)$ . The classical laminated plate theory is an eighth-order theory. This implies that there are eight boundary conditions and that in every point of the boundary four conditions [Dirichlet and/or Neumann] must be defined. The boundary conditions are defined with respect to a  $ns$  coordinate system [Figure below].

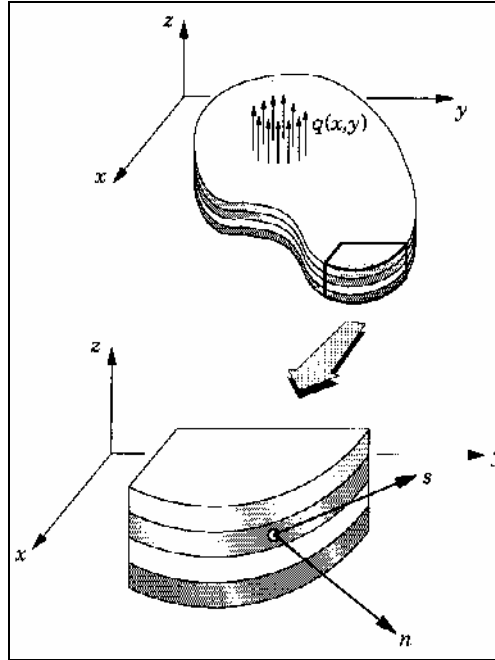


Figure 3.5 : Geometry of a laminated plate with curved boundary.

$$u_n^o, u_s^o, w^o, \frac{\partial w^o}{\partial n} \quad [\text{Dirichlet boundary conditions}]$$

$$N_n, N_{ns}, V_n, M_n \quad [\text{Neumann boundary conditions}]$$

The Neumann boundary condition  $V_n$  is known as the Kirchhoff free-edge condition.

In addition to the boundary conditions, initial conditions are required to solve the differential equations. These initial conditions are specified initial deflection and velocity profiles:

$$\begin{array}{ll} u_n^o(x, y, 0) & \dot{u}_n^o(x, y, 0) \\ u_s^o(x, y, 0) & \dot{u}_s^o(x, y, 0) \\ w^o(x, y, 0) & \dot{w}^o(x, y, 0) \end{array} \quad [\text{Defined at } t = 0]$$

### 3.1.3 Solution methods

Exact solutions of the governing differential equations can be obtained for certain boundary and loading conditions, and circular and rectangular geometries. The Navier solutions can be developed for rectangular plates when all four edges of the plates are simply supported. The Lévy solutions can be developed for rectangular plates with two opposite edges simply supported and the remaining two edges having any possible combination of boundary conditions: free, simple support or fixed support. Exact solutions can be found in books by Reddy (Ref. 9) and by Timoshenko (Ref 10).

In many practical situations either the geometrical or material properties vary, or it may be that the shape of the boundaries cannot be described in terms of known functions. In these situations it is impossible to obtain exact solutions of the governing differential equations which satisfy the boundary conditions. This difficulty is overcome by seeking approximate solutions which satisfy Hamilton's principle. There are a number of techniques available for determining approximate solutions to Hamilton's principle. One of the most widely used procedures is the Rayleigh-Ritz method. This method approximates the solution with a finite expansion of the form

$$\tilde{u}^o(x, y, t) = \sum_{j=1}^l \Phi_j(x, y)q_j(t)$$

$$\tilde{v}^o(x, y, t) = \sum_{j=l+1}^m \Phi_j(x, y)q_j(t)$$

$$\tilde{w}^o(x, y, t) = \sum_{j=m+1}^n \Phi_j(x, y)q_j(t)$$

where the  $q_j(t)$  are unknown generalized coordinates and the trial functions  $\Phi_j(x, y)$  are prescribed functions of  $x$  and  $y$ . A continuous deformable body consists of an infinity of material points, and therefore, it has infinitely many degrees of freedom. By assuming that the motion is given by the above expressions, the continuous system has been reduced to a system with a finite number of degrees of freedom. In this case a  $n$  degree of freedom system.

If the integrals in the statement of Hamilton involve derivatives up to order  $p$ , then the trial functions  $\Phi_j(x, y)$  must satisfy the following criteria in order to ensure convergence of the solution.

- (1) Be linearly independent.
- (2) Be continuous and have continuous derivatives up to order  $(p - 1)$ .
- (3) Satisfy the geometric [Dirichlet] boundary conditions. These involve derivatives up to order  $(p - 1)$ .
- (4) Form a complete series. A series of functions is complete if the 'mean square error'

vanishes in the limit, that is 
$$\lim_{n \rightarrow \infty} \int_0^L \left( u - \sum_{j=1}^n \Phi_j q_j \right)^2 dx = 0.$$

The trial solutions  $\tilde{u}^o(x, y, t)$ ,  $\tilde{v}^o(x, y, t)$  and  $\tilde{w}^o(x, y, t)$  are substituted in the expressions for the kinetic energy  $T$ , potential energy  $U$  and the virtual work done by non-conservative forces  $\delta W_{nc}$ . Afterwards, the kinetic energy  $T$  is only function of  $\dot{q}_j$  ( $j = 1, \dots, n$ ) and the strain energy  $U$  is only function of  $q_j$  ( $j = 1, \dots, n$ ), that is

$$T = T(\dot{q}_1, \dot{q}_2, \dots, \dot{q}_n)$$

$$U = U(q_1, q_2, \dots, q_n)$$

and

$$\delta T = \sum_{j=1}^n \frac{\partial T}{\partial \dot{q}_j} \delta \dot{q}_j$$

$$\delta U = \sum_{j=1}^n \frac{\partial U}{\partial q_j} \delta q_j$$

The work done by the non-conservative forces can be written in the form (Ref. 11)

$$\delta W_{nc} = \sum_{j=1}^n Q_j \delta q_j$$

where the  $Q_j$  are generalized forces.

Substituting the above expressions in Hamilton's principle gives

$$\sum_{j=1}^n \int_{t_1}^{t_2} \left( \frac{\partial T}{\partial \dot{q}_j} \delta \dot{q}_j - \frac{\partial U}{\partial q_j} \delta q_j + Q_j \delta q_j \right) dt = 0$$

Integrating the first term by parts gives

$$\begin{aligned} \int_{t_1}^{t_2} \frac{\partial T}{\partial \dot{q}_j} \delta \dot{q}_j dt &= \left[ \frac{\partial T}{\partial \dot{q}_j} \delta q_j \right]_{t_1}^{t_2} - \int_{t_1}^{t_2} \frac{d}{dt} \left( \frac{\partial T}{\partial \dot{q}_j} \right) \delta q_j dt \\ &= - \int_{t_1}^{t_2} \frac{d}{dt} \left( \frac{\partial T}{\partial \dot{q}_j} \right) \delta q_j dt \end{aligned}$$

since the  $\delta q_j = 0$  at  $t = t_1$  and  $t_2$ .

Hamilton's principle becomes

$$\sum_{j=1}^n \int_{t_1}^{t_2} \left( -\frac{d}{dt} \left( \frac{\partial T}{\partial \dot{q}_j} \right) - \frac{\partial U}{\partial q_j} + Q_j \right) \delta q_j dt = 0$$

Since the virtual displacements  $\delta q_j$  are arbitrary and independent, one arrives at the Lagrange's equations:

$$\boxed{\frac{d}{dt} \left( \frac{\partial T}{\partial \dot{q}_j} \right) + \frac{\partial U}{\partial q_j} = Q_j \quad j = 1, 2, \dots, n}$$

The procedure can be made more systematic by using matrix notation. The kinetic energy and strain energy can be written in matrix forms

$$T = \frac{1}{2} \{\dot{\mathbf{q}}\}^T [\mathbf{M}] \{\dot{\mathbf{q}}\}$$

$$U = \frac{1}{2} \{\mathbf{q}\}^T [\mathbf{K}] \{\mathbf{q}\}$$

where

$\{\mathbf{q}\}$  is the column matrix of system displacements

$\{\dot{\mathbf{q}}\}$  is the column matrix of system velocities

$[\mathbf{M}]$  is the square symmetric matrix of inertia coefficients

$[\mathbf{K}]$  is the square symmetric matrix of stiffness coefficients

The separate terms in Lagrange's equations become

$$\left\{ \frac{d}{dt} \left( \frac{\partial T}{\partial \dot{q}_j} \right) \right\} = [\mathbf{M}] \{\ddot{\mathbf{q}}\}$$

$$\left\{ \frac{\partial U}{\partial q_j} \right\} = [\mathbf{K}] \{\mathbf{q}\}$$

Lagrange's equations therefore yield the following equations of motion in matrix form

$$\boxed{[\mathbf{M}] \{\ddot{\mathbf{q}}\} + [\mathbf{K}] \{\mathbf{q}\} = \{\mathbf{Q}\}}$$

It is only necessary to obtain the energy expressions in matrix form in order to determine the matrix coefficients in the equation of motion. This algebraic equation is solved for  $\{\mathbf{q}\}$ , which are then substituted into the trial solution. As such, one obtains an approximate solution to the problem at hand.

## **3.2 The finite element solution**

### **3.2.1 The Finite Element Method as a generalization of the Rayleigh-Ritz Method**

When analyzing structures of complex shape, difficulties arise in constructing a set of trial functions  $\Phi_j(x, y)$  which satisfy the geometric boundary conditions. These difficulties can be overcome by using the Finite Element Displacement Method. The main difference between the Finite Element Method and the classical Rayleigh-Ritz Method lies in the construction of the trial functions.

- (1) The trial functions are developed for subdomains into which a given domain is divided. The subdomains, called finite elements, are geometrically simple shapes that permit a systematic construction of trial functions.
- (2) The trial functions are algebraic polynomials developed according to the principle of interpolation. To interpolate is to devise a continuous function that satisfies prescribed conditions at a finite number of points also called 'nodes'. Each trial function has a unit value at one node and becomes zero at all other nodes. Hence, the generalized coordinates represent the value of the trial solution at a node and get important physical meaning.
- (3) The trial functions are the same for each finite element. As a result, the derivation of the stiffness and mass matrices can be carried out very efficiently by first deriving element stiffness and mass matrices and then assembling them into matrices for the whole system.

In order to ensure convergence of the solution, the trial functions must satisfy the following criteria

- (1) Be linearly independent.
- (2) Be continuous and have continuous derivatives up to order  $(p - 1)$  both within the element and across element boundaries. An element which satisfies this condition is referred to as a 'conforming' element.
- (3) The polynomial functions should be complete at least to degree  $p$ . If any terms of degree greater than  $p$  are used, they need not be complete. The rate of convergence is governed by the order of completeness of the polynomial.
- (4) Satisfy the geometric boundary conditions.

In the Rayleigh-Ritz method, convergence is obtained as the number of trial functions is increased. To increase the number of trial functions in the finite element method, the number of node points and therefore the number of elements is increased.

### 3.2.2 Derivation of element matrices

#### *Linear rectangular membrane element*

The energy expressions for a membrane element are

$$T_e = \frac{1}{2} \int_{A_e} \rho H (\dot{u}_o^2 + \dot{v}_o^2) dA$$

$$U_e = \frac{1}{2} \int_{A_e} H \left[ \frac{\partial u^o}{\partial x} \quad \frac{\partial v^o}{\partial y} \quad \frac{\partial u^o}{\partial y} + \frac{\partial v^o}{\partial x} \right] \begin{bmatrix} \bar{Q}_{11} & \bar{Q}_{12} & 0 \\ \bar{Q}_{12} & \bar{Q}_{22} & 0 \\ 0 & 0 & \bar{Q}_{66} \end{bmatrix} \begin{bmatrix} \partial u^o / \partial x \\ \partial v^o / \partial y \\ \partial u^o / \partial y + \partial v^o / \partial x \end{bmatrix} dA$$

$$\delta W_e = \int_{S_e} (p_x \delta u^o + p_y \delta v^o) ds$$

The highest spatial derivative appearing in these expressions is the first. Hence, it is only necessary to take  $u^o$  and  $v^o$  as degrees of freedom at each node to ensure continuity. Also, complete polynomials of at least degree one should be used for the trial functions  $N_j(x, y)$ . The element trial solutions can be written as

$$\tilde{u}^o(x, y, t) = \sum_{j=1}^4 N_j(x, y) u_j(t)$$

$$\tilde{v}^o(x, y, t) = \sum_{j=1}^4 N_j(x, y) v_j(t)$$

Or written in matrix form

$$\begin{bmatrix} \tilde{u}^o \\ \tilde{v}^o \end{bmatrix} = \begin{bmatrix} N_1 & 0 & N_2 & 0 & N_3 & 0 & N_4 & 0 \\ 0 & N_1 & 0 & N_2 & 0 & N_3 & 0 & N_4 \end{bmatrix} \begin{bmatrix} u_1 \\ v_1 \\ u_2 \\ v_2 \\ u_3 \\ v_3 \\ u_4 \\ v_4 \end{bmatrix} \quad \text{or} \quad \begin{bmatrix} \tilde{u}^o \\ \tilde{v}^o \end{bmatrix} = [\mathbf{N}] \{\mathbf{u}\}_e$$

The expressions for the element trial solution are substituted in the membrane energy expressions, one obtains

$$T_e = \frac{1}{2} \{\dot{\mathbf{u}}\}_e^T [\mathbf{m}]_e \{\dot{\mathbf{u}}\}_e$$

$$U_e = \frac{1}{2} \{\mathbf{u}\}_e^T [\mathbf{k}]_e \{\mathbf{u}\}_e$$

where

$$[\mathbf{m}]_e = \int_{Ae} \rho H [\mathbf{N}]^T [\mathbf{N}] dA$$

$$[\mathbf{k}]_e = \int_{Ae} H [\mathbf{B}]^T \begin{bmatrix} \bar{Q}_{11} & \bar{Q}_{12} & 0 \\ \bar{Q}_{12} & \bar{Q}_{22} & 0 \\ 0 & 0 & \bar{Q}_{66} \end{bmatrix} [\mathbf{B}] dA$$

$$[\mathbf{B}] = \begin{bmatrix} \partial/\partial x & 0 \\ 0 & \partial/\partial y \\ \partial/\partial y & \partial/\partial x \end{bmatrix} [\mathbf{N}]$$

### Thin rectangular plate bending element

The energy expressions for a thin plate bending element are

$$T_e = \frac{1}{2} \int_{Ae} \rho H \dot{w}_o^2 dA$$

$$U_e = \frac{1}{2} \int_{Ae} \frac{H^3}{12} \begin{bmatrix} \frac{\partial^2 w^o}{\partial x^2} & \frac{\partial^2 w^o}{\partial y^2} & 2 \frac{\partial^2 w^o}{\partial x \partial y} \end{bmatrix} \begin{bmatrix} \bar{Q}_{11} & \bar{Q}_{12} & 0 \\ \bar{Q}_{12} & \bar{Q}_{22} & 0 \\ 0 & 0 & \bar{Q}_{66} \end{bmatrix} \begin{bmatrix} \frac{\partial^2 w^o}{\partial x^2} \\ \frac{\partial^2 w^o}{\partial y^2} \\ 2 \frac{\partial^2 w^o}{\partial x \partial y} \end{bmatrix} dA$$

$$\delta W_e = \int_{Ae} p_z \delta w^o dA$$

The highest spatial derivative appearing in these expressions is the second. Hence, for convergence, it will be necessary to ensure that  $w^o$  and its first derivatives  $\partial w^o / \partial x$  and  $\partial w^o / \partial y$  are continuous between elements. These three quantities are taken as degrees of freedom at each node. Also, complete polynomials of at least degree two should be used for the trial functions  $N_j(x, y)$ . The element trial solution can be written as

$$\begin{aligned} \tilde{w}^o(x, y, t) = & N_1(x, y)w_1(t) + N_2(x, y) \frac{\partial w_1}{\partial x}(t) + N_3(x, y) \frac{\partial w_1}{\partial y}(t) \dots \\ & + N_{10}(x, y)w_4(t) + N_{11}(x, y) \frac{\partial w_4}{\partial x}(t) + N_{12}(x, y) \frac{\partial w_4}{\partial y}(t) \end{aligned}$$

Or written in matrix form

$$\tilde{w}^o(x, y, t) = \begin{bmatrix} N_1 & N_2 & N_3 & \dots & N_{10} & N_{11} & N_{12} \end{bmatrix} \begin{bmatrix} w_1 \\ \partial w_1 / \partial x \\ \partial w_1 / \partial y \\ \vdots \\ w_4 \\ \partial w_4 / \partial x \\ \partial w_4 / \partial y \end{bmatrix} \quad \text{or} \quad \tilde{w}^o(x, y, t) = [\mathbf{N}] \{\mathbf{w}\}_e$$

The expression for the element trial solution is substituted in the plane bending energy expressions, one obtains

$$T_e = \frac{1}{2} \{\dot{\mathbf{w}}\}_e^T [\mathbf{m}]_e \{\dot{\mathbf{w}}\}_e$$

$$U_e = \frac{1}{2} \{\mathbf{w}\}_e^T [\mathbf{k}]_e \{\mathbf{w}\}_e$$

where

$$\begin{aligned}
 [\mathbf{m}]_e &= \int_{Ae} \rho H [\mathbf{N}]^T [\mathbf{N}] dA \\
 [\mathbf{k}]_e &= \int_{Ae} \frac{H^3}{12} [\mathbf{B}]^T \begin{bmatrix} \bar{Q}_{11} & \bar{Q}_{12} & 0 \\ \bar{Q}_{12} & \bar{Q}_{22} & 0 \\ 0 & 0 & \bar{Q}_{66} \end{bmatrix} [\mathbf{B}] dA \\
 [\mathbf{B}] &= \begin{bmatrix} \partial^2 / \partial x^2 \\ \partial^2 / \partial y^2 \\ 2\partial^2 / \partial x \partial y \end{bmatrix} [\mathbf{N}]
 \end{aligned}$$

### Facet shell element

In a shell, the element generally will be subject both to bending and to ‘in-plane’ force resultants. For a flat element these cause independent deformations, provided the local deformations are small. Therefore, the shell matrices can be obtained by combining the membrane and bending element matrices. Figure 3.6 illustrates a rectangular facet shell element.

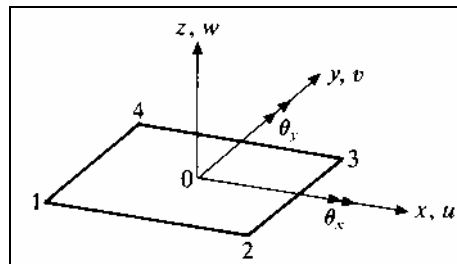


Figure 3.6 : Geometry of a rectangular facet shell element and local element xyz-coordinate system

The kinetic energy of a rectangular membrane element with four nodes is of the form

$$T_m = \frac{1}{2} \{\dot{\mathbf{u}}\}^T [\mathbf{m}]^m \{\dot{\mathbf{u}}\}$$

where the subscript  $e$  has been omitted and a superscript  $m$  has been introduced to denote membrane motion. Also

$$\{\mathbf{u}\}^T = [u_1 \quad v_1 \quad u_2 \quad v_2 \quad u_3 \quad v_3 \quad u_4 \quad v_4]$$

and

$$[\mathbf{m}]^m = \begin{bmatrix} \mathbf{m}_{11}^m & & & & & & & \text{Sym} \\ \mathbf{m}_{21}^m & \mathbf{m}_{22}^m & & & & & & \\ \mathbf{m}_{31}^m & \mathbf{m}_{32}^m & \mathbf{m}_{33}^m & & & & & \\ \mathbf{m}_{41}^m & \mathbf{m}_{42}^m & \mathbf{m}_{43}^m & \mathbf{m}_{44}^m & & & & \end{bmatrix}$$

Each submatrix  $\mathbf{m}_{ij}^m$  is of order  $(2 \times 2)$ .

The kinetic energy of a rectangular plate bending element with four nodes is of the form

$$T_b = \frac{1}{2} \{\dot{\mathbf{w}}\}^T [\mathbf{m}]^b \{\dot{\mathbf{w}}\}$$

where

$$\{\mathbf{w}\}^T = [w_1 \quad \partial w_1 / \partial x \quad \partial w_1 / \partial y \quad \dots \quad w_4 \quad \partial w_4 / \partial x \quad \partial w_4 / \partial y]$$

and

$$[\mathbf{m}]^b = \begin{bmatrix} \mathbf{m}_{11}^b & & & \text{Sym} \\ \mathbf{m}_{21}^b & \mathbf{m}_{22}^b & & \\ \mathbf{m}_{31}^b & \mathbf{m}_{32}^b & \mathbf{m}_{33}^b & \\ \mathbf{m}_{41}^b & \mathbf{m}_{42}^b & \mathbf{m}_{43}^b & \mathbf{m}_{44}^b \end{bmatrix}$$

Each submatrix  $\mathbf{m}_{ij}^b$  is of order  $(3 \times 3)$ .

Combining  $T_m$  and  $T_b$  gives the kinetic energy of the shell element  $T_s$ .

$$T_s = \frac{1}{2} \{\dot{\mathbf{u}}\}_s^T [\mathbf{m}]^s \{\dot{\mathbf{u}}\}_s$$

where

$$\{\mathbf{u}\}_s^T = \begin{bmatrix} u_1 & v_1 & w_1 & \partial w_1 / \partial x & \partial w_1 / \partial y & \dots \\ & u_4 & v_4 & \partial w_4 / \partial x & \partial w_4 / \partial y \end{bmatrix}$$

and

$$[\mathbf{m}]^s = \begin{bmatrix} \mathbf{m}_{11}^s & & & \text{Sym} \\ \mathbf{m}_{21}^s & \mathbf{m}_{22}^s & & \\ \mathbf{m}_{31}^s & \mathbf{m}_{32}^s & \mathbf{m}_{33}^s & \\ \mathbf{m}_{41}^s & \mathbf{m}_{42}^s & \mathbf{m}_{43}^s & \mathbf{m}_{44}^s \end{bmatrix}$$

Here each submatrix is of order  $(5 \times 5)$  and is of the form

$$\mathbf{m}_{ij}^s = \begin{bmatrix} \mathbf{m}_{ij}^m & \mathbf{0} \\ \mathbf{0} & \mathbf{m}_{ij}^b \end{bmatrix}$$

Similarly, the strain energy of a facet shell element is of the form

$$U_s = \frac{1}{2} \{\mathbf{u}\}_s^T [\mathbf{k}]^s \{\mathbf{u}\}_s$$

where

$$[\mathbf{k}]^s = \begin{bmatrix} \mathbf{k}_{11}^s & & & & \text{Sym} \\ \mathbf{k}_{21}^s & \mathbf{k}_{22}^s & & & \\ \mathbf{k}_{31}^s & \mathbf{k}_{32}^s & \mathbf{k}_{33}^s & & \\ \mathbf{k}_{41}^s & \mathbf{k}_{42}^s & \mathbf{k}_{43}^s & \mathbf{k}_{44}^s & \\ & & & & \end{bmatrix}$$

and

$$\mathbf{k}_{ij}^s = \begin{bmatrix} \mathbf{k}_{ij}^m & \mathbf{0} \\ \mathbf{0} & \mathbf{k}_{ij}^b \end{bmatrix}$$

The submatrices  $\mathbf{k}_{ij}^m$  and  $\mathbf{k}_{ij}^b$ , of order (2×2) and (3×3) respectively, are the appropriate submatrices of the membrane and bending stiffness matrices.

### 3.2.3 Derivation of structural matrices

The element matrices in the previous section are derived in a local element xyz-coordinate system. Figure 3.7 shows a typical element coordinate system for a shell element.

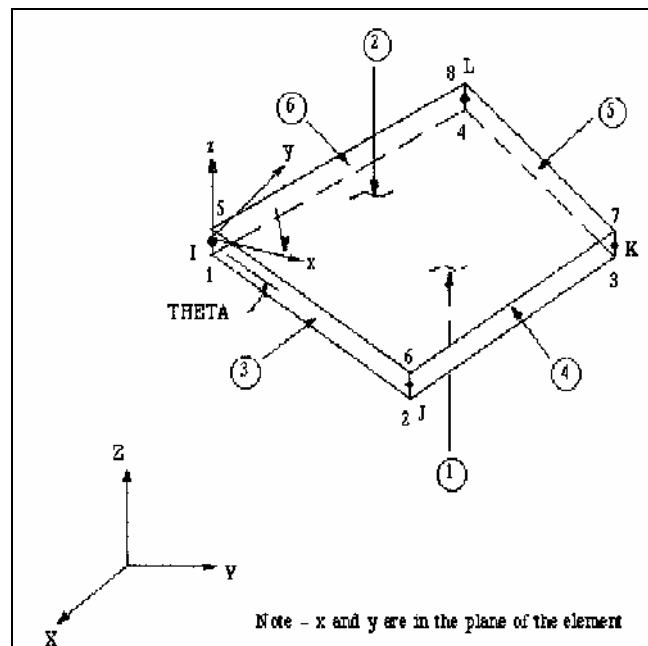


Figure 3.7 : shell element local xyz-coordinate system and global XYZ coordinate system

The element coordinate systems are right-handed, orthogonal systems as in figure. The default orientation has the x-axis aligned with element I-J side and the z-axis normal to the shell surface. The outward direction of the z-axis is determined by the right-hand rule around the element from node I to J to K. The y-axis is perpendicular to the x- and z-axis. This convention is also used in figure 3.6 .

Orthotropic material input directions are defined with respect to the local element coordinate system. When constructing a mesh of the structure, one has to make sure that all element coordinate systems are properly aligned conform the convention used in the mathematical model. That is, the local x-axis must lie in the span direction of the beam and the local y-axis is perpendicular to the x-axis and lies in the plane of the element.

In practice, an analysis is defined with respect to a global coordinate system. The element matrices are transformed into expressions involving nodal degrees of freedom relative to the common global system. These element matrices are assembled and one obtains the structural matrices. The assembly process is based on interelement continuity of primary variables and balance of secondary variables. Primary variables are displacements and slopes, secondary variables are forces and moments.

Continuity of primary variables is assured at the nodes. Interelement continuity is, however, not always assured. A point in case is the plate bending element derived previously. For this element the displacement  $w$  will vary as a cubic along any  $x$  constant or  $y$  constant line. The element boundaries or interfaces are composed of such lines. As a cubic is uniquely defined by four constants, the two end values of slopes and the two displacements at the ends will therefore define the displacements along the boundaries uniquely. As such end values are common to adjacent elements continuity of  $w$  will be imposed along any interface. The gradient of  $w$  normal to any of the boundaries also varies along it in a cubic way. As on such lines only two values of the normal slope are defined, the cubic is not specified uniquely and, in general, a discontinuity of normal slope will occur. Elements that violate the continuity of any primary unknowns across element boundaries are called ‘nonconforming’. The element, however, passes the patch tests and yields good results.

Another point in case concerns the facet shell element. Consider figure 3.8 . In this case, continuity of displacement along the common edge between two elements meeting at right angles is lost. The membrane displacement in the vertical element should be equal to the bending displacement of the horizontal element. This is not true between nodes since membrane displacements vary linearly whilst bending displacements have a cubic variation.

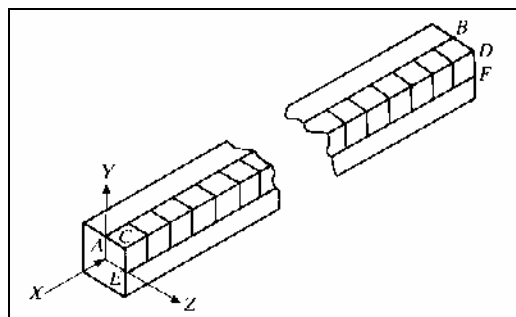


Figure 3.8 : Hollow box-beam modeled with Facet shell elements.

### 3.2.4 Solving the equation of motion for modal data

Finally, one arrives at the governing equation of motion for the discrete system. This equation takes the form

$$[\mathbf{M}]\{\ddot{\mathbf{u}}(t)\} + [\mathbf{K}]\{\mathbf{u}(t)\} = \{\mathbf{f}(t)\}$$

with

- $[\mathbf{M}]$  the structural mass matrix
- $[\mathbf{K}]$  the structural stiffness matrix
- $\{\mathbf{f}(t)\}$  the force vector in the time domain
- $\{\ddot{\mathbf{u}}(t)\}$  the acceleration vector
- $\{\dot{\mathbf{u}}(t)\}$  the velocity vector
- $\{\mathbf{u}(t)\}$  the displacement vector

The governing equation represent a system of  $n$  coupled, second-order ordinary differential equations in time. With  $n$  the number of degrees of freedom of the structure. Each equation constitutes a semidiscretization, that is, nodal degrees of freedom  $\{\mathbf{u}(t)\}$  are discrete functions of space but continuous functions of time.

To study the natural vibrations of the structure, the force vector  $\{\mathbf{f}(t)\}$  is identically zero. For a structure without damping, all points move in phase with one another and at the same frequency  $\omega$ . Hence, the solution is of the form  $\{\mathbf{u}(t)\} = \{\boldsymbol{\psi}\} \sin \omega t$ . The amplitudes  $\{\boldsymbol{\psi}\}$  are independent of time and  $\omega$  is the frequency of vibration. The solution substituted in the equation of motion gives

$$-[\mathbf{M}]\omega^2 \{\boldsymbol{\psi}\} \sin \omega t + [\mathbf{K}]\{\boldsymbol{\psi}\} \sin \omega t = \{\mathbf{0}\}$$

or

$$\boxed{\{[\mathbf{K}] - \omega^2 [\mathbf{M}]\}\{\boldsymbol{\psi}\} = \{\mathbf{0}\}}$$

What remains is a general eigenvalue problem of order  $n$ . The condition that these equations should have a non-zero solution is that the determinant of coefficients should vanish, that is

$$\det \{[\mathbf{K}] - \omega^2 [\mathbf{M}]\} = |[\mathbf{K}] - \omega^2 [\mathbf{M}]| = 0$$

This equation can be expanded to give a polynomial of degree  $n$  in  $\omega^2$ . This polynomial equation will have  $n$  roots  $\omega_1^2, \omega_2^2, \dots, \omega_n^2$  called 'eigenvalues'. The quantities  $\omega_1, \omega_2, \dots, \omega_n$  are approximate values of the first  $n$  natural frequencies of the system.

With each eigenvalue  $\omega^2$  corresponds an eigenvector  $\{\psi\}$ . These vectors are unique only in the sense that the ratio between any two components  $\psi_i$  and  $\psi_j$  is constant. The vector is rendered unique by means of a process known as normalization. Here the eigenvector is scaled with respect to the global mass matrix of the structure, that is  $\{\psi\}^T [\mathbf{M}] \{\psi\} = 1$ .

To solve an eigenvalue problem, the approach based on the characteristic determinant is not recommended when the number of degrees of freedom is three and higher. Today, a large variety of efficient numerical algorithms exists capable of solving eigenvalue problems for systems with many degrees of freedom. FEMtools uses a Lanczos subspace method to solve the eigenvalue problem. In case of free/free problems (free vibration and no boundary constraints), a minimum frequency must be specified to filter out extraction of rigid body modes.

The coefficients of the mass matrices  $[\mathbf{M}]$  can be lumped into the leading diagonal. This procedure reduces the cost of eigenvector calculation for an acceptable loss of accuracy. In this case, rotational mass inertia are not taken into account.

### 3.2.5 Sources of error

Results computed by finite element procedures contain error, except in instances where the mathematical model is so simple that finite element analysis is unnecessary. By “error” we mean disagreement between finite element results and the exact solution of the mathematical model. Possible sources of error can be grouped in the following way.

#### *Modeling error*

Modeling error refers to the difference between a physical system and its mathematical model. What is analyzed is not the actual problem, but its mathematical model, which is a simplification in which fine detail of the actual problem is omitted. Details of small holes, geometric irregularities and nonuniformity of material properties are ignored. In summary, modeling error refers to reasonable and considered approximations made deliberately rather than by mistake.

#### *Discretization error*

Discretization error is error introduced by representing the mathematical model by a finite element model. The number of degrees of freedom is infinite in the mathematical model but finite in a finite element model. The finite element solution is influenced by the number of elements used, the number of nodes per element, the nature of element shape functions and other formulation details of particular elements. Discretization error is estimated by comparing successive solutions with refined mesh density. More elements will result in a more exact solution of the mathematical model. When the difference between successive solutions is minimal, the mesh is “convergence”.

#### *Numerical error*

Numerical error is the combined result of truncation error and manipulation error. Truncation error refers to loss of information due to truncation or rounding of numbers to fit a finite computer word length. Manipulation error is introduced as equations are processed.

### *User error*

User error refers to mistakes made by the software user after the physical problem has been understood, the question to be answered by analysis have been decided and an appropriate mathematical model has been created. Included in user error are choosing the wrong general element type, choosing poor element sizes and shapes and outright blunders in data input so that the model described is not the model intended. One might also include in this category an inability to interpret computed results.

## **Chapter Four: Model Updating**

### **4.1 Principle of model updating**

To answer this question, let us have a look at what we have discussed already. Chapter Two explains the experimental procedure to determine modal properties of a structure. Modal properties depend only on mass and stiffness distribution in the structure. To obtain natural frequencies  $f_{\text{exp}}$ , it is sufficient to measure a ‘good’ frequency response. This frequency response is analyzed using the peak picking method, resulting in the natural frequencies  $f_{\text{exp}}$  of the structure. This can be done with minimal effort and cost. Measuring mode shapes  $\{\Psi\}_{\text{exp}}$  requires high-tech expensive measuring apparatus such as a laser vibrometer. Most small to midsize companies have no disposal of such high-tech measuring equipment. The method developed here must be applicable in industry. Consequently, it is assumed that only the natural frequencies  $f_{\text{exp}}$  are known.

Chapter Three outlines the major steps in developing a virtual model of the structure. Choosing an appropriate mathematical model is a first important step. The mathematical model is appropriate if it represents mass and stiffness properties of the physical beam in sufficient detail. The composite material is modeled as global homogeneous orthotropic material. All other mass and stiffness related properties of the physical structure are known and as such implemented into the mathematical model. Finally, the model is solved for modal data using finite element procedures. The output contains the analytical natural frequencies  $f_{\text{analyt}}$  with corresponding mode shapes  $\{\Psi\}_{\text{analyt}}$ .

At this moment, two sets of modal data are available. The experimental natural frequencies  $f_{\text{exp}}$  and the analytical natural frequencies  $f_{\text{analyt}}$  with corresponding mode shapes  $\{\Psi\}_{\text{analyt}}$ . However, it is highly unlikely that the analytical frequencies will have the same value as the experimental frequencies. That is because the virtual model is solved for modal data making use of some initial ‘good guessed’ orthotropic properties. The ultimate goal is to modify the orthotropic properties in such a way that the analytical frequencies correspond with the experimental frequencies. If both models have the same natural frequencies and mode shapes, they possess the same global mass and stiffness properties. The process of modifying the material properties in such a way that both sets of modal data correspond, is called model updating. The principle of model updating is summarized in Figure 4.1. This chapter gives an overview of the most important aspects concerning model updating.

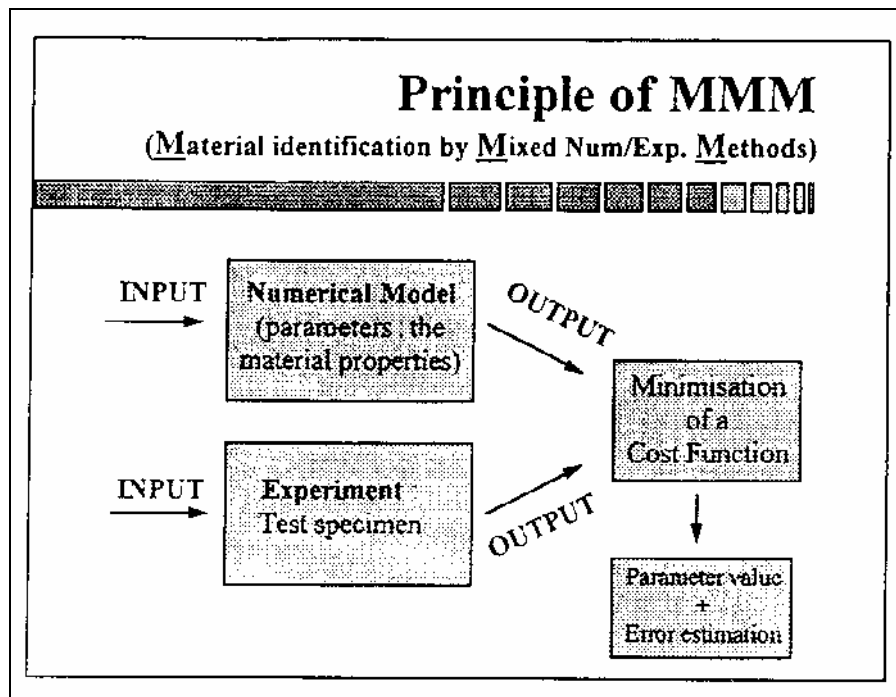


Figure 4.1 : Principle model updating

## 4.2 Mathematics of Model Updating

From a mathematical point of view, the difficulty with model updating is that the relation between output vector [natural frequencies] and the parameter vector [orthotropic material properties] is nearly always non linear. This means that updating the parameter values from an initial value to a final value has to be done iteratively. The value of the output for some new parameter values can be estimated with a Taylor expansion. The Taylor series can be cut off after the linear term or can be cut after some higher order terms. Figure 4.2 illustrates the mathematics involved in model updating.

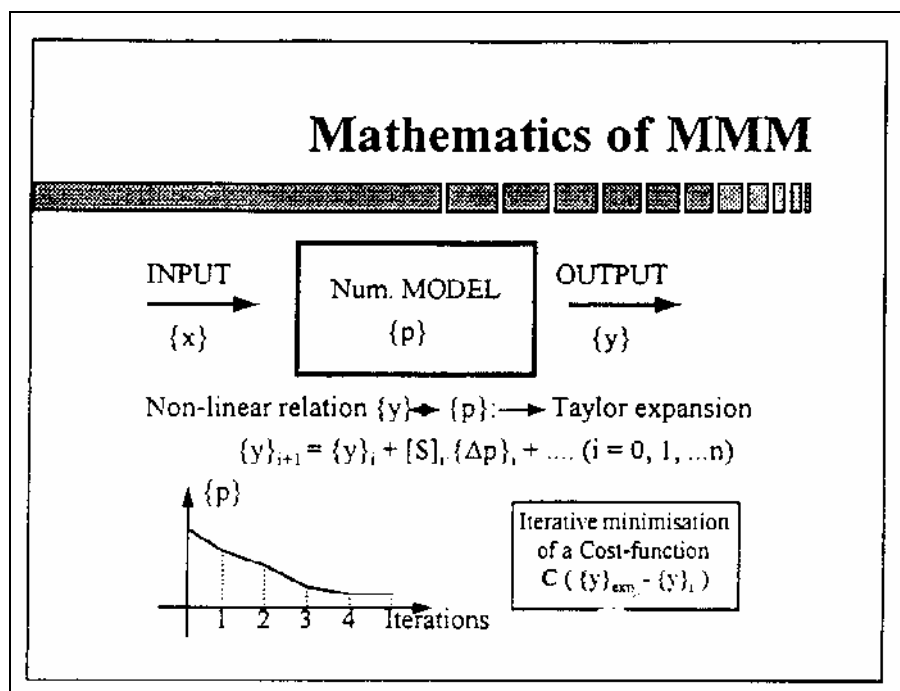


Figure 4.2 : Mathematics of model updating

The matrix  $[S]$  that appears in the linear Taylor term is called the sensitivity matrix. It contains the partial derivatives of the output components for the different parameter values. The success of model updating is highly dependant from the numerical condition of the sensitivity matrix because  $[S]$  must be inverted in every iteration step to obtain the parameter correction  $\{\Delta p\}$ .

Convergency from an initial parameter value  $\{p\}_0$  to the final value is obtained by minimization of a cost function in every iteration step. Graphically, this means that the cost function evolves iteratively from an initial point in the  $(m+1)$  dimensional parameter space towards a global minimum. The parameter values in the global minimum are the optimal parameter values. Figure 4.3 illustrates the principle.

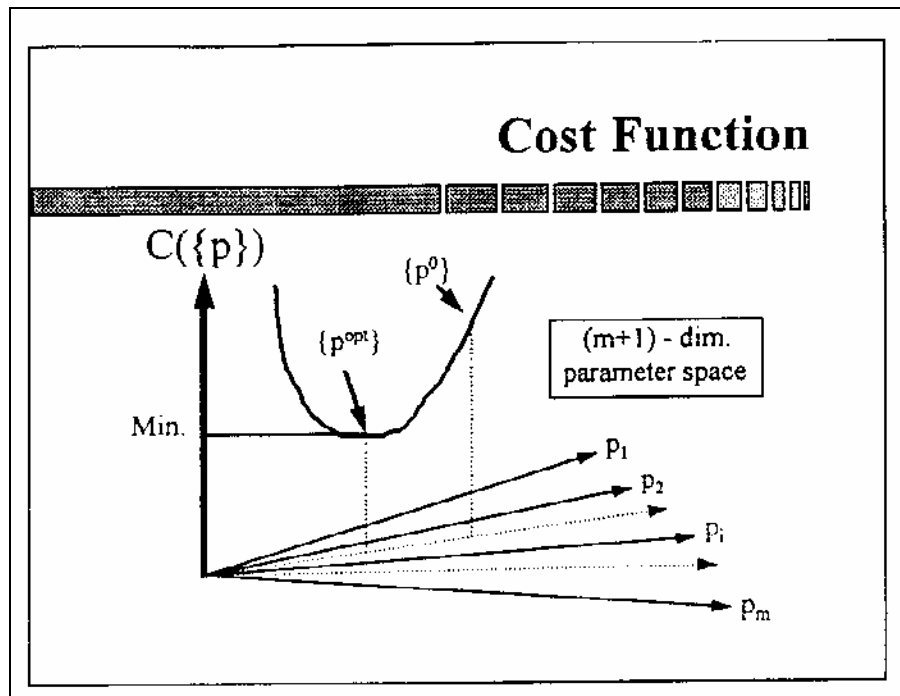


Figure 4.3 : Minimizing of cost function

One of the most simple cost functions leads to a weighted least squares estimator. In this cost function, a weighting matrix  $[W]$  is pre- and post multiplied with the difference between the measured and the computed response in a point in the parameter space. The weighting matrix  $[W]$  allows to express a different confidence in the different measured data points. This is illustrated in Figure 4.4 .

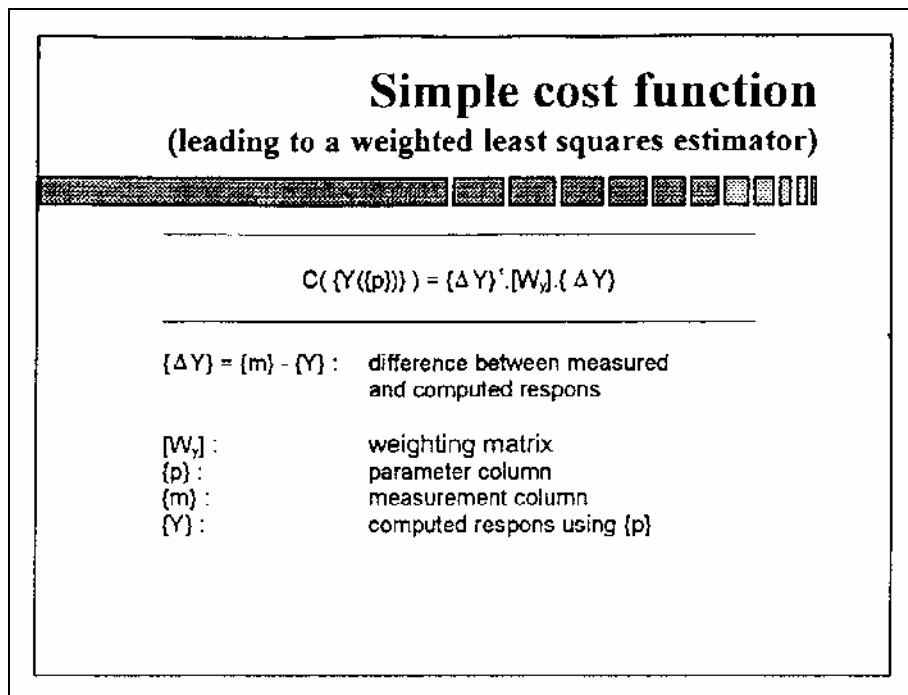


Figure 4.4 : Simple cost function

A more elaborated cost function also takes the initial parameter values into account. A second term is added to the cost function in which a weighting matrix is pre- and post multiplied with the difference between the initial and the current parameter value. Again, a weighting matrix allows to express a different confidence in the different initial parameter values.

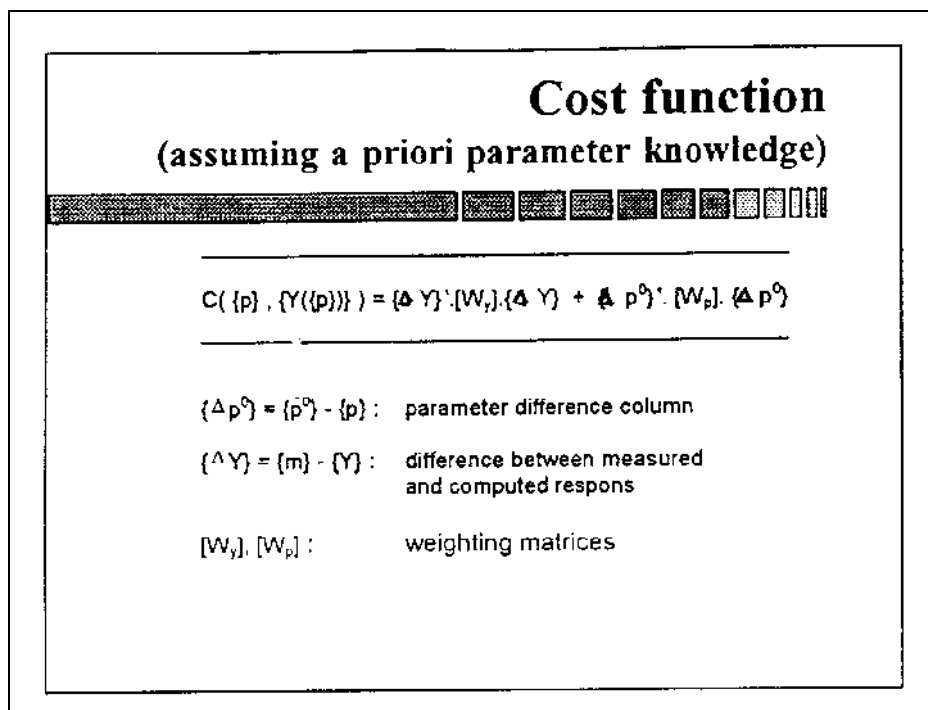


Figure 4.5 : Cost function

The matrix  $[W]_p$  represents the weighting matrix expressing the confidence in the model parameters, while  $[W]_y$  is a weighting matrix expressing the confidence in the reference response test data.

### 4.3 Successful Model Updating

The success of model updating strongly depends on the following considerations.

#### *Accuracy numerical model*

A first aspect is the quality of the mathematical model. All known mass and stiffness properties must be correctly represented in the mathematical model. Secondly, this model is solved using the finite element method. Error due to discretization of the mathematical model is introduced. The discretization error must be kept to a minimum. A coarse mesh density is not as flexible as the mathematical model with infinite degrees of freedom. Hence, the calculated natural frequencies will be overestimated. The model updating will result in physically incorrect material properties. Discretization error is estimated by comparing successive solutions with refined mesh density. More elements will result in a more exact solution of the mathematical model. When the difference between successive solutions is minimal, the mesh is “convergence”. The accuracy of the analysis is related to the mesh density.

#### *Experimental error*

Incorrect input can not result in physical correct material properties. Experimental error can be divided into two categories. Random errors and Systematic errors. The random errors can be treated with statistical procedures. Modal analysis software is capable in minimizing random errors. Systematic errors are a lot more difficult to detect and to solve. A damaged accelerometer will produce systematically an error on his output. Experimental tests on an analytical known problem can indicate a systematic error.

#### *Controllability*

A numerical model is controllable if it is possible to tune the model output from an arbitrary point  $\{y\}_0$  in the parameter space to a measured point  $\{y\}_{exp}$  with the selected parameter set. This is further explained in figure (below).

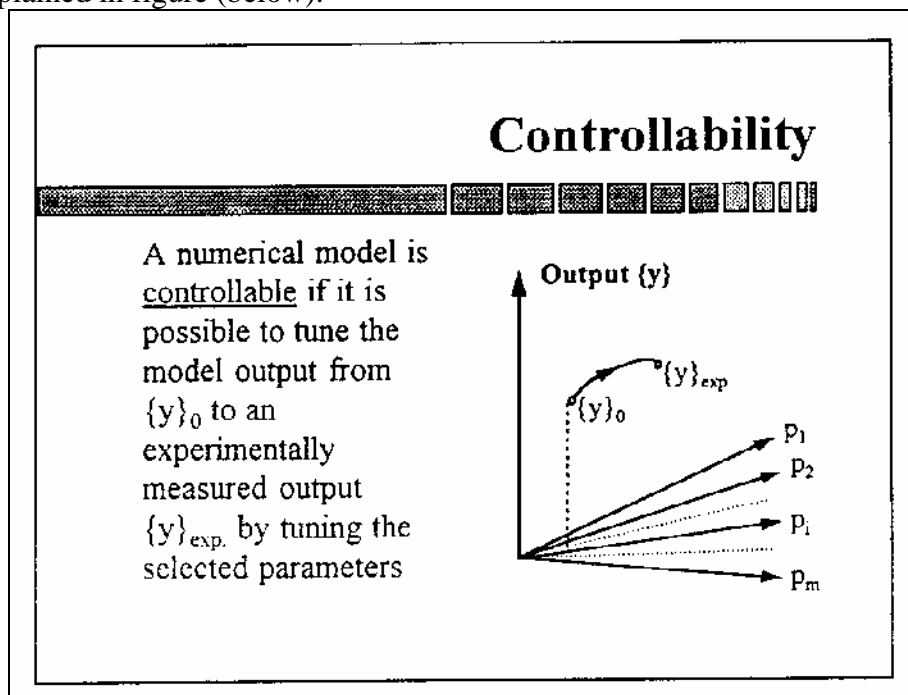


Figure 4.6 : Controllability

Non-controllability can be turned into controllability by selecting more or more appropriate parameter. A parameter is appropriate if the sensitivity with respect to the response is sufficiently high.

### *Observability*

A numerical model is observable if measurement of the output contains sufficient information for the identification of the selected parameters. A natural frequency do not contain information concerning the color of the structure. It is impossible to identify a color by measuring the natural frequency of the structure. Figure 4.7 summarize the definition of observability.

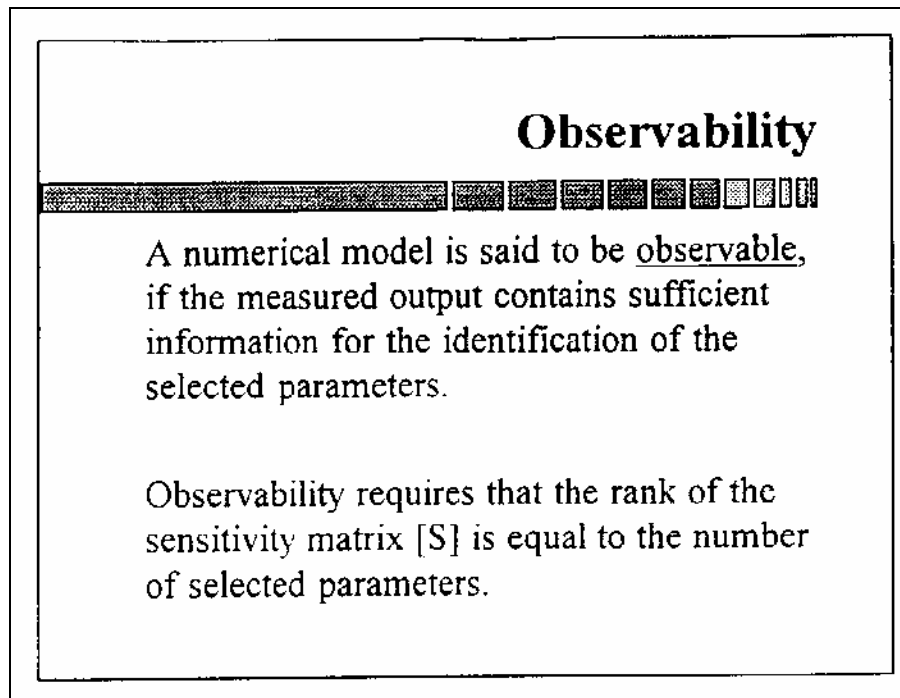


Figure 4.7 : Observability

Of course, one wants to identify all four orthotropic material properties by measuring a certain amount of frequencies. Unfortunately, depending on the structure, not every parameter will be identifiable. To investigate observability, FEMtools offers sensitivity sum curves. Such a curve sums all sensitivity values for all responses as a function of parameter number. A low sensitivity sum value shows that none of the responses contains sufficient information for the identification of that parameter. If this occurs, one can add more experimental measurements or conclude that the parameter in question can not be identified by frequency measurement.

### *Initial parameter values*

Model updating requires initial parameter values  $\{\mathbf{p}\}_0$ . The quality of the initial parameter values can effect both the speed of convergence and whether or not convergence to the 'true' parameters is achieved. The parameter estimation problem is often posed as a problem of constraint minimization and in the case of non-linearity in parameters, a particular minimum is sought on a surface which contains many minima and maxima. Usually either a local minimum is sought, when there is confidence in the initial model, or else the problem is to determine the unique global minimum.

At the Vrije Universiteit Brussel Professor Hugo Sol has developed a method which can detect orthotropic material properties of a layered plate. The Resonalyser Method makes use of experimental measured frequencies to tune a corresponding numerical model. It is in fact also a mixed numerical experimental method. More information about this test can be found in the addendum. However, the Resonalyser uses a plate of material. Only small plates could be prepared because of the minimal width of the structures. In practice, small plates are not ideal to obtain initial parameter properties.

To obtain initial values for the longitudinal moduli  $E_x$  and  $E_y$ , the first bending frequency of a beam specimen is determined. To identify  $E_x$  a beam model in the span direction of the structure is used. No limit on the length of this specimen. Identification of  $E_y$  uses a specimen in the width direction of the structure. The length of this specimen is restricted by the width of the structure. The most ideal manner to excite this kind of specimen is by means of acoustical energy. Figure 4.8 shows a beam specimen during EMA.



Figure 4.8 : EMA conducted on beam specimen to obtain initial parameter values

Knowledge of the bending frequency and dimensions of the specimen renders the elastic modulus of the material. The formula used to estimate the elasticity modulus (Ref. 12):

$$E = 7.89e-2 * (\text{frequency})^2 * (\text{length})^4 * \text{density} * \text{transverse\_section} * (\text{moment of inertia})^{-1}$$

## 4.4 Model updating using FEMtools

### *Sensitivity calculation*

The matrix  $[S]$  that appears in the linear Taylor term is called the sensitivity matrix. It contains the partial derivatives of the output components for the different parameter values. There are two basic approaches to compute sensitivities: (i) using differential sensitivities and (ii) using a finite difference approximation. Which one to use depends on the parameter type. For non-proportional parameters, such as the Young's modulus for orthotropic materials, FEMtools uses finite difference sensitivities. In this method derivatives are approximated with a forward finite difference approach. This is done using the results of two finite element analysis for two states of the parameter  $p_j$ . The element  $ij$  of the matrix  $[S]$  becomes

$$\frac{\Delta y_i}{\Delta p_j} = \frac{y_i(p_j - \Delta p_j) - y_i(p_j)}{\Delta p_j}$$

The sensitivities discussed so far are absolute sensitivities. This means that they use the units of the response and parameter value. The absolute sensitivities can be made independent of the units used for the response and parameter values. They are then referred to as normalized sensitivities. A normalized sensitivity shows the percentage change of the response value for one percent change of the parameter value. The element  $ij$  of the matrix  $[S_n]$  can be written as

$$S_{ij(n)} = \frac{\Delta y_i}{\Delta p_j} \times \frac{p_j}{y_i}$$

### *Mode shape pairing*

During model updating, the algorithm will try to drive the predicted analytical response to the experimental reference data in the test database. This implies that the algorithm knows which analytical response has to match with which experimental response. This can be defined using sequential mode shape pairing. Sequential mode pairing means that analytical mode 1 will be paired with experimental mode 1, analytical mode 2 with experimental mode 2, etc. If during model updating a switch of mode shapes occur, this method fails. The resulting frequencies will probably be close but the mode shapes are different. There is no possibility to connect a mode shape to a particular experimental reference response.

To deal with the above problem, the program will copy the analytical frequencies, predicted by the initial values for parameters  $E_x$ ,  $E_y$ ,  $G_{xy}$  and  $\nu_{xy}$ , to the test database. The user of the program knows exactly the sequence of these modes [the program will previously show them]. It is now up to the user to connect the correct experimental reference frequency with the corresponding mode shape. In other words, the **test database** must **reflect the correct physical response** [natural frequency with corresponding mode shape]. Automatic mode shape pairing can now be used to drive the analytical response to the experimental reference response in the test database.

During model updating, automatic mode shape pairing makes a relation between those frequencies which have the highest Modal Assurance Criterion (MAC). The MAC is a measure of the squared cosine of the angle between two mode shapes. To compute the MAC between an analytical and experimental mode shape, the following equation is used:

$$\text{MAC}(\Psi_{\text{analyt}}, \Psi_{\text{exp}}) = \frac{\left| \left( \{\Psi_a\}^T \{\Psi_e\} \right)^2 \right|}{\left( \{\Psi_a\}^T \{\Psi_a\} \right) \left( \{\Psi_e\}^T \{\Psi_e\} \right)}$$

After model updating, a MAC value can be calculated between the updated fem model and the physical test modal. If no mode switch occurred during model updating this MAC matrix is a diagonal matrix.

### *Aspects of convergence*

CCABSOLUTE: Average value of weighted absolute relative differences between predicted and reference resonance frequencies.

CCMEAN: Average value of weighted relative differences between predicted and reference resonance frequencies.

In model updating, the above correlation coefficients are interpreted as an objective function that needs to be minimized. With each iteration loop the values of the correlation coefficients will be verified to check if a convergence criterion is satisfied. The following criteria are used:

- (1) The value of the reference correlation coefficient is less than an imposed margin:

$$CC_t < \varepsilon_1$$

where:

$CC_t$  Reference correlation coefficient at iteration t

$\varepsilon$  Convergence margin

- (2) Two consecutive values of the reference correlation coefficient are within a given margin.

$$|CC_{t+1} - CC_t| < \varepsilon_2$$

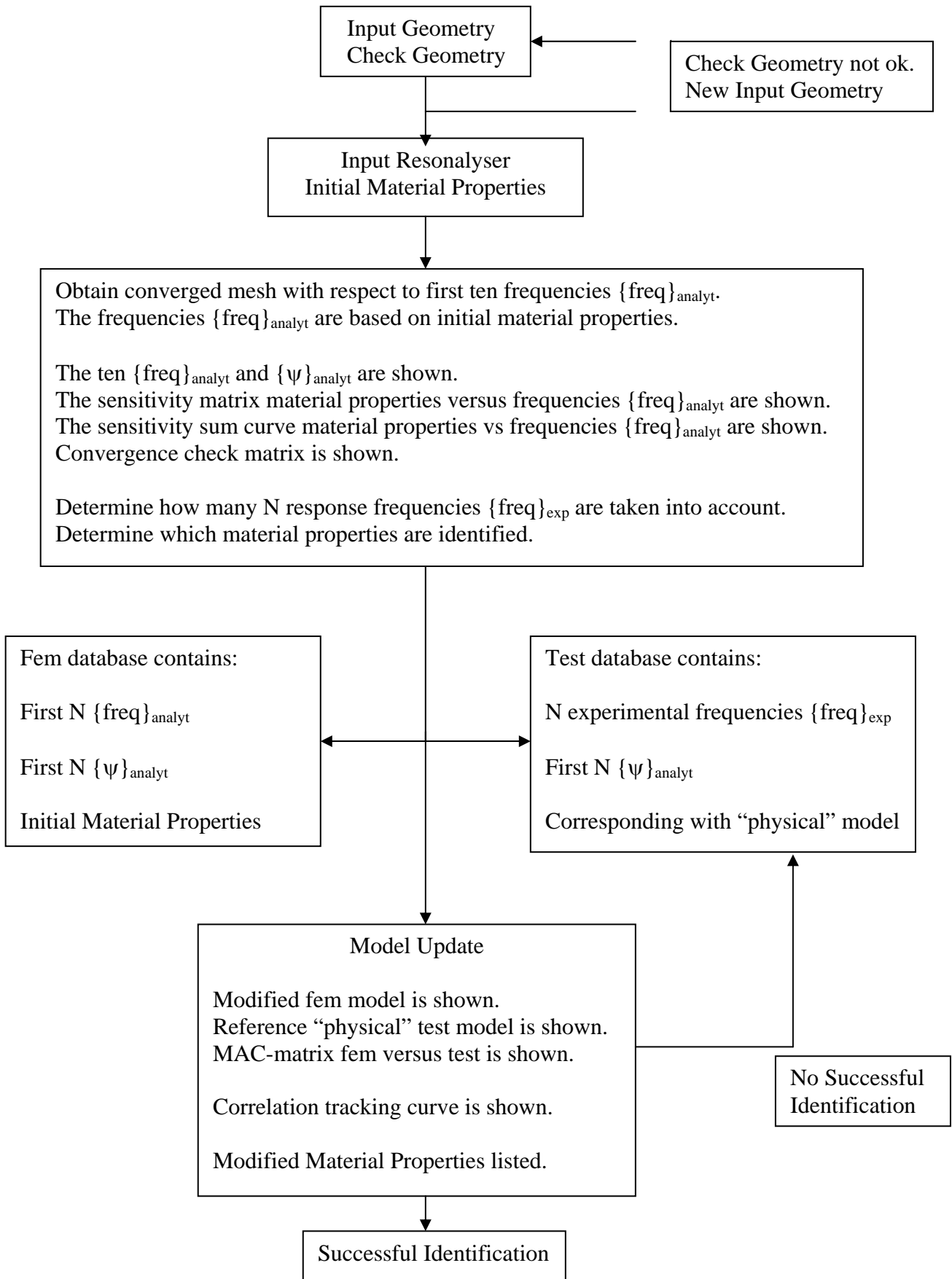
The iteration loop in model updating will be stopped as soon as one of these tests is satisfied.

Default values for  $\varepsilon_1$  and  $\varepsilon_2$  are used namely 0.08

Default values are also used for weighting coefficients and other settings

## Chapter Five: Outline program

### 5.1 Flowchart program



## 5.2 Input box “Define Geometry Beam”

This graphical user interface (GUI) is used to define the cross section and the length of the beam. Arbitrary open and multi-celled closed cross sections can be constructed. The cross section is defined by a series of rectangular segments. The segments are input such that they make a continuous outline of the cross section – the end point of one segment is the beginning point of the next segment. Segments may be given a zero thickness in order to backtrack over previously defined segments to continue the outline. The thickness in (X coord, Y coord, Thickness) is the thickness of the segment that is defined by this point and the previous point. The thickness of the first point is therefore not used.

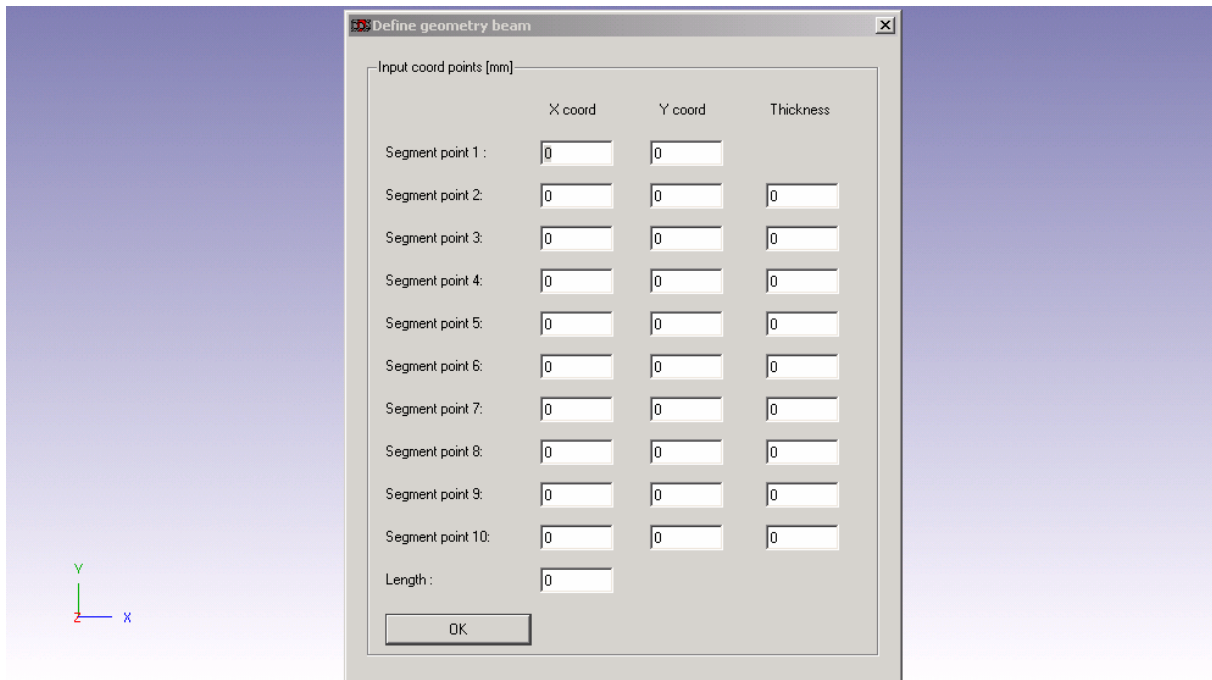


**Figure 5.1 :** GUI Define geometry beam

### Input Restrictions:

Zero thickness (backtrack) segments must follow the original geometry. They cannot enclose an area.

No backtrack possible to point (0, 0).

A straight zero thickness line must have the same number segments as the original straight line.

A single straight line cross section is permitted.

Multiple celled closed sections (such as a double box beam) are allowed.

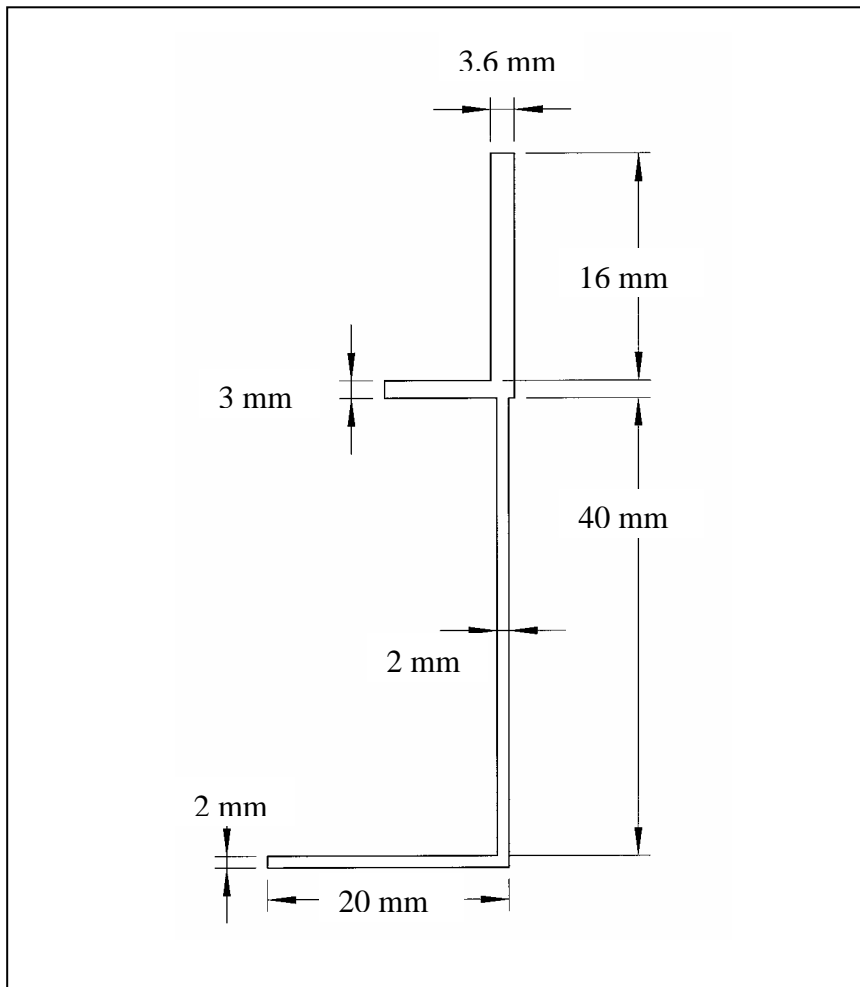
Thickness must be a positive number (including zero).

Length of the beam must be a positive number (excluding zero).

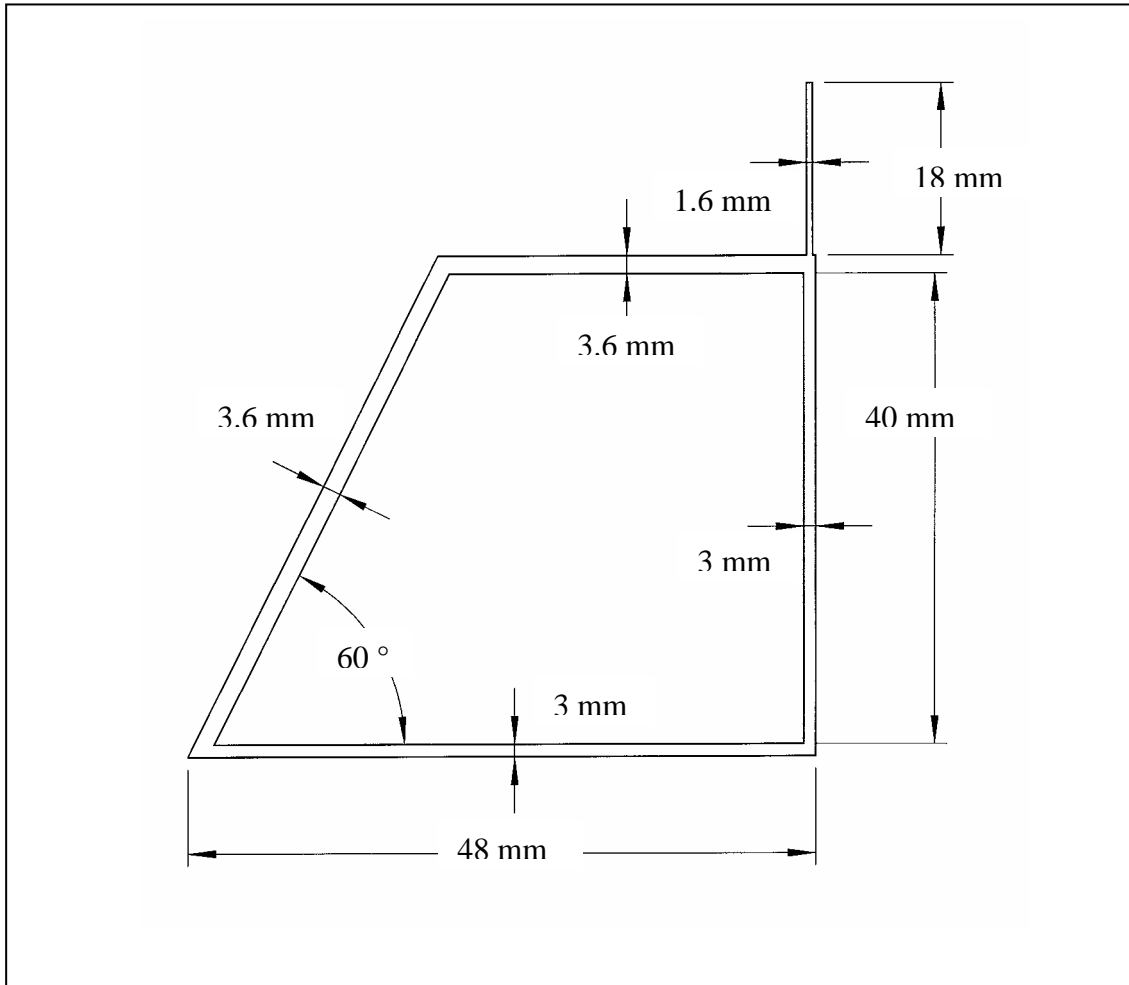
Segment point 1 and segment point 2 cannot have the same coordinates.

When these restrictions are not met, the program will stop and indicate the problem.

The best way to become familiar with the interface is to study the next two example inputs. One input concerns an arbitrary open cross section, the other is an arbitrary closed cross section.



	X coord	Y coord	Thickness
Segment point 1	0	0	
Segment point 2	19	0	2
Segment point 3	19	42,5	2
Segment point 4	19	60	3,6
Segment point 5	19	42,5	0
Segment point 6	10	42,5	3
Segment point 7	0	0	0
Segment point 8	0	0	0
Segment point 9	0	0	0
Segment point 10	0	0	0
Length	400		



	X coord	Y coord	Thickness
Segment point 1	0	0	
Segment point 2	44,7	0	3
Segment point 3	44,7	43,3	3
Segment point 4	44,7	63,1	1,6
Segment point 5	44,7	43,3	0
Segment point 6	25	43,3	3,6
Segment point 7	0	0	3,6
Segment point 8	0	0	0
Segment point 9	0	0	0
Segment point 10	0	0	0
Length	600		

When the input is accepted the program will calculate a characteristic element length. The characteristic length determines the size of the elements in the initial mesh. To calculate the characteristic element length it is assumed that the area of one element is ten times the mean thickness.

$$\begin{aligned}\text{Area element} &= 10 \times \text{mean thickness} \\ \text{Span element} \times \text{width element} &= 10 \times \text{mean thickness}\end{aligned}$$

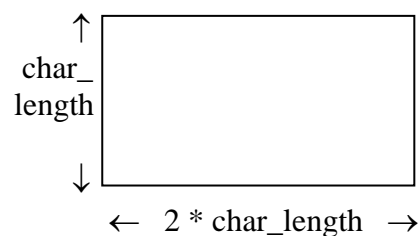
The structures of interest are slender beams for which the length is much greater than the width. Therefore the span of an element is twice the width of the element.

$$\begin{aligned}2 \times (\text{width element})^2 &= 10 \times \text{mean thickness} \\ \text{Width element} &= \sqrt{10 \times \text{mean thickness} / 2}\end{aligned}$$

Finally this result in the next expression for the characteristic element length.

$$\text{Char\_length} = 2 \times \sqrt{10 \times \text{mean thickness} / 2}$$

Working with a characteristic element length results in a uniform mesh. All elements are rectangular in shape (aspect ratio 0.5) and have more or less the same dimensions, that is:



To illustrate the procedure, look at the input of the first profile. The mean thickness equals:

$$\begin{aligned}\text{Mean thickness} &= \frac{2 + 2 + 3.6 + 3}{4} \\ \text{Mean thickness} &= 2.65 \\ \text{Char\_length} &= 7.28\end{aligned}$$

The line with points (0, 0) and (19, 0) has a length of 19 mm. Consequently,  $19 / 7.28 = 2.6$  and two elements with a width of 9.5 mm are constructed. The line with points (19, 0) and (19, 42.5) has a length of 42.5 mm. Consequently,  $42.5 / 7.28 = 5.8$  and five elements with a width of 8.5 mm are constructed. The length of the beam equals 400 mm. Consequently,  $400 / (2 \times 7.28) = 27.4$  and twenty-seven elements with a length of 14.8 mm are constructed. This can be verified in the next figure.

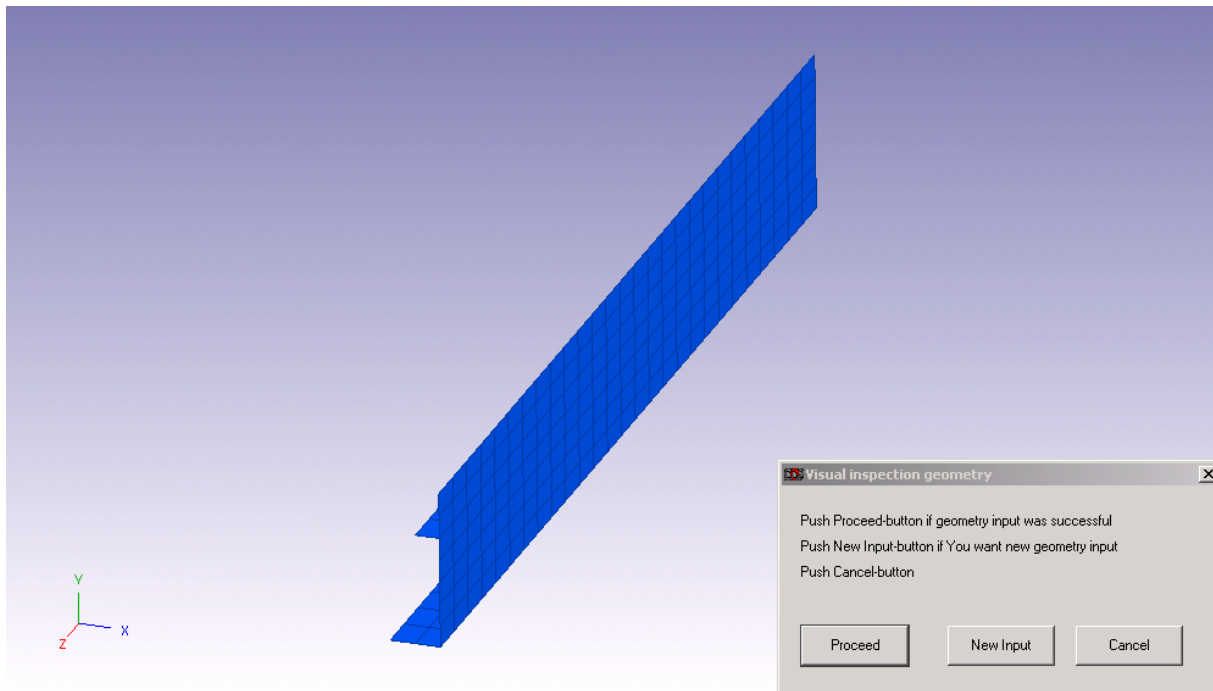


Figure 5.2 : Visual inspection geometry

The mean thickness has direct impact on the characteristic element length. When the mean thickness increases the characteristic element length will also increase. The situation can occur that the mean thickness and consequently the characteristic element length become too large to construct elements in a certain area. In this case the program will show the message “Shell model is probably not appropriate”.

After the geometry input one has the possibility to visual check the input data. If the input is successful the user can go to the next step by pushing the button “Proceed”. For new input click the button “New Input”. The “Cancel” button will clear the database and stop the program. The “Visual Inspection Geometry Box” is shown in the figure above.

### 5.3 Input box “Inputmenu Resanalyser”

This input box will ask initial values for the next properties:

Ex modulus length direction beam [N/mm<sup>2</sup>]  
 Ey modulus width direction beam [N/mm<sup>2</sup>]  
 Gxy shear modulus in the xy plane [N/mm<sup>2</sup>]  
 Nuxy major poisson's ratio [ ]

The use of Poisson's ratios for orthotropic materials sometimes causes confusion, so that care should be taken in their use. In practice, orthotropic material data are most often supplied in the major Poisson's ratio format or,

$$\frac{N_{uxy}}{E_x} = \frac{N_{uyx}}{E_y}$$

To estimate good initial values one can use the Resanalyser procedure. For more details about the Resanalyser device see reference.

The mass density is also required at this stage. In fact this is not an initial value because the mass density is not a parameter during model updating. Consequently, this exact value will be used during model updating.

Input Restrictions:

The elastic properties and the mass density must be positive values

The poisson's ratio must lie between 0.01 and 1.5

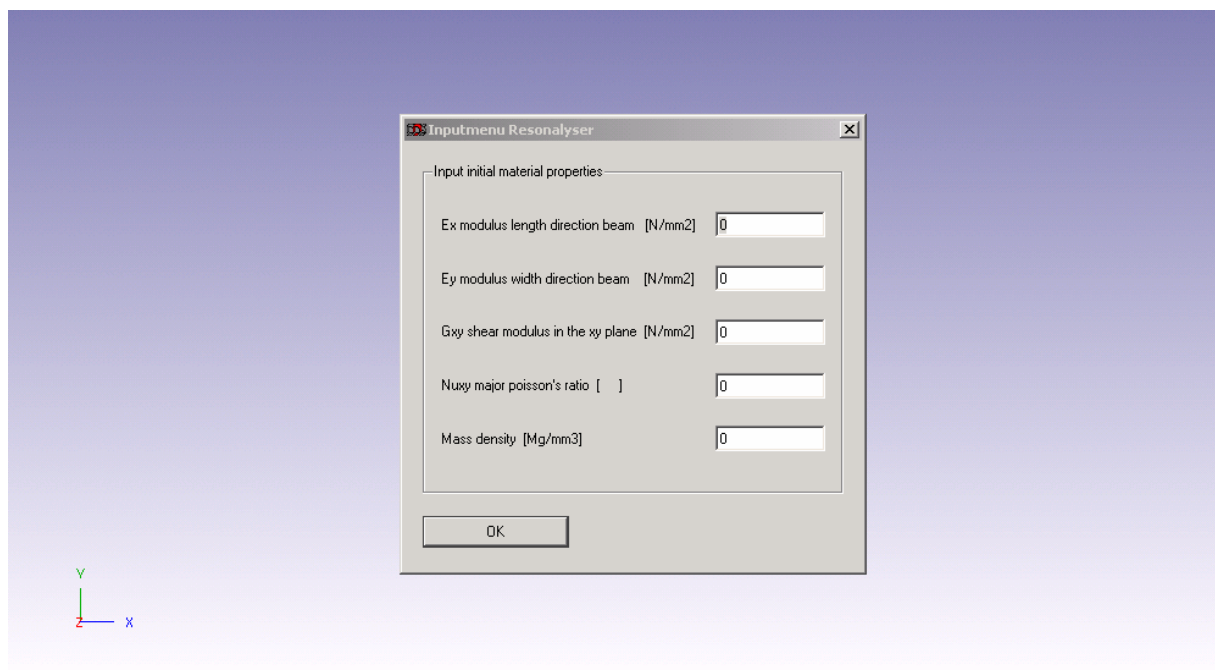


Figure 5.3 : Inputmenu Resanalyser

## **5.4 Generate converged mesh**

This step requires no extra input and is not directly visible to the user. A finite element analysis implies different kind of assumptions. One significant assumption that can be addressed only after a run is the assumption that the mesh was sufficient to capture the behavior of interest. An initial mesh must typically be refined multiple times to accurately capture this behavior. The process of successive mesh refinement to produce the optimal results is called convergence. The importance of a converged mesh cannot be overemphasized.

Natural frequencies are used as reference response during model updating. Therefore the accurate prediction of natural frequencies is of prime importance.

To obtain a converged mesh the program calculates the first ten natural frequencies of the structure at hand. This calculation is done with the initial mesh size. This result is stored in the first column of the matrix `freq_monitor`. Next the characteristic element length is divided by two. Consequently, the initial mesh is refined by a factor two. This refined mesh is used to calculate the first ten natural frequencies. This result is stored in the second column of the matrix `freq_monitor`. This process will go on until the difference between succeeding results is minimal. In the context of this work, minimal takes the value of 1 pro cent.

To illustrate the process, consider the next figures.

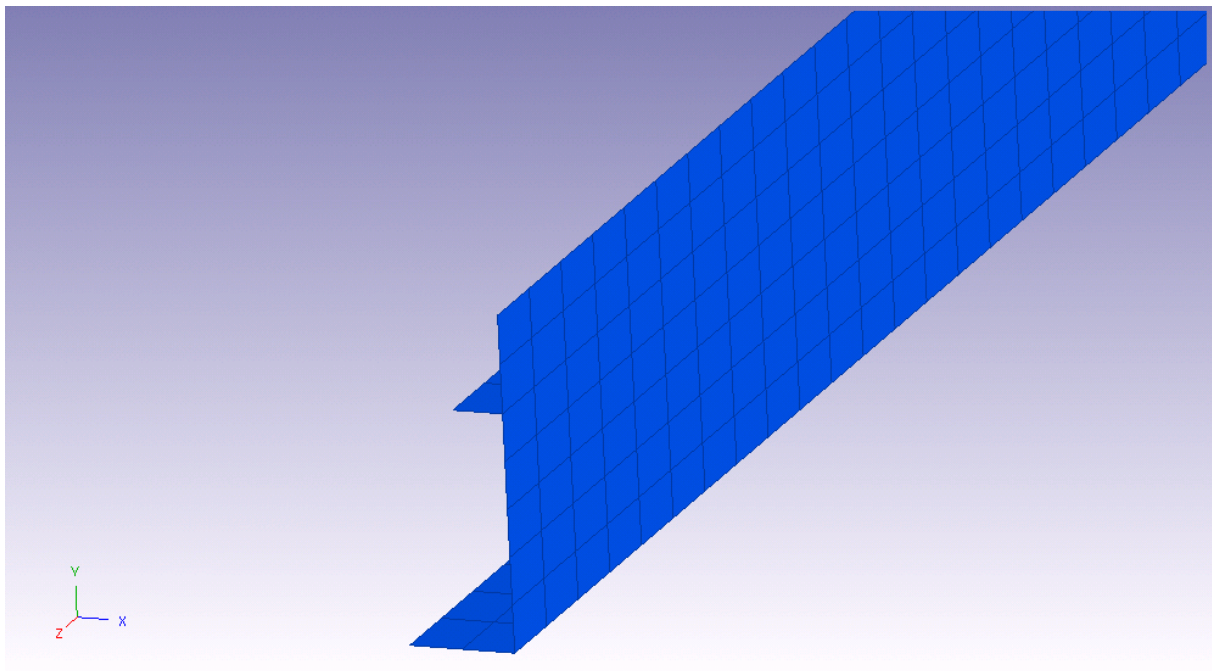


**Figure 5.4 : Initial mesh**

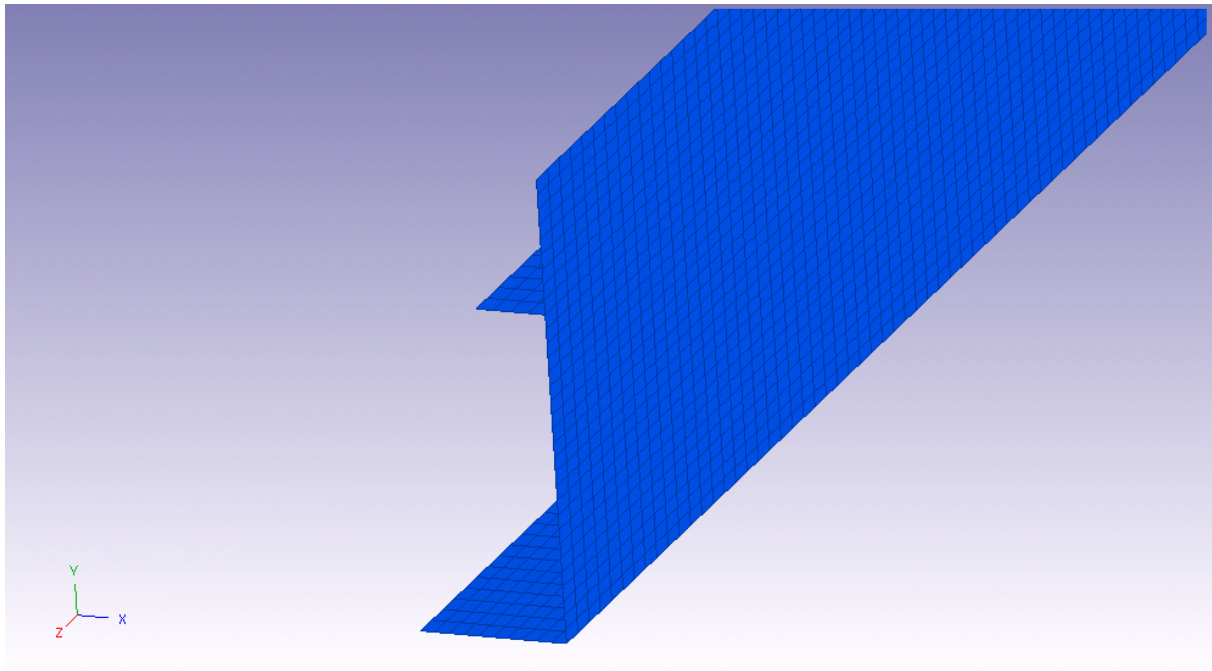


Figure 5.5 : Converged mesh

The next table shows the succeeding results.

Matrix freq_monitor	Initial mesh	Refined mesh	Refined refined mesh
freq 1	158,3	158,2	158,2
freq 2	266,1	264,9	264,6
freq 3	602,9	600,5	600
freq 4	624,1	619,1	617,6
freq 5	1126	1113	1109
freq 6	1321	1320	1320
freq 7	1343	1345	1345
freq 8	1350	1351	1351
freq 9	1398	1391	1389
freq 10	1623	1626	1627

Matrix freq\_monitor: values

Difference between two red values is higher than 1 pro cent. Therefore the refined mesh is refined again.

The matrix freq\_monitor is also available as matrix bitmap.

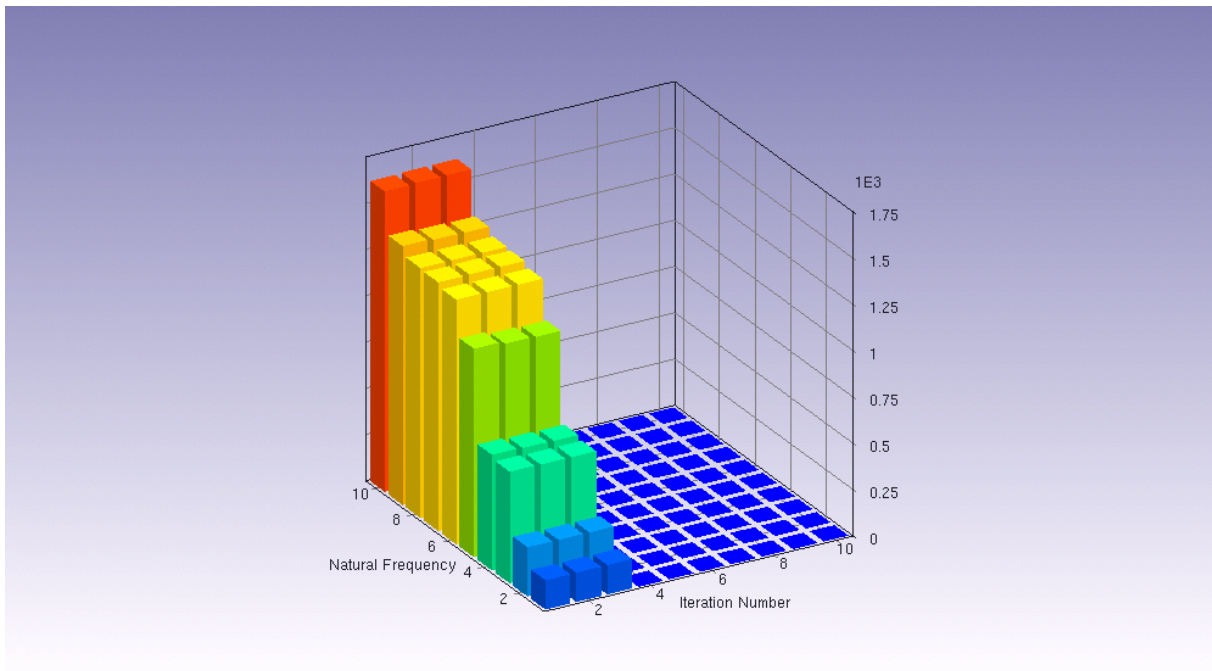


Figure 5.6 : Matrix freq\_monitor: matrix bitmap

## 5.5 Check Sensitivity Box

Here the program will supply the user with the following information:

- (1) first ten natural frequencies  $\{\text{freq}\}_{\text{analyt}}$  and corresponding mode shapes  $\{\psi\}_{\text{analyt}}$
- (2) the sensitivity matrix material properties versus frequencies  $\{\text{freq}\}_{\text{analyt}}$
- (3) the sensitivity sum curve material properties versus frequencies  $\{\text{freq}\}_{\text{analyt}}$
- (4) the convergence check matrix

These results are very useful. First, the output shows which mode shapes occur based on initial material properties. This information can be used during EMA.

The sensitivity matrix material properties versus analytical frequencies shows which parameter(s) can be identified by measuring the first natural frequencies of the structure. The sensitivity sum curve contains similar information.

The above information must give an answer to the next questions:

How many N response frequencies  $\{\text{freq}\}_{\text{exp}}$  are taken into account?

Which material properties can be identified?

## **5.6 Input box “Tune InputBox”**

This input box asks for the N reference response data  $\{\text{freq}\}_{\text{exp}}$ . Remember that the analytical mode shapes based on initial material properties are copied to the test database. It is important that the frequencies  $\{\text{freq}\}_{\text{exp}}$  correspond with the correct analytical mode shapes in the test database. Hence, **the test database reflects the behavior of the physical structure.**

A checkbox is available to indicate which material property will be treated as parameter during the identification.

From here the model updating can be launched. If the identification is done the program gives the updated values for the parameter(s). There is also an indication concerning convergence [CCABS and CCMEAN]. Both the fem model and test model are shown and one can investigate the correlation between the two models. If mode switching occurred during the update process, the MAC matrix is not diagonal any more.

## Chapter Six: Application of the program

All the tools and issues discussed in the previous chapters, are brought together in this chapter. The ultimate goal is to identify global effective orthotropic material properties by measuring natural frequencies of the structure at hand.

As a first test, the program is used to estimate the isotropic material properties of a steel beam. Initial values are input which deviate from the standard properties of steel. Natural frequencies are calculated based on the standard material properties of steel. If the program works properly, correct steel properties must result.

In the sequel, the program is employed to identify global effective orthotropic material properties of four composite profiles. There is one closed box profile and three open profiles in the set of four. Initial values for  $E_x$  and  $E_y$  are determined in the manner explained previously. No initial values are available for the shear moduli  $G_{xy}$  and Poisson coefficient  $\nu_{xy}$ . Common values are applied instead. Natural frequencies and corresponding mode shapes are measured using a laser vibrometer. To keep the **text readable**, the **mode shapes**, based on **initial material properties**, calculated by the program are placed in addendum. For the same reason, **experimental** measured **mode shapes** can be found in **addendum**.

The purpose is to identify all four orthotropic material properties. However, in view of practical applications, one is mainly interested in the effective properties  $E_x$  and  $G_{xy}$ . The knowledge of these values result in the longitudinal bending stiffness and the torsional stiffness of the beam. Properties of major importance in practical design.

The same convention is used for coordinate system and area properties as in Chapter One: Mechanical behavior of structural elements. Reference is made to a global orthogonal rectangular coordinate system  $xyz$ . The origin of this system is placed in the centroid  $G$  of the section at hand. The  $x$ -axis is directed along the span direction of the beam; the  $y$ - and  $z$ - axis are the principal central axes of the section. The position of the shear center is indicated with  $Q$ .

The sensitivity matrix shows the sensitivities of four parameters versus ten responses. Here the next convention is used:

Parameter 1:  $E_x$

Parameter 2:  $E_y$

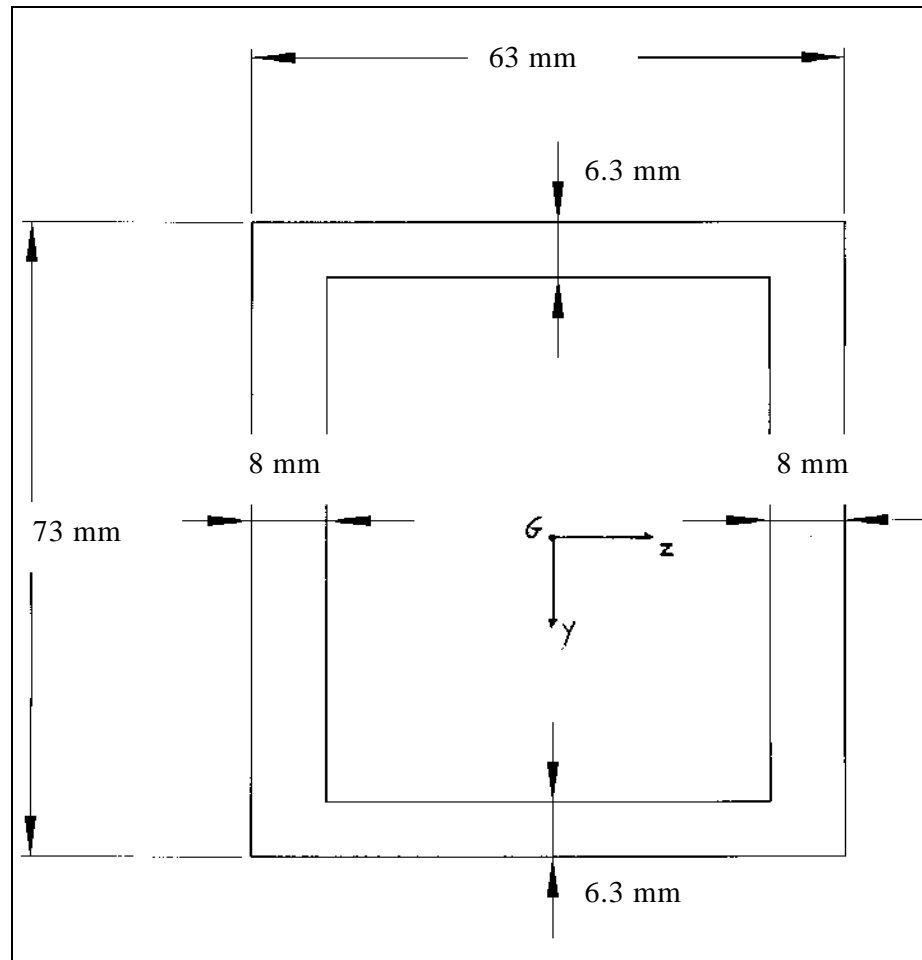
Parameter 3:  $G_{xy}$

Parameter 4:  $\nu_{xy}$

Ten responses: first ten analytical frequencies  $\{\text{freq}\}_{\text{analyt}}$  based on initial material properties.

## 6.1 Closed box profile made out of steel

As a first test, the program is used to identify the material properties of steel. Known analytical solutions are available to calculate the bending and torsional natural frequencies of beams [Ref Inman]. These frequencies are used as reference response in the program. A perturbation of 25 % is given to the material properties of steel. These values are used as initial material properties in the program. Consider the next profile section.



### *Section properties*

Dimensions according to figure (above)

Moment of inertia  $I_y$ : 998544 mm<sup>4</sup>

Moment of inertia  $I_z$ : 1179306 mm<sup>4</sup>

Torsional stiffness factor  $J$ : 1393340 mm<sup>4</sup>

Length: 2000 mm

### *Reference properties of steel*

$E$ : 210 000 N/mm<sup>2</sup>

$G$ : 84 000 N/mm<sup>2</sup>

$\nu$ : 0.25

Density: 7.87e-9 Mg/mm<sup>3</sup>

### Reference response data

The formula to calculate bending frequencies of a beam can be written as:

$$\omega_n = \beta_n^2 \sqrt{EI / \rho A}$$

where

$\omega_n$  is the  $n^{th}$  angular natural frequency [rad/sec]

$\beta_n$  are known numerical values [see Engineering vibrations by Inman p335]

$E$  is the elasticity modulus of steel

$\rho$  is the density of steel

$A$  is the cross sectional area of the beam

This formula applied to the box beam, results in the next reference frequencies.

Bending Y-axis [Hz]	Bending Z-axis [Hz]
109,5	119
302	328
560	612

The formula to calculate torsional frequencies of a bar can be written as:

$$\omega_n = \frac{n \pi c}{l}$$

where

$\omega_n$  is the  $n^{th}$  angular natural frequency [rad/sec]

$c = \sqrt{GJ / \rho I_{polar}}$ ,  $G$  the shear modulus of steel,  $J$  the torsional stiffness factor of the section,

$\rho$  is the density of steel,  $I_{polar}$  the polar moment of area of the section

$l$  is the length of 2000 mm of the beam

This formula applied to the box beam, results in the next reference frequencies.

Torsional vibration [Hz]
685,8
1335

### Initial values

A deviation of 25 % is given on the known properties of steel. This result in the next initial values.

Material Property	Initial value [N/mm <sup>2</sup> ]
Ex	157500
Ey	180000
Gxy	63000
Vxy	0,25

### Results modal updating

Initial values [N/mm <sup>2</sup> ]				Parameter selection				Fem data based on initial values versus Exp. data [Hz]			Mode switch		Difference initial final values [%]		Final parameter values [N/mm <sup>2</sup> ]			
Ex	Ey	Gxy	Vxy	Ex	Ey	Gxy	Vxy	Fem value	Exp. value	Description mode	Yes	No	CCABS	CCMEAN	Ex	Ey	Gxy	Vxy
157500	180000	63000	0.25	X		X		93	109,5	1bending Y-axis		X	14 // 1	- 14 // O	218557	180000	80709	0,25
								102	119	1bending Z-axis								
								252	302	2bending Y-axis								
								276	328	2bending Z-axis								
								481	560	3bending Y-axis								
								528	612	3bending Z-axis								
								606	685,8	1 torsion								

The updated values for  $E_x$  and  $G_{xy}$  show good correspondence with the target values of respectively 210000 N/mm<sup>2</sup> and 84000 N/mm<sup>2</sup>. A deviation of 25 % is reduced to a deviation of respectively 4.1 % and 3.9 %.

## 6.2 Closed box profile

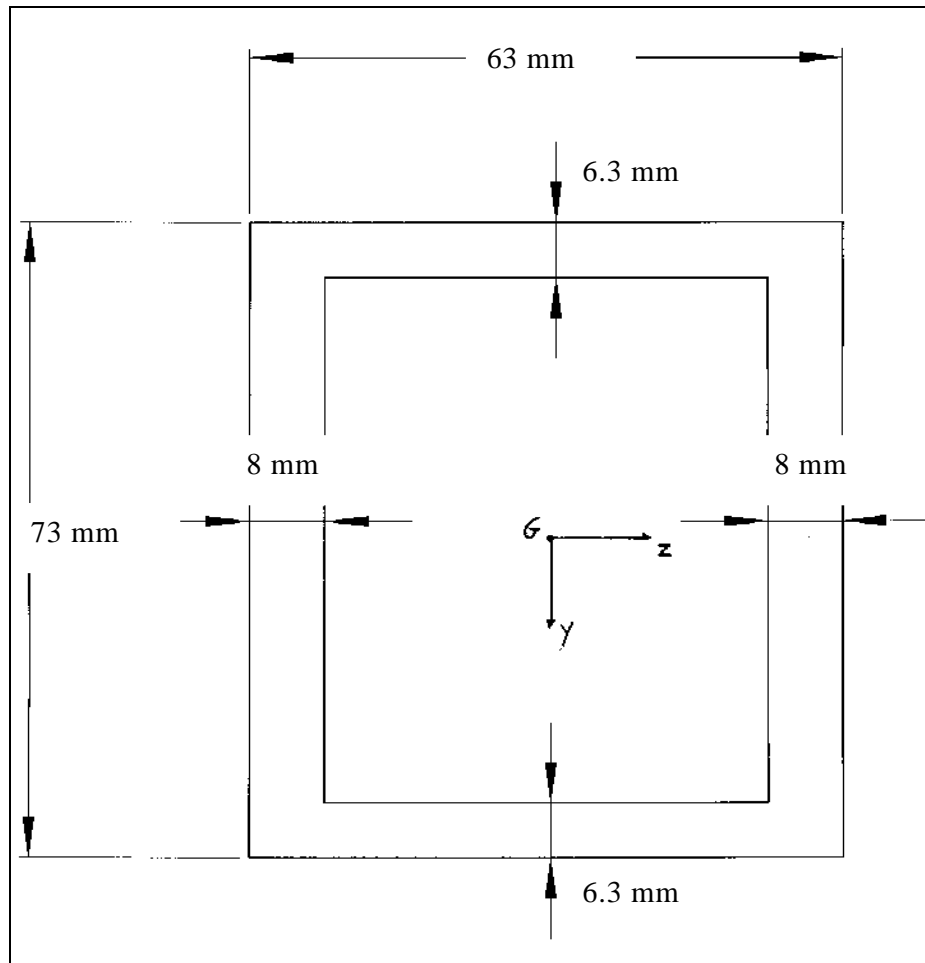
### *Section properties*

Dimensions according to figure (below)

Moment of inertia  $I_y$  : 998544 mm<sup>4</sup>

Moment of inertia  $I_z$  : 1179306 mm<sup>4</sup>

Torsional stiffness factor  $J$  : 1393340 mm<sup>4</sup>



### *Volume properties*

Volume : 2587494 mm<sup>3</sup>

Mass : 5132 gram

Density : 1.995e-9 Mg/mm<sup>3</sup>

Length : 1470 mm

### *Input geometry*

	X coord	Y coord	Thickness
Segment point 1	27.5	-33.35	
Segment point 2	27.5	33.35	8
Segment point 3	-27.5	33.35	6.3
Segment point 4	-27.5	-33.35	8
Segment point 5	27.5	-33.35	6.3
Length	1470		

### *Estimation initial values*

An initial value for  $E_x$  is obtained using the Resonalyser procedure. An initial value for  $E_y$  could not be obtained because the thickness versus width of the profile is too high. Typical engineering properties of a glass-polymer composite are used instead for  $E_y$ ,  $G_{xy}$  and  $\nu_{xy}$  (Ref. 1). The initial values are

	Initial value (N/mm <sup>2</sup> )	Method used to obtain value
<b>Ex</b>	35000	Resonalyser
<b>Ey</b>	16000	Literature
<b>Gxy</b>	5000	Literature
<b>νxy</b>	0,3	Literature

### *Experimental natural frequencies*

Two different planes of the beam are measured. First the shaker is attached to a small plane of the beam and the laser measured the response of the opposite small plane. These results can be found in column **Box\_LaserMeasuredOnSmallPlane**. Next the shaker is attached to a large plane of the beam and the laser measured the response of the opposite large plane. These results are shown in column **Box\_LaserMeasuredOnLargePlane**. The results with corresponding mode shapes are included in addendum.

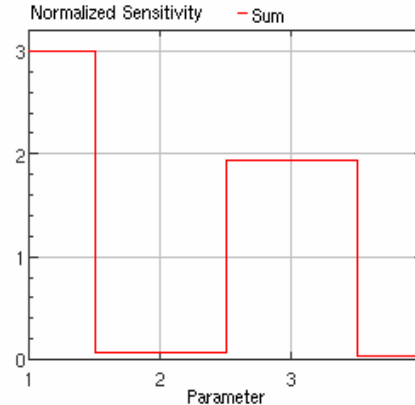
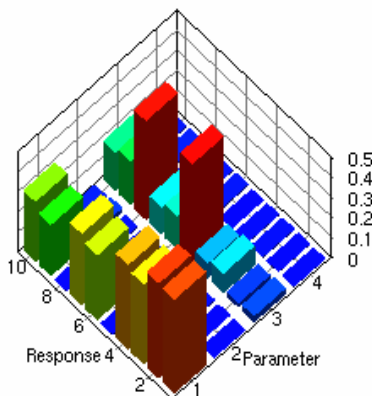
<b>Box_LaserMeasuredOnSmallPlane [Hz]</b>	<b>Description mode shape</b>	<b>Box_LaserMeasuredOnLargePlane [Hz]</b>	<b>Description mode shape</b>
180	1 bending mode Z-axis	166,9	1 bending mode Y-axis
471,3	2 bending mode Z-axis	428,8	2 bending mode Y-axis
543,1	1 torsion mode	543,8	1 torsion mode

### Check sensitivity box: program output

The Check sensitivity box is definitely the most useful part of the program. It gives information about frequencies and mode shapes based on initial material properties. Moreover, the sensitivity matrix is shown. One can investigate if the first ten frequencies contain sufficient information for the identification of all four parameters. Additionally, a sensitivity sum curve is shown. A low sensitivity sum value shows that none of the responses was sensitive to the parameter change. This means that the parameter is ineffective for all responses and should not be included in the selection for model updating.

The results are summarized in the next table and figures.

	{freq}analyt based on initial material properties [Hz]	Description modeste
Mode 1	157	1 bending mode Y-axis
Mode 2	172	1 bending mode Z-axis
Mode 3	399	2 bending mode Y-axis
Mode 4	444	2 bending mode Z-axis
Mode 5	466	1 torsion mode
Mode 6	701	3 bending mode Y-axis
Mode 7	797	3 bending mode Z-axis
Mode 8	929	2 torsion mode
Mode 9	1024	4 bending mode Y-axis
Mode 10	1192	4 bending mode Z-axis



The initial values are quite good in the sense that predicted mode shapes correspond with measured ones. The calculated modal data do not indicate closely spaced modes. Although the first torsion mode is in the neighborhood of the second bending around Z-axis.

It is immediately clear that  $E_y$  and  $\nu_{xy}$  can not be identified by measuring frequencies of the structure. The advantage is that values found in literature can be used as initial values, since they have minor influence on the output.

The first four modes contain information with respect to  $E_x$ . The fifth torsion mode is very sensitive for a change in value of  $G_{xy}$ . It is therefore logical to use the first five measured frequencies as reference response.

### Model Updating results

Initial values [N/mm <sup>2</sup> ]				Parameter selection				Fem data based on initial values versus Exp. data [Hz]			Mode shape switch occur		Difference initial final values [%]		Final parameter values [N/mm <sup>2</sup> ]			
Ex	Ey	Gxy	Vxy	Ex	Ey	Gxy	Vxy	Fem value	Exp. value	Description mode	Yes	No	CCABS	CCMEAN	Ex	Ey	Gxy	Vxy
35000	16000	5000	0,3	X		X		157,4	166,9	1 bending Y		X	7,5 / 0,5	7 / 0	38466	16000	6819	0,3
								172,4	180	1 bending Z								
								398,6	428,8	2 bending Y								
								444,3	471,3	2 bending Z								
								465,8	543,4	1 torsion								

### Model Updating results: deviation on initial values

Initial values [N/mm <sup>2</sup> ]				Parameter selection				Fem data based on initial values versus Exp. data [Hz]			Mode shape switch occur		Difference initial final values [%]		Final parameter values [N/mm <sup>2</sup> ]			
Ex	Ey	Gxy	Vxy	Ex	Ey	Gxy	Vxy	Fem value	Exp. value	Description mode	Yes	No	CCABS	CCMEAN	Ex	Ey	Gxy	Vxy
42000	16000	4000	0,3	X		X		170	166,9	1 bending Y		X	6,5 / 0,5	-4 / 0	38467	16000	6819	0,3
								187	180	1 bending Z								
								416,6	428,8	2 bending Y								
								416,9	543,4	1 torsion								
								469	471,3	2 bending Z								

Initial values [N/mm <sup>2</sup> ]				Parameter selection				Fem data based on initial values versus Exp. data [Hz]			Mode shape switch occur		Difference initial final values [%]		Final parameter values [N/mm <sup>2</sup> ]			
Ex	Ey	Gxy	Vxy	Ex	Ey	Gxy	Vxy	Fem value	Exp. value	Description mode	Yes	No	CCABS	CCMEAN	Ex	Ey	Gxy	Vxy
28000	16000	6000	0,3	X		X		142	166,9	1 bending Y		X	12 / 0,5	-12 / 0	38467	16000	6819	0,3
								155	180	1 bending Z								
								369	428,8	2 bending Y								
								408	471,3	2 bending Z								
								510	543,4	1 torsion								

### 6.3 SymmetricU-profile

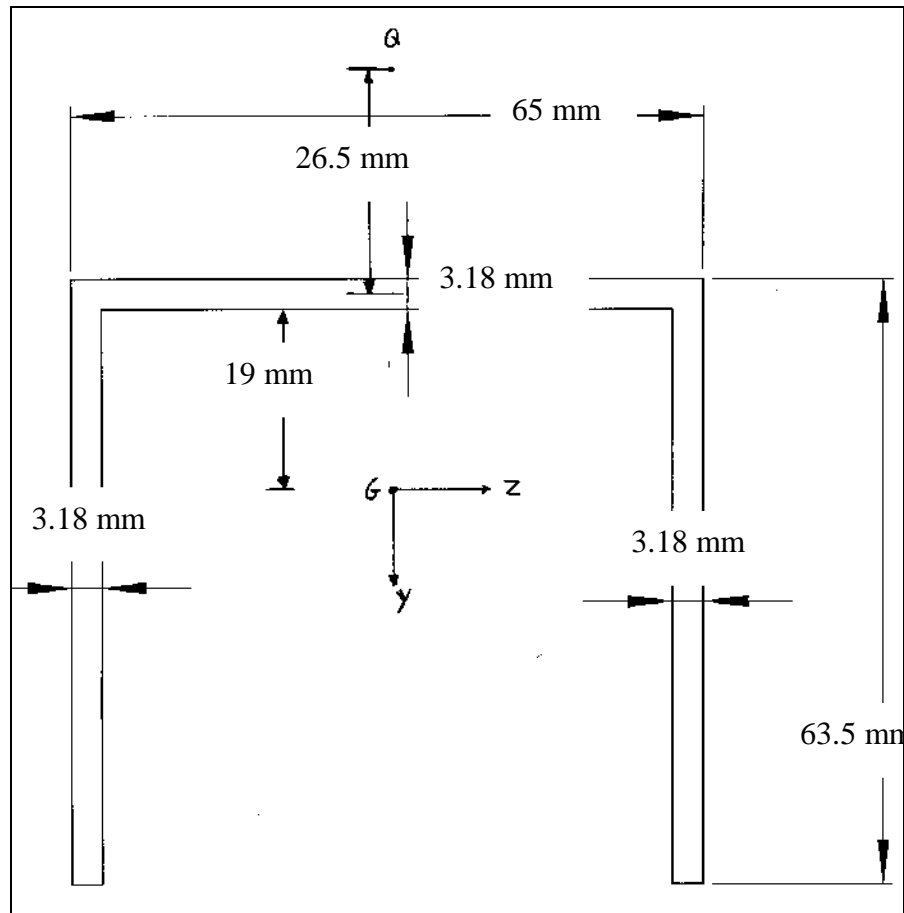
#### *Section properties*

Dimensions according to figure (below)

Moment of inertia  $I_y$  : 439635 mm<sup>4</sup>

Moment of inertia  $I_z$  : 251905 mm<sup>4</sup>

Torsional stiffness factor  $J$  : 1990 mm<sup>4</sup>



#### *Volume properties*

Volume : 867793 mm<sup>3</sup>

Mass : 1599 gram

Density : 1.8426e-9 Mg/mm<sup>3</sup>

Length : 1470 mm

### *Input geometry*

	X coord	Y coord	Thickness
Segment point 1	0	0	
Segment point 2	0	61.91	3.18
Segment point 3	-61.82	61.91	3.18
Segment point 4	-61.82	0	3.18
Length	1470		

### *Estimation initial values*

The initial values for  $E_x$  are obtained by measuring the first bending mode of beam specimen in the span direction of the structure. Initial values  $E_y$  are obtained by measuring the first bending mode of a beam specimen in the width direction of the structure. Results are summarized in next table.

Name	Dimensions (widthxlengthxthickness) [mm]	Mass [ton]	Volume [mm <sup>3</sup> ]	Density [ton/mm <sup>3</sup> ]	Transverse section [mm <sup>2</sup> ]	Moment of inertia [mm <sup>4</sup> ]	Frequency first bending mode [Hz]	Elasticity Modulus [N/mm <sup>2</sup> ]
X spec1	20,3 x 182 x 3,2	21,2 e-6	11823	1,8 e-9	65	55,4	342,5	21447
X spec2	19,5 x 182 x 3,2	21,0 e-6	11357	1,9 e-9	62,4	53,3	341,3	22431
Y spec1	20 x 56,9 x 3,2	6,7 e-6	3642	1,8 e-9	64	54,6	2523	11108
Y spec2	20 x 56,3 x 3,2	6,7 e-6	3603	1,9 e-9	64	54,6	2667	12557

Typical engineering properties of a glass-polymer composite are used for  $G_{xy}$  and  $\nu_{xy}$  (Ref. 1).

The initial values are

	Initial value (N/mm <sup>2</sup> )	Method used to obtain value
<b>E<sub>x</sub></b>	22000	Resonalyser
<b>E<sub>y</sub></b>	11800	Resonalyser
<b>G<sub>xy</sub></b>	5000	Literature
<b>ν<sub>xy</sub></b>	0,3	Literature

**Experimental natural frequencies**

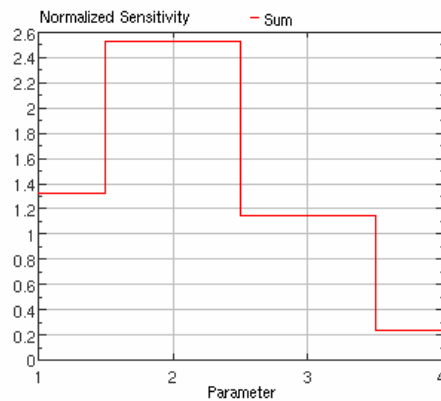
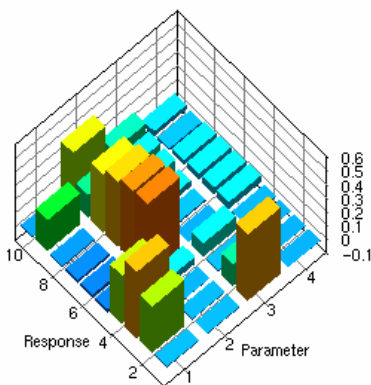
The shaker is attached to the upper plane [65x1470] of the beam and response measured on the same plane. Results are found in column **SymU\_LaserMeasuredOnUpperPlane**. Next the shaker is attached to one of the side planes [63.5x1470] of the beam and the laser measured the response of the opposite side plane. These results are shown in column **SymU\_LaserMeasuredOnSidePlane**. The results with corresponding mode shapes are included in addendum.

SymU_LaserMeasuredOnUpperPlane [Hz]	Description mode shape	SymU_LaserMeasuredOnSidePlane [Hz]	Description mode shape
32.5	1 torsion mode	146.9	2 complex bending Y-axis
66.25	1 complex bending Y-axis		
135.6 – 139.4	1 bending mode Z-axis		

**Check sensitivity box: program output**

Modal data calculated based on initial values can be found in addendum.

	{freq}analyt based on initial material properties [Hz]	Description modes hape
Mode 1	32	1 torsion mode
Mode 2	61	1 complex bending mode Y-axis
Mode 3	116	1 bending mode Z-axis
Mode 4	140	2 complex bending mode Y-axis
Mode 5	197	1 (rigid) open/close mode side planes
Mode 6	199	2 open/close mode side planes
Mode 7	207	Higer order modes
Mode 8	217	
Mode 9	221	
Mode 10	235	



The initial values are quite good in the sense that predicted mode shapes correspond with measured ones. The first four modes are well separated; with a first torsion mode halve the value of the second mode. After the first four modes, the calculation indicates closely spaced modes as there are five modes in a frequency band of 24 Hz. This situation was also encountered in practice. Closely spaced modes are more difficult to measure.

The sensitivity matrix indicates that the first torsion mode contains information about the shear modulus  $G_{xy}$ . The next three modes are particular sensitive to a change in value of parameter one, the modulus  $E_x$ . Remark the fact that the response is also sensitive to a change in value of  $E_y$ . Especially, modes five and six are sensitive with respect to a change in  $E_y$ . None of the responses are sensitive to a change in value of  $\nu_{xy}$ . No attempt should be made to identify  $\nu_{xy}$  by measuring natural frequencies.

There was no indication, what so ever, of modes five and six in the measured data with vibrometer. Probably due to the fact that a single shaker is not optimal to excite mode five. Additionally, both modes are extremely close to each other. Consequently, further discussion will focus on the determination of  $E_x$  and  $G_{xy}$ . The first four modes are used to identify  $E_x$  and  $G_{xy}$ .

### Model Updating results

Initial values [N/mm <sup>2</sup> ]				Parameter selection				Fem data based on initial values versus Exp. data [Hz]			Mode shape switch occur		Difference initial final values [%]		Final parameter values [N/mm <sup>2</sup> ]			
Ex	Ey	Gxy	Vxy	Ex	Ey	Gxy	Vxy	Fem value	Exp. value	Description mode	Yes	No	CCABS	CCMEAN	Ex	Ey	Gxy	Vxy
22000	11800	5000	0,3	X		X		32	32,5	1 torsion		X	7,5 / 2,5	7,5 / 0	28944	11800	5014	0,3
								61	66,25	1complex bend Y								
								116	137,5	1 bending Z								
								140	146,9	2complex bend Y								

### Model Updating results: deviation on initial values

Initial values [N/mm <sup>2</sup> ]				Parameter selection				Fem data based on initial values versus Exp. data [Hz]			Mode shape switch occur		Difference initial final values [%]		Final parameter values [N/mm <sup>2</sup> ]			
Ex	Ey	Gxy	Vxy	Ex	Ey	Gxy	Vxy	Fem value	Exp. value	Description mode	Yes	No	CCABS	CCMEAN	Ex	Ey	Gxy	Vxy
26400	11800	4000	0,3	X		X		29	32,5	1 torsion		X	6.5 / 2.8	-6 / 0	28945	11800	5015	0,3
								63	66,25	1complex bend Y								
								126	137,5	1 bending Z								
								146	146,9	2complex bend Y								

Initial values [N/mm <sup>2</sup> ]				Parameter selection				Fem data based on initial values versus Exp. data [Hz]			Mode shape switch occur		Difference initial final values [%]		Final parameter values [N/mm <sup>2</sup> ]			
Ex	Ey	Gxy	Vxy	Ex	Ey	Gxy	Vxy	Fem value	Exp. value	Description mode	Yes	No	CCABS	CCMEAN	Ex	Ey	Gxy	Vxy
17600	11800	6000	0,3	X		X		35	32,5	1 torsion		X	14 / 2.8	-10 / 0	28948	11800	5015	0,3
								59	66,25	1complex bend Y								
								104	137,5	1 bending Z								
								132	146,9	2complex bend Y								

## 6.4 Asymmetric U-profile

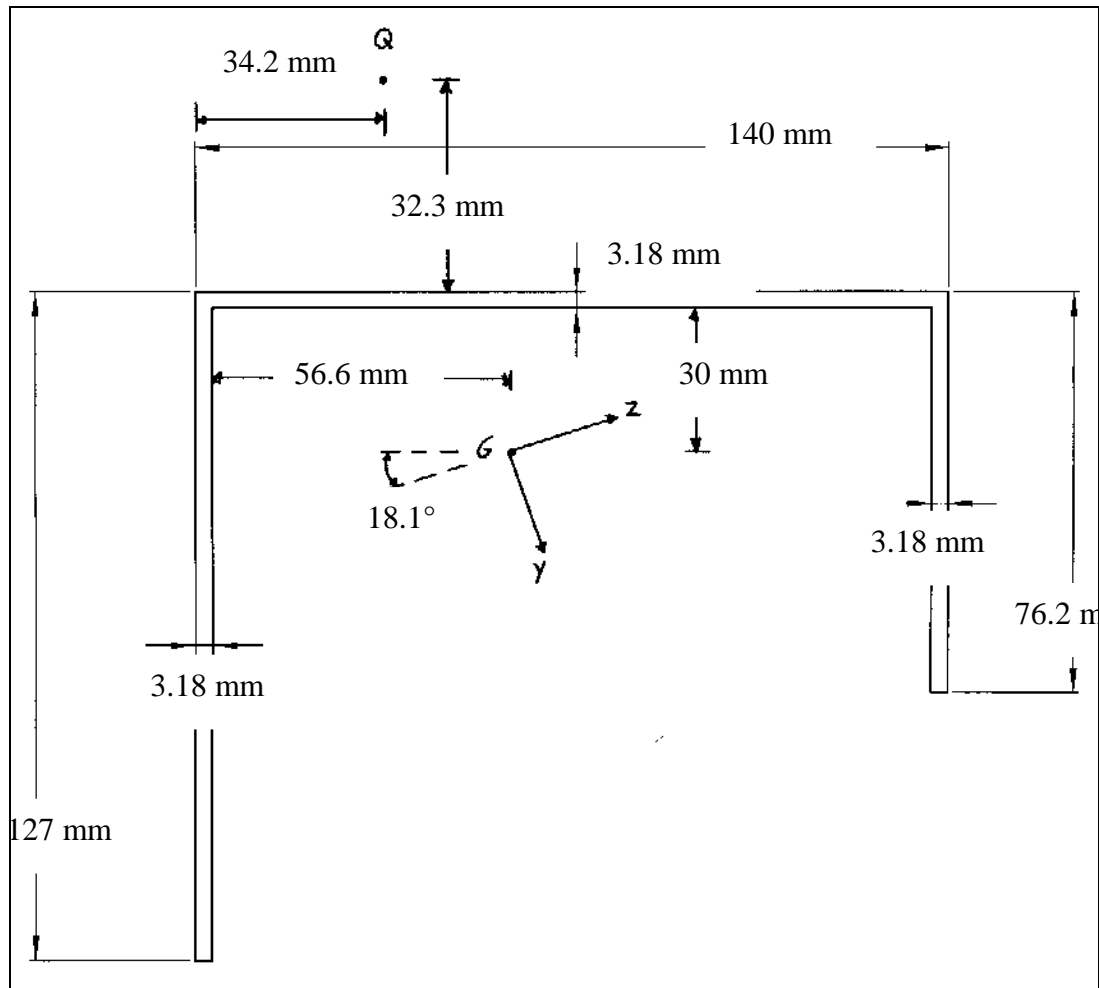
### *Section properties*

Dimensions according to figure (below)

Moment of inertia  $I_y$ : 3788688 mm<sup>4</sup>

Moment of inertia  $I_z$ : 1216052 mm<sup>4</sup>

Torsional stiffness factor  $J$ : 3611 mm<sup>4</sup>



### *Volume properties*

Volume : 1576509 mm<sup>3</sup>

Mass : 3000 gram

Density : 1.9029e-9 Mg/mm<sup>3</sup>

Length : 1470 mm

### *Input geometry*

	X coord	Y coord	Thickness
Segment point 1	0	0	
Segment point 2	0	125.41	3.18
Segment point 3	136.82	125.41	3.18
Segment point 4	136.82	50.8	3.18
Length	1470		

### *Estimation initial values*

The initial values for  $E_x$  are obtained by measuring the first bending mode of beam specimen in the span direction of the structure. Initial values  $E_y$  are obtained by measuring the first bending mode of a beam specimen in the width direction of the structure. Results are summarized in next table.

Name	Dimensions (widthxlengthxthickness) [mm]	Mass [ton]	Volume [mm <sup>3</sup> ]	Density [ton/mm <sup>3</sup> ]	Transverse section [mm <sup>2</sup> ]	Moment of inertia [mm <sup>4</sup> ]	Frequency first bending mode [Hz]	Elasticity Modulus [N/mm <sup>2</sup> ]
X spec1	20,2 x 158 x 3,2	19,4 e-6	10213	1,9 e-9	64,6	55,2	507,5	28159
X spec2	20,3 x 158 x 3,2	19.5 e-6	10264	1,9 e-9	65	55,4	540	31963
Y spec1	20,2 x 124,2 x 3,2	15,3 e-6	8028	1,9 e-9	64,6	55,2	560	13091
Y spec2	20,2 x 124,2 x 3,2	15,3 e-6	8028	1,9 e-9	64,6	55,2	567,5	13444

Typical engineering properties of a glass-polymer composite are used for  $G_{xy}$  and  $\nu_{xy}$  (Ref. 1).

The initial values are

	Initial value (N/mm <sup>2</sup> )	Method used to obtain value
<b>E<sub>x</sub></b>	30000	Resonalyser
<b>E<sub>y</sub></b>	13260	Resonalyser
<b>G<sub>xy</sub></b>	5000	Literature
<b>ν<sub>xy</sub></b>	0,3	Literature

**Experimental natural frequencies**

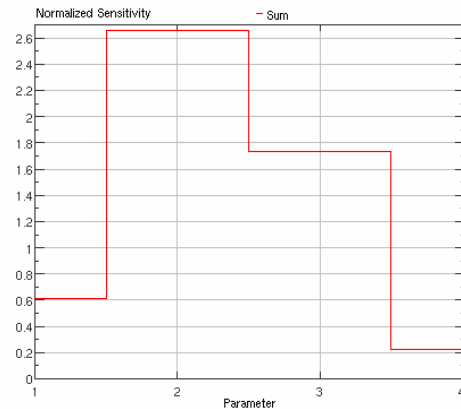
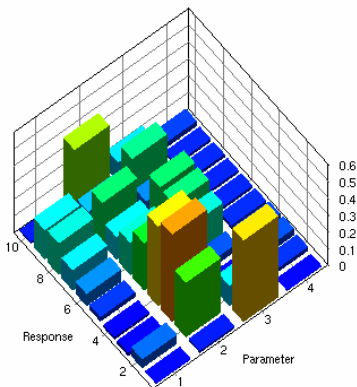
The shaker is attached to the upper plane [140x1470] of the beam and response measured on the same plane. Results are found in column **AsymU\_LaserMeasuredOnUpperPlane**. Next the shaker is attached to the large side plane and response is measured on the opposite small [76.2x1470] plane. These results are shown in column **AsymU\_LaserMeasuredOnSmallSidePlane**. Finally, the shaker is attached to the small side plane and response is measured on the opposite large [127x1470] plane. Results are shown in column **AsymU\_LaserMeasuredOnLargeSidePlane**. The results with corresponding mode shapes are included in addendum.

AsymU_Laser MeasuredOn UpperPlane [Hz]	Description modeshape	AsymU_Laser MeasuredOn SmallSidePlane [Hz]	Description modeshape	AsymU_Laser MeasuredOn LargeSidePlane [Hz]	Description modeshape
17,5	1 torsion mode	58,75	1 open / close mode side planes	58,75	1 open / close mode side planes
58,75	1 open / close mode side planes			70,63	4 open / close mode side planes
70,63	4 open / close mode side planes			83,75	5 open / close mode side planes

**Check sensitivity box: program output**

Modal data calculated based on initial values can be found in addendum.

	{freq}analyt based on initial material properties [Hz]	Description modeshape
Mode 1	16	1 torsion mode
Mode 2	60	1 open/close mode side planes
Mode 3	66	2 (rigid) open/close mode side planes
Mode 4	68	3 open/close mode side planes
Mode 5	74	4 open/close mode side planes
Mode 6	90	5 open/close mode side planes
Mode 7	111	6 open/close mode side planes
Mode 8	120	1 bending mode Z-axis
Mode 9	136	7 open/close mode side planes
Mode 10	152	2 bending mode Z-axis

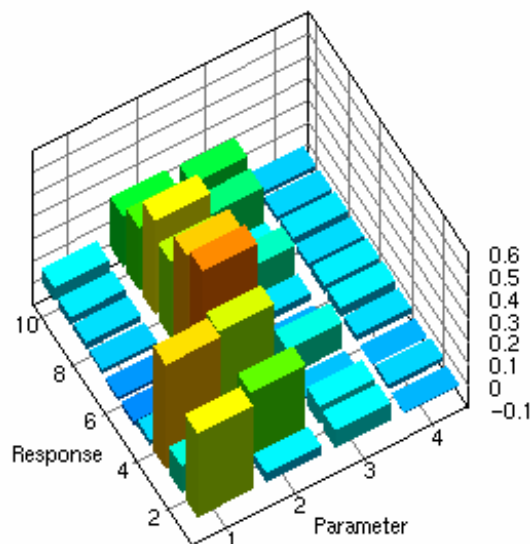


For this profile (torsion excluded), all modes behave in a similar manner. The upper plane of the profile has almost no movement, instead the webs of the profile are moving out- or inwards. These modes are called “open/close mode side planes” and are particular sensitive for a change in value of  $E_y$ .

Unfortunately, modes three and four are very difficult to measure in practice. First, they are very close to each other. Secondly, a single shaker is not optimal to excite this kind of modes.

Again the first torsion mode, has a high sensitivity for parameter three or  $G_{xy}$ . Initial value calculation indicates that this mode will not interfere with higher order modes.

The first ten response frequencies show a very low sensitivity for parameter 1 or  $E_x$ . Consequently, it is not possible to identify  $E_x$  by measuring the first natural frequencies of this profile. Longitudinal bending modes do not occur. This is probably the reason why the sensitivity for  $E_x$  is so low. The same profile with longer span can probably solve this problem. The longer the beam, the more likely longitudinal bending modes will occur. To investigate the above statement, the sensitivity matrix is calculated for a beam with same section properties but with double span length [2940 mm]. This sensitivity matrix is shown below.



As expected, the response of a longer beam is more sensitive with respect to parameter  $E_x$ . However, note that shear modulus  $G_{xy}$  sensitivity is very low. The original beam's [1470 mm span] first mode is very sensitive to a change in value of  $G_{xy}$ . The program can be used to analyse one particular structure of a certain length. This is in fact what is done in this thesis. However, the **program** can also be **used to** investigate the influence of the length on the sensitivity response versus parameter. As such, one can **determine** the **most ideal length** to **identify** a **certain material property**.

In the sequel, the model is updated for parameters  $E_y$  and  $G_{xy}$  making use of the first two responses.

### Model Updating results

Initial values [N/mm <sup>2</sup> ]				Parameter selection				Fem data based on initial values versus Exp. data [Hz]			Mode shape switch occur		Difference initial final values [%]		Final parameter values [N/mm <sup>2</sup> ]			
Ex	Ey	Gxy	Vxy	Ex	Ey	Gxy	Vxy	Fem value	Exp. value	Description mode	Yes	No	CCABS	CCMEAN	Ex	Ey	Gxy	Vxy
30000	13260	5000	0,3		X	X		16	17,5	1 torsion		X	6 / 0	- 4 / 0	30000	11185	6275	0,3
								60	58,75	1 open/close mode side planes								

Modes five and six are measured with the vibrometer. The frequencies of these two modes are respectively 70.63 Hz and 83.75 Hz. Recalculation with updated material properties, gives a frequency of 74 Hz and 90 Hz for modes five and six.

### Model Updating results: deviation on initial values

Initial values [N/mm <sup>2</sup> ]				Parameter selection				Fem data based on initial values versus Exp. data [Hz]			Mode shape switch occur		Difference initial final values [%]		Final parameter values [N/mm <sup>2</sup> ]			
Ex	Ey	Gxy	Vxy	Ex	Ey	Gxy	Vxy	Fem value	Exp. value	Description mode	Yes	No	CCABS	CCMEAN	Ex	Ey	Gxy	Vxy
30000	15912	4000	0,3		X	X		14	17,5	1 torsion		X	13 / 0	-6.5 / 0	30000	11194	6267	0,3
								62	58,75	1 open/close mode side planes								

Initial values [N/mm <sup>2</sup> ]				Parameter selection				Fem data based on initial values versus Exp. data [Hz]			Mode shape switch occur		Difference initial final values [%]		Final parameter values [N/mm <sup>2</sup> ]			
Ex	Ey	Gxy	Vxy	Ex	Ey	Gxy	Vxy	Fem value	Exp. value	Description mode	Yes	No	CCABS	CCMEAN	Ex	Ey	Gxy	Vxy
30000	10608	6000	0,3		X	X		17	17,5	1 torsion		X	2.2 / 0	-2.2 / 0	30000	11149	6273	0,3
								57	58,75	1 open/close mode side planes								



### *Volume properties*

Volume : 2898840 mm<sup>3</sup>

Mass : 5457 gram

Density : 1.8825e-9 Mg/mm<sup>3</sup>

Length : 1470 mm

### *Input geometry*

	X coord	Y coord	Thickness
Segment point 1	0	0	
Segment point 2	87.27	0	5.08
Segment point 3	87.27	70.1	5.08
Segment point 4	87.27	144.42	5.08
Segment point 5	87.27	70.1	0
Segment point 6	50.49	70.1	5.08
Segment point 7	50.49	144.42	5.08
Segment point 8	50.49	70.1	0
Segment point 9	0	70.1	5.08
Length	1470		

### *Estimation initial values*

The initial values for  $E_x$  are obtained by measuring the first bending mode of beam specimen in the span direction of the structure. Initial values  $E_y$  are obtained by measuring the first bending mode of a beam specimen in the width direction of the structure. Results are summarized in next table.

Name	Dimensions (widthxlengthxthickness) [mm]	Mass [ton]	Volume [mm <sup>3</sup> ]	Density [ton/mm <sup>3</sup> ]	Transverse section [mm <sup>2</sup> ]	Moment of inertia [mm <sup>4</sup> ]	Frequency first bending mode [Hz]	Elasticity Modulus [N/mm <sup>2</sup> ]
X spec1	20,6 x 157,5 x 5,1	30,8 e-6	16547	1,9 e-9	105,1	227,7	645	17714
X spec2	20,8 x 159 x 5,1	30,5 e-6	16867	1,8 e-9	106,1	230,0	642,5	17285
Y spec1	20,6 x 64 x 5,1	12,5 e-6	6724	1,9 e-9	105,1	227,7	4063	19164
Y spec2	20,4 x 64 x 5,1	12,5 e-6	6659	1,9 e-9	104	225,5	4063	19148

Typical engineering properties of a glass-polymer composite are used for  $G_{xy}$  and  $\nu_{xy}$  (Ref. 1).

The initial values are

	Initial value (N/mm <sup>2</sup> )	Method used to obtain value
<b>E<sub>x</sub></b>	17500	Resonalyser
<b>E<sub>y</sub></b>	19156	Resonalyser
<b>G<sub>xy</sub></b>	5000	Literature
<b>ν<sub>xy</sub></b>	0,3	Literature

**Experimental natural frequencies**

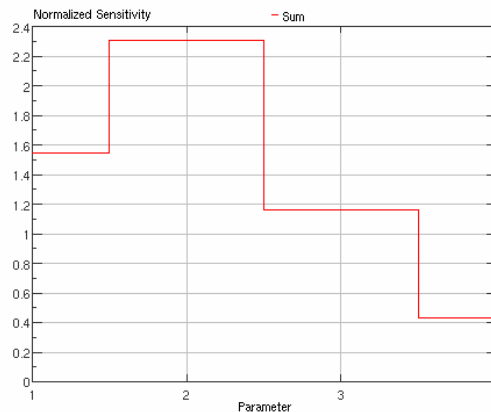
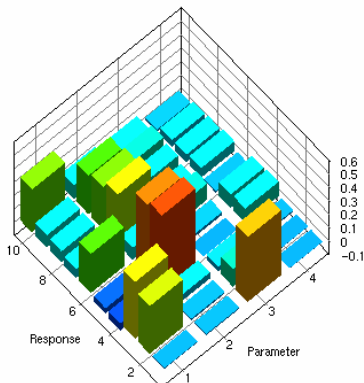
The shaker is attached to the lower plane [89.8x1470] of the beam and response measured on the opposite top plane. Results are found in column **Complex\_LaserMeasuredOnUpperPlane**. Next the shaker is attached to the large side plane and response is measured on the same plane [147x1470] plane. These results are shown in column **Complex\_LaserMeasuredOnSidePlane**. Finally, the shaker is attached to the top plane and response is measured on the opposite bottom [89.8x1470] plane. Results are shown in column **Complex\_LaserMeasuredOnBottomPlane**. The results with corresponding mode shapes are included in addendum.

<b>Complex_Laser MeasuredOn UpperPlane [Hz]</b>	<b>Description modeshape</b>	<b>Complex_Laser MeasuredOn SidePlane [Hz]</b>	<b>Description modeshape</b>	<b>Complex_Laser MeasuredOn BottomPlane [Hz]</b>	<b>Description modeshape</b>
38.75	1 torsion mode	38.13	1 torsion mode	105.6	mode 2
		105.6	mode 2	151.9	1 bending mode Y-axis
		151.3	1 bending mode Y-axis		

**Check sensitivity box: program output**

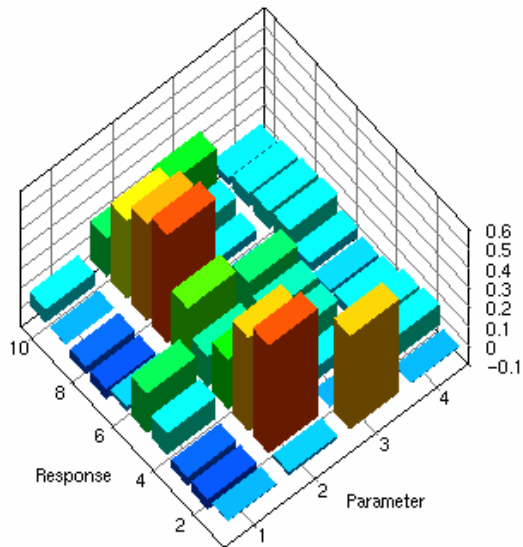
Modal data calculated based on initial values can be found in addendum.

	<b>{freq}analyt based on initial material properties [Hz]</b>	<b>Description modeshape</b>
Mode 1	33	1 torsion mode
Mode 2	90	mode 2
Mode 3	128	1 bending mode Y-axis
Mode 4	191	1 (rigid) open/close mode side planes
Mode 5	194	2 open/close mode side planes
Mode 6	199	mode 6
Mode 7	210	3 open/close mode side planes
Mode 8	228	4 open/close mode side planes
Mode 9	272	5 open/close mode side planes
Mode 10	280	mode 10



Here again, modes four and five are “open/close modes side planes” and show a high sensitivity with respect to parameter  $E_y$ . Also here the measured data did not contain any information about those two modes.

What would be the effect of halving the span length [735 mm] of the beam? Probably, the sensitivities for  $E_x$  will go down, while the first mode will stay the torsion mode. This can be investigated by using the program. The resulting sensitivity matrix is shown below.



For the short beam, the torsion frequency is still the first mode encountered and has a value of 65 Hz. The next mode at 190 Hz is the “rigid open/close side planes” mode. It is clear that by modifying the length of the beam, one can make the responses more sensitive to a preferred parameter. Moreover, one can tune the length in such a way that succeeding frequencies are well separated. Hence, the different frequencies are more easily detected during measurements.

The torsion mode is well separated from the higher order modes and shows good sensitivity with respect to  $G_{xy}$ . The first mode is used to identify  $G_{xy}$ . Mode two and three are used to identify  $E_x$ .

**Model Updating results**

Initial values [N/mm <sup>2</sup> ]				Parameter selection				Fem data based on initial values versus Exp. data [Hz]			Mode shape switch occur		Difference initial final values [%]		Final parameter values [N/mm <sup>2</sup> ]			
Ex	Ey	Gxy	Vxy	Ex	Ey	Gxy	Vxy	Fem value	Exp. value	Description mode	Yes	No	CCABS	CCMEAN	Ex	Ey	Gxy	Vxy
17500	19156	5000	0,3	X		X		33	38,75	1 torsion		X	14 / O	-14 / O	25331	19156	6782	0,3
								90	105,6	mode 2								
								128	151,6	1 bending Y								

*Mode Updating results: deviation on initial values*

Initial values [N/mm <sup>2</sup> ]				Parameter selection				Fem data based on initial values versus Exp. data [Hz]			Mode shape switch occur		Difference initial final values [%]		Final parameter values [N/mm <sup>2</sup> ]			
Ex	Ey	Gxy	Vxy	Ex	Ey	Gxy	Vxy	Fem value	Exp. value	Description mode	Yes	No	CCABS	CCMEAN	Ex	Ey	Gxy	Vxy
21000	19156	4000	0,3	X		X		30	38,75	1 torsion		X	15 / 1	-15 / 0	25331	19156	6782	0,3
								94	105,6	mode 2								
								137	151,6	1 bending Y								

Initial values [N/mm <sup>2</sup> ]				Parameter selection				Fem data based on initial values versus Exp. data [Hz]			Mode shape switch occur		Difference initial final values [%]		Final parameter values [N/mm <sup>2</sup> ]			
Ex	Ey	Gxy	Vxy	Ex	Ey	Gxy	Vxy	Fem value	Exp. value	Description mode	Yes	No	CCABS	CCMEAN	Ex	Ey	Gxy	Vxy
14000	19156	6000	0,3	X		X		36	38,75	1 torsion		X	16 / 1	- 16 / 0	25331	19156	6782	0,3
								86	105,6	mode 2								
								117	151,6	1 bending Y								

## **Chapter Seven: Conclusions**

This thesis gives an answer to the question: “Is it possible to determine global effective orthotropic material properties by measuring a certain amount of natural frequencies of a composite structure?”. A program written in FEMtools is developed. In first instance the program is used to identify the material properties of a steel beam. Results are in line of expectation. Afterwards, the program is applied to four composite structures with unknown material properties. In the set of four, there is one closed box beam and three beams with an open cross-section. This set is too small to state some general conclusions concerning the identification of material properties of slender composite structures. However, some general trends are clearly observed.

For the closed box beam, values for  $E_x$  and  $G_{xy}$  can be identified using the program. The natural frequencies of the beam are not sensitive to change in value of  $E_y$  and  $\nu_{xy}$ . Hence, it is not possible to determine these values by measuring natural frequencies.

The natural frequencies of beams with open cross section are sensitive to a change in value of  $E_x$ ,  $E_y$  and  $G_{xy}$ . Hence, there is a possibility to identify these properties by measuring natural frequencies. The frequencies sensitive to a modification of  $E_y$ , are more difficult to measure in practise. The mode shapes corresponding with these frequencies, are those in which the section goes open and close. It is not possible to identify values for  $\nu_{xy}$ .

The program needs initial values for orthotropic material properties, before identification can start. The initial values are obtained making use of the Resonalyser procedure. A deviation of 25 % given on estimated initial values, results in the same final updated values for the parameters. Hence, the final updated results are almost not sensitive to a deviation of initial values.

The program can also be used to study the influence of the length of the structure on the possibility to identify certain parameters. Consequently, an optimal length can be determined for which the first (two) frequencies are very sensitive to a change in value of a preferred parameter. Making it possible to identify orthotropic material properties in a more easy and structured manner.

## References

- (Ref. 1) Stress analysis of fiber-reinforced composite materials  
Michael W. Hyer  
McGraw-Hill
- (Ref. 2) Roark's formulas for stress and strain  
Warren C. Young  
McGraw-Hill
- (Ref. 3) Bert C W 1973, "Simplified analysis of static shear factors for beams of non homogeneous cross section", J. Comp. Mat. 7:525-529
- (Ref. 4) Vinson J R and R L Sierakowski 1987. The behavior of structures composed of composite materials Dordrecht Martinus Nijhoff Publishers
- (Ref. 5) Whiney J M, C E Browning and A Mair 1974 "Analysis of the flexure test for laminated composite materials", Composite Materials: testing and design (Third Conference)
- (Ref. 6) Tsai, S W 1988 Composites Design Dayton OH: Think composites
- (Ref. 7) Barbero E J, R Lopez-Anido and J F Davalos 1993 "On the mechanics of thin-walled laminated composite beams" J Comp Mat 27(8): 806-829
- (Ref 8) Modal Testing: Theory and Practice  
D J Ewins  
Research studies press
- (Ref. 9) Energy and variational methods in applied mechanics  
J N Reddy  
John Wiley & Sons
- (Ref.10) Theory of plates and shells  
Stephen P Timoshenko  
Woinowsky-Krieger  
McGraw-Hill
- (Ref.11) Introduction to finite element vibration analysis  
Maurice Petyt  
Cambridge University Press
- (Ref.12) Engineering Vibration  
Daniel J Inman  
Prentice Hall